Tesi di Dottorato in

Design and synthesis of peptides involved in the inhibition of influenza virus infection

Dottorando   **Tutore**

Dott. *Maria Carmina Scala*   **Chiar.mo** Prof. *Pietro Campiglia*

Coordinatore: Chiar.mo Prof. *Gianluca Sbardella*

Index

Chapter IV

Investigation on side-products formation during the preparation of a cyclic peptide contained a lactam bridge

Figure captions

Chapter III:

Chapter IV:

Table captions

Chapter II:

Chapter III:

Scheme captions

Chapter III:

Chapter IV:

CHAPTER I

Hemagglutinin: a promising target against influenza virus

Abstract

Influenza is a highly contagious, acute respiratory illness, which represents one of the main plagues worldwide. Even though some antiviral drugs are available, the alarming increase of virus strains resistant to them, highlights the need to find new antiviral compounds. The high mutation rate of the RNA genome of the influenza virus, combined with assortment of its multiple genomic segments, promotes antigenic diversity and new subtypes, allowing the virus to evade vaccines and become resistant to antiviral drugs. Thus, there is a continuing need for new anti-influenza therapy using novel targets and creative strategies.

On the basis of the above considerations, an ideal target for therapy should be a viral component, whose function is essential for virus infection.

In this contest, the influenza A virus hemagglutinin (HA) represents a very promising target.

Keywords: Influenza, virus, drug, resistance, therapy, hemagglutinin.

Abbreviations

IAVs, Influenza A virus; ORFs, open reading frames, HA, hemagglutinin; NA, neuraminidase; M2, matrix 2; M1, matrix 1; NEP, nuclear export protein; NS2, nonstructural protein 2; RNP, ribonucleoprotein; NP, nucleoprotein; HEF, hemagglutinin-esterase-fusion protein; NLSs, nuclear localization signals; cRNA, complementary RNA; NAIs, neuraminidase inhibitors; DANA, 2-deoxy-2,3-didehydro- N-acetyl neuraminic acid; FANA, 2-deoxy-2,3-dehydro-N-trifluoroacetylneuraminic acid.

1.1. Introduction

Influenza is a contagious respiratory infection and it is considered to be one of the life-threatening infectious diseases.[1] It is a viral infection, associated with seasonal outbreaks of respiratory illness during the winter months in regions with temperate climates and during rainy seasons in tropical regions.

In some countries seasonal influenza affects annually up to 40% of the population and 500 million people die from it worldwide every year.[2-4]

The reasons for seasonal epidemics of influenza are not definitely known. They probably involve a combination of environmental factors such as low humidity and low temperature and social behaviors that facilitate person-to-person transmission of influenza virus. At unpredictable intervals, influenza pandemics occur with very high attack rates and severe disease. In the population, influenza follows the general pattern that now appears to characterize essentially all respiratory infections. It can be particularly hazardous to individuals with poor immunity such as children and the elderly, and those with pulmonary, cardiovascular or other complications. Because of a lack of prior immunity, humans can be highly susceptible to infection and disease from these subtypes.

Influenza in otherwise healthy persons is characterized predominantly by fever, myalgias, cough and other respiratory symptoms, and malaise. In most persons, recovery from these symptoms occurs in 5 to 7 days, but even in healthy persons symptoms of fatigue and malaise may not completely resolve for several weeks.

Influenza may cause more severe pulmonary symptoms through direct invasion of the lung (leading to primary viral pneumonia) or by altering lung defense mechanisms in a variety of ways that lead to bacterial superinfection. This superinfection, which may occur simultaneously with influenza or follow it by days to weeks, may be responsible for much of the disease burden

associated with influenza. Although the primary target and clinically relevant tissue in influenza virus infection is the respiratory epithelium,[2] facultative infection of other organs, such as the cardiac or skeletal muscle, is possible and has occasionally been documented in cell culture and experimental animal infections.[5-9]

1.2 Influenza viruses

Influenza viruses, belonging to the Orthomyxoviridae family, are enveloped negative-strand RNA viruses with segmented genomes containing seven to eight gene segments.[4]

One genus includes influenza A and B viruses, and the other comprises influenza C viruses. The three virus types differ in host range and pathogenicity. [10] Type B and C influenza viruses are isolated almost exclusively from humans, although influenza B viruses have been isolated from seals and influenza C viruses have been isolated from pigs and dogs.[11-12]

Influenza A viruses, however, infect a wide variety of warm-blooded animals, including birds, swine, horses, humans, and other mammals. Influenza A and B viruses have a similar structure, whereas influenza C is more divergent. Influenza A- and B-type viruses contain eight discrete single-stranded RNA gene segments, each encoding at least one protein. Only Influenza A virus (IAVs) pose a significant risk of zoonotic infection, host switch, and the generation of pandemic IAVs. IAVs are enveloped with a host cell-derived lipid membrane. The eight gene segments encode at least 11 open reading frames (ORFs) (Figure 1.1).
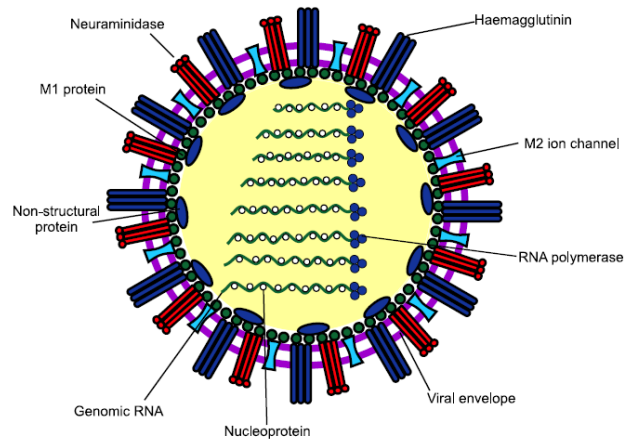
Figure 1.1 *Diagrammatic representation of an Influenza A Virus, the two major surface glycoproteins, hemagglutinin (HA) and neuraminidase (NA), along with small numbers of the matrix 2 (M2) ion channel protein, are embedded in a lipid bilayer (according to Ludwig et al. 2003). Adapted from "Antiviral agents targeting the influenza virus: a review and publication analysis," by L. Eyer and K. Hruska, 2013, Veterinarni Medicina, 58, 113-185.*

The envelope bilayer harbors the two spike glycoproteins, hemagglutinin (HA) and neuraminidase (NA), and the M2 proton channel. HA is a glycosylated type I integral membrane protein with functions both as the viral receptor-binding protein and fusion protein. NA cleaves glycosidic bonds with terminal SA facilitating the release of budding virions from the cell. There are 16 known HA (H1 to H16) and 9 NA (N1 to N9) subtypes in influenza A,[4, 13] leading to the current HxNy nomenclature. Routine human infections of seasonal influenza are mainly due to H1N1, H1N2 and influenza B; however, H3N2 is gradually becoming more abundant.[14] The small protein M2 is a proton channel necessary for viral replication.

1.2.1 Virion structure and organization

Influenza A and B viruses are virtually indistinguishable by electron microscopy. They are spherical or filamentous in shape, with the spherical forms on the order of 100 nm in diameter and the filamentous forms often in excess of 300 nm in length. The influenza A virion is studded with glycoprotein spikes of HA and NA, in a ratio of approximately four to one, projecting from a host cell–derived lipid membrane.[4]

A smaller number of matrix ion channels (M2) traverse the lipid envelope, with an M2:HA ratio on the order of one M2 channel per 101-102 HA molecules.[15] The envelope and its three integral membrane proteins HA, NA, and M2 overlay a matrix of M1 protein, which encloses the virion core. Internal to the M1 matrix are found the nuclear export protein (NEP; also called nonstructural protein 2, NS2) and the ribonucleoprotein (RNP) complex, which consists of the viral RNA segments coated with nucleoprotein (NP) and the heterotrimeric RNAdependent RNA polymerase, composed of two "polymerase basic" and one "polymerase acidic" subunits (PB1, PB2, and PA). The organization of the influenza B virion is similar, with four envelope proteins: HA, NA, and, instead of M2, NB and BM2. Influenza C virions are structurally distinct from those of the A and B viruses; on infected cell surfaces, they can form long cordlike structures on the order of 500 μm. However, influenza C virions are compositionally similar, with a glycoprotein-studded lipid envelope overlying a protein matrix and the RNP complex. The influenza C viruses have only one major surface glycoprotein, the hemagglutinin-esterase-fusion (HEF) protein, which corresponds functionally to the HA and NA of influenza A and B viruses, and one minor envelope protein, CM2.[4]

1.2.2 The influenza virus replication cycle

1.2.2.1 Virus attachment

Influenza viruses recognize N-acetylneuraminic (sialic) acid on the host cell surface. Sialic acids are nine-carbon acidic monosaccharides commonly found at the termini of many glycoconjugates. The sialic acid moiety is recognized and bound by the HA spikes on the surface of influenza viruses.[16]
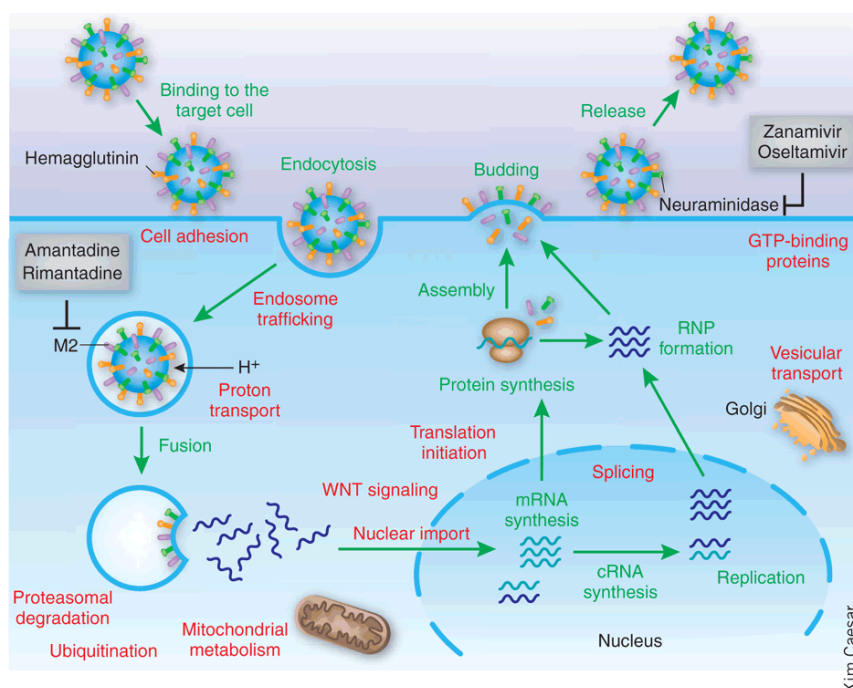
Figure 1.2 *Cellular targets for anti-influenza drugs in the context of the replication cycle of influenza virus. Stages of influenza A virus replication are in green. Cellular pathways shown by siRNA screens to be essential for completion of the viral replication cycle are shown in red. Adapted from "Cellular targets for influenza drugs," by J. Min and K. Subbarao, 2010, Nature Biotechnology, 28, 239-240.*

1.2.2.2 Virus Entry

Following attachment of the influenza virus HA to sialic acid, the virus is endocytosed. The acidity of the endosomal compartment is crucial to influenza virus uncoating in two ways. First, low pH triggers a conformational change in the HA, exposing a fusion peptide that mediates the merging of the viral envelope with the endosomal membrane, thus opening a pore through which the viral RNP's are released into the host cell cytoplasm.[17, 18] Second, hydrogen ions from the endosome are pumped into the virus particle via the M2 ion channel. The M2 protein, a transmembrane ion channel found only in influenza A virus, has portions external to the viral envelope, along with the HA and NA.[19, 20] Internal acidification of the influenza virion via the M2 channel disrupts internal protein-protein interactions, allowing viral RNPs to be released from the viral matrix into the cellular cytoplasm.[21]

1.2.2.3 Synthesis of Viral RNA

Once liberated from the virion, RNPs are trafficked to the host cell nucleus by means of viral proteins' nuclear localization signals (NLSs), which direct cellular proteins to import the RNPs and other viral proteins into the host cell nucleus.[22] The nucleus is the location of all influenza virus RNA synthesis. The viral RNAdependent RNA polymerase – a component of the RNPs imported into the nucleus – uses the negative-sense vRNA as a template to synthesize two positive-sense RNA species: mRNA templates for viral protein synthesis, and complementary RNA (cRNA) intermediates from which the RNA polymerase subsequently transcribes more copies of negative-sense, genomic vRNA. Nuclear export of vRNA segments, however, is mediated by the viral proteins M1 and NEP/NS2.[22] M1 interacts with both vRNA and NP and it also associates with the nuclear export protein NEP, which mediates the M1-RNP export via nucleoporins into the cytoplasm.

1.2.2.4 Virus Budding and Release

Influenza virus budding occurs at the cell membrane, probably initiated by an accumulation of M1 matrix protein at the cytoplasmic side of the lipid bilayer. When budding is complete, HA spikes continue to bind the virions to the sialic acid on the cell surface until virus particles are actively released by the sialidase activity of the NA protein. The NA is a mushroom-shaped tetramer, anchored to the viral envelope by a transmembrane domain.[23, 24] It possesses receptor destroying activity, cleaving terminal sialic acid residues from cell-surface glycoproteins and gangliosides to release progeny virus from the host cell. In viruses with inactive or absent NA, or in the presence of neuraminidase inhibitors, virus particles clump at the cell surface and infectivity is consequently reduced. The NA also removes sialic acid residues from the virus envelope itself, which prevents viral particle aggregation to enhance infectivity.[25, 26] The NA is also thought to aid virus infectivity by breaking down the mucins in respiratory tract secretions and allowing the virus to penetrate through to the respiratory epithelium, and it may play a role in virus entry into respiratory epithelial cells.[27] Host antibodies to the NA, as well as neuraminidase inhibitors, prevent virus release from infected cells and thus inhibit viral replication.

1.3 Anti-influenza therapy

1.3.1 Vaccine

The vaccination represent the main strategy for preventing infections. However, the vaccines are not able to follow the rapid virus antigenic drift, so that vaccine antigen composition needs to be updated annually based on global influenza surveillance. Efforts to influenza prevention by vaccination are made difficult by the virus ability to rapidly mutate and recombine into antigenically

new viral particles, sometimes leading to the emergence of a totally new virus. For this reason, at present, the development of antiviral drugs represents a crucial strategy in the control and prevention of seasonal and pandemic influenza infections.[28] Antiviral drugs can overcome the limitations of vaccination strategies, such as the time-consuming vaccine design, insufficient protection for immunocompromised patients and the unpredictable antigenic changes in influenza strains which render vaccination ineffective.

The anti-influenza drugs are usually classified according to their target in the viral life-cycle, which is schematically depicted in Figure 1.2. Antiviral molecules are particularly used as inhibitors of the following processes: attachment of the virus to host cell receptors, endocytosis and fusion of viral and cell membranes, replication and transcription of the viral genome, synthesis of viral proteins, assembly of the viral progeny and release of the new virions into the outside environment. Two classes of antiviral drugs, the adamantane derivatives (amantadine and rimantadine) and neuraminidase inhibitors (NAIs; zanamivir and oseltamivir), have been approved for treatment and prophylaxis of influenza.[4, 29, 30]

1.3.2 M2 ion channel blockers

M2 ion channel is a transmembrane viral protein (Figure 1.1) that mediates the selective transport of protons into the interior of the influenza virion. Conductance of protons acidifies the internal space of the viral particle and facilitates the haemagglutinin-mediated membrane fusion, which in turn results in the uncoating of the influenza nucleocapsid and import of the viral genome into the nucleus.[31] Adamantanes are potent M2 channel blockers, which are known as the first synthetic anti-influenza drugs described in the mid-1960s.[32] Two adamantane derivatives, amantadine and rimantadine (Figure 1.3), have been licensed for influenza control and are commercially available under the

trademarks Symmetrel® and Flumadine®, respectively.[33] The adamantanes are relatively cheap, highly stable in storage and show strong anti-influenza activity at micromolar concentrations. At present, the application of adamantanes for prevention and treatment of influenza infections is, however, not recommended because of the rapid emergence of drug-resistant virus variants that retain full virulence and transmissibility.[34, 35]
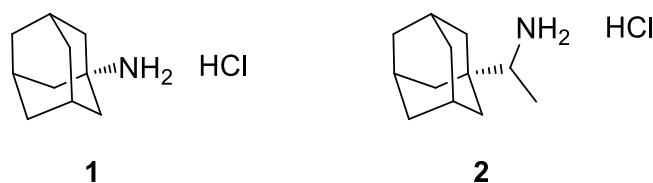
Figure 1.3 *Structure of M2 ion channel inhibitors:*

amantadine (1) and rimantadine (2).

1.3.3 Inhibitors of neuraminidase

Neuraminidase, also referred to as sialidase, is an antigenic glycoprotein anchored in the surface envelope of the influenza virions, which hydrolytically cleaves the terminal sialic acid from the host cell receptors (Figure 1.2). Thus, it plays a crucial role in the release of viral progeny from the membranes of infected cells, prevents self-aggregation of virions and facilitates the movement of the infectious viral particles in the mucus of the respiratory epithelia.[27, 36] Influenza neuraminidase has been established as a key drug target for the prophylaxis and treatment of influenza infections, predominantly for the following reasons: firstly, the structure of the influenza neuraminidase active site is highly conserved between influenza A and B strains, making neuraminidase an attractive target for the development of broad-spectrum inhibitors.[37] Secondly, resistance to neuraminidase inhibitors develops less

commonly than to other anti-influenza drugs. Nevertheless, the intensive application of neuraminidase inhibitors for influenza treatment results in a permanently increasing number of drug-resistant strains.[38] Thirdly, in contrast to adamantanes, neuraminidase inhibitors are mostly well tolerated in patients under therapy.[39] Finally, neuraminidase protein is a freely accessible target for antiviral molecules with an extracellular mode of action. The development of neuraminidase inhibitors started in the middle 1970s, when the first structural analogues of sialic acid were described and denoted as DANA (2-deoxy-2,3-didehydro- N-acetyl neuraminic acid) and its trifluoroacetyl derivative FANA (2-deoxy-2,3-dehydro-N-trifluoroacetylneuraminic acid).[40] At present, several licensed anti-influenza medications are available on the market, most notably the inhalant zanamivir with the trademark Releza®, and the orally administered oseltamivir (Tamiflu®) having excellent bioavailability and relatively long half-life *in vivo* (Figure 1.4).[41, 42]
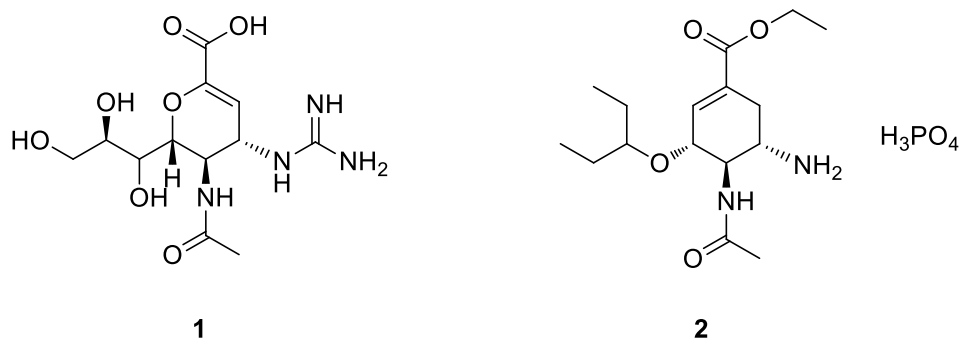
Figure 1.4 *Structure of neuraminidase inhibitors: zanamivir (1) and oseltamivir (2).*

In response to the emergence of some oseltamivir-resistant influenza strains, peramivir and laninamivir have been recently developed (Figure 1.5).[43, 44]
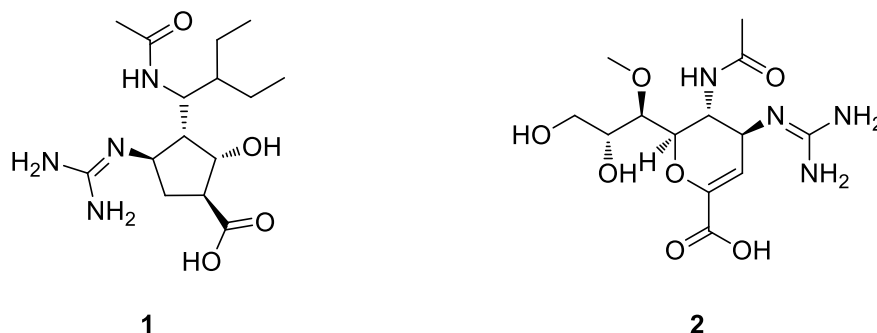
Figure 1.5 *Structure of peramivir (1) and laninamivir (2).*

New-generation neuraminidase inhibitors are currently under investigation, e.g., multimeric forms of zanamivir,[45] dual-targeted bifunctional antivirals[46] and several herbal remedies, such as flavonols, alkaloids and saponins.[47]

1.4 Influenza drug resistance

The propagation of viruses in the presence of antiviral drugs increases the selection pressure for mutations in the viral target proteins, which results in the induction of virus drug resistance. As an example, adamantane resistant strains are typically characterised by a single substitution in the transmembrane region of the M2 ion channel.[48, 49] On the other hand, resistance to neuraminidase inhibitors can result from mutations in the neuraminidase active cavity, but also from amino acid substitutions on the molecular surface of the neuraminidase protein.[37, 50] It is noteworthy that resistance to adamantanes is acquired rapidly and by a high number of virus strains,[34] while neuraminidase inhibitor resistance has developed over a longer time period and occurs with a relatively lower frequency.[38] This may be due to the fact that some mutations significantly affect viral infectivity and ability to replicate in the host cell.

Therefore, the capability of viruses to mutate the target proteins represents an obstacle for efficient treatment with these drugs. On the basis of the above it

is apparent the need to provide for new compounds against influenza virus able to overcome the disadvantages of the known therapies.[51, 52]

Therefore, the identification of new target for therapy of influenza virus infection and development of new therapeutic agents are the global public health priority.

1.5 Hemagglutinin: a new promising target

An attractive antiviral strategy is the blocking of influenza virus entry into the host cell. This process is mediated by the viral hemagglutinin (HA), a glycosylated type I integral membrane protein. HA is responsible for the binding of the virus to the target cell and, after virus uptake into endosomes, fusion of the virus with the cell membranes.[53]

The crystal structure of the HA molecule is a trimer with two structurally distinct regions: a stem, comprising a triple-stranded coiled-coil of alpha-helices, and a globular head of antiparallel beta-sheet, positioned atop the stem.[54]

The head contains the sialic acid receptor binding site, which is surrounded by the predicted variable antigenic determinants, designated A, B, C, and D in the H3 subtype[55] and Sa, Sb, Ca1, Ca2, and Cb in the H1 subtype (Figure 1.6).[4]
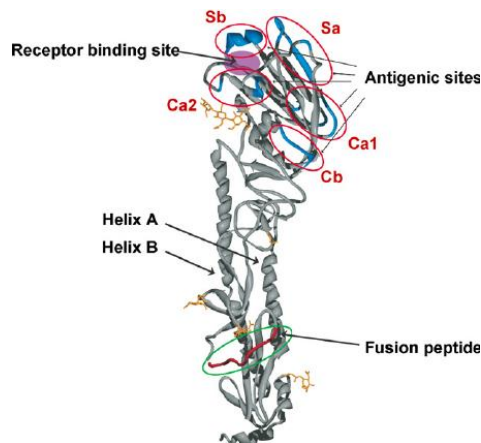
Figure 1.6 *Ribbon diagram of an uncleaved hemagglutinin monomer from an influenza A virus (H1N1). The head contains the sialic acid receptor-binding site, which is surrounded by the five predicted antigenic sites (Sa, Sb, Ca1, Ca2, and Cb). The stem comprises helices A and B and the fusion peptide, as shown. Adapted from "The biology of influenza viruses," by N. M. Bouvier and P. Palese, 2008, Vaccine, 26, 1-10.*

During virus replication, the HA protein is cleaved by serine proteases into HA1 and HA2; this post-translational modification is necessary for virus infectivity. The HA2 portion is thought to mediate the fusion of virus envelope with cell membranes, while the HA1 portion contains the receptor binding and antigenic sites.[56] Antibodies to HA neutralize virus infectivity, so virus strains evolve frequent amino acid changes at the antigenic sites; however, the stem-head configuration of the HA molecule remains conserved among strains and subtypes. These relatively minor changes accumulate in a process called *antigenic drift*. Eventually, mutations in multiple antigenic sites result in a virus strain that is no longer effectively neutralized by host antibodies to the parental virus, and the host becomes susceptible again to productive infection by the drifted strain.

Hemagglutinin has been chosen since it is the major surface protein of the Influenza A virus and is essential to the entry process so representing an

attractive target for antiviral therapy. An initial attachment of HA to specific receptors on the host cell surface and a membrane fusion of HA matured by protease digestion are required for virus infection. As a matter of fact, neutralizing compounds targeting HA represent a useful tool in neutralizing viral infection, clearing virus, and suppressing viral spread.

References

[1]   Mulder, J.; Hers, J. F. P. Influenza. Groningen: Wolters-Noordhoff. **1972**, 287.

[2]   Metersky, M. L.; Masterton, R.G.; Lode, H.; File, T. M., Jr.; Babinchak, T. Epidemiology, microbiology, and treatment considerations for bacterial pneumonia complicating influenza. *Int J Infect Dis.* **2012**, 16, 321-331.

[3]   Hale, B. G.; Albrecht, R. A.; García-Sastre, A. Innate immune evasion strategies of influenza viruses. *Future Microbiol.* **2010**, 5, 23-41.

[4]   Palese, P.; Shaw, M. L. Orthomyxoviridae: the viruses and their replication. In Fields Virology. 5 edition. Edited by: Knipe, D. M.; Howley, P. M. Philadelphia, PA: Lippincott Williams **2007**, 1647-1689.

[5]   Haessler, S.; Paez, A.; Rothberg, M.; Higgins, T. 2009 pandemic H1N1-associated myocarditis in a previously healthy adult. *Clin Microbiol Infect.* **2011**, 17, 572-574.

[6]   Kumar, K.; Guirgis, M.; Zieroth, S.; Lo, E.; Menkis, A. H.; Arora, R. C.; Freed, D. H. Influenza myocarditis and myositis: case presentation and review of the literature. *Can J Cardiol.* **2011**, 27, 514-522.

[7]   Pan, H. Y.; Yamada, H.; Chida, J.; Wang, S.; Yano, M.; Yao, M.; Zhu, J.; Kido, H. Upregulation of ectopic trypsins in the myocardium by influenza A virus infection triggers acute myocarditis. *Cardiovasc Res.* **2011**, 89, 595-603.

[8]   Ru, Y. X.; Li ,Y.C.; Zhao, Y.; Zhao, S. X.; Yang, J. P.; Zhang, H. M.; Pang, T.X. Multiple organ invasion by viruses: pathological characteristics in three fatal cases of the 2009 pandemic influenza A/H1N1. *Ultrastruct Pathol.* **2011**, 35, 155-161.

[9]   Toffan, A.; Serena Beato, M.; De Nardi, R.; Bertoli, E.; Salviato, A.; Cattoli, G.; Terregino, C.; Capua, I. Conventional inactivated bivalent H5/H7 vaccine prevents viral localization in muscles of turkeys infected experimentally with low pathogenic avian influenza and highly pathogenic avian influenza H7N1 isolates. *Avian Pathol.* **2008**, 37, 407-412.

[10]   Wright, P.F.; Neumann, G.; Kawaoka, Y. Orthomyxoviruses. In: Knipe DM, Howley PM, editors. Fields Virology. Williams & Wilkins; Philadelphia, Lippincott: **2007**, 1691–1740.

[11]   Osterhaus, A. D.; Rimmelzwaan, G. F.; Martina, B. E.; Bestebroer, T. M.; Fouchier, R. A. Influenza B virus in seals. *Science*. **2000**, 288, 1051–1053.

[12]   Youzbashi, E.; Marschall, M.; Chaloupka, I.; Meier-Ewert, H. Distribution of influenza C virus infection in dogs and pigs in Bavaria. *Tierarztl. Prax.* **1996**, 24, 337–342.

[13]   Webster, R. G.; Bean, W. J.; Gorman, O. T.; Chambers, T. M.; Kawaoka, Y. Evolution and ecology of influenza A viruses. *Microbiol Rev*. **1992**, 56, 152-179.

[14]   Centers for Disease Control and Prevention: Seasonal influenza (flu) - information on H3N2 variant influenza A viruses.[http://www.cdc.gov/flu/swineflu/influenza-variant-viruses-h3n2v.htm.

[15]   Zebedee, S. L.; Lamb, R. A. Influenza A virus M2 protein: monoclonal antibody restriction of virus growth and detection of M2 in virions. *J Virol*. **1988**, 62, 2762–2772.

[16]   Couceiro, J. N.; Paulson, J. C.; Baum, L. G. Influenza virus strains selectively recognize sialyloligosaccharides on human respiratory epithelium; the role of the host cell in selection of hemagglutinin receptor specificity. *Virus Res*. **1993**, 29,155–165.

[17]   Sieczkarski, S. B.; Whittaker, G. R. Viral entry. *Curr Top Microbiol Immunol*. **2005**, 285, 1–23.

[18]   Stegmann, T. Membrane fusion mechanisms: the influenza hemagglutinin paradigm and its implications for intracellular fusion. *Traffic*. **2000**, 1, 598–604.

[19]   Pinto, L. H.; Holsinger, L. J.; Lamb, R. A. Influenza virus M2 protein has ion channel activity. *Cell*. **1992**, 69, 517-528.

[20]   Wharton, S. A.; Belshe, R. B.; Skehel, J. J.; Hay, A. J. Role of virion M2 protein in influenza virus uncoating: specific reduction in the rate of membrane fusion between virus and liposomes by amantadine. *J Gen Virol*. **1994**, 75, 945-948.

[21]   Martin, K.; Helenius, A. Transport of incoming influenza virus nucleocapsids into the nucleus. *J Virol*. **1991**, 65, 232–244.

[22]   Cros, J. F.; Palese, P. Trafficking of viral genomic RNA into and out of the nucleus: influenza, Thogoto and Borna disease viruses. *Virus Res*. **2003**, 95, 3–12.

[23]   Colman, P. M.; Varghese, J. N.; Laver, W. G. Structure of the catalytic and antigenic sites in influenza virus neuraminidase. *Nature*. **1983**, 303, 41-44.

[24]   Varghese, J. N.; Laver, W. G.; Colman, P. M. Structure of the influenza virus glycoprotein antigen neuraminidase at 2.9 A resolution. Nature. **1983**, 303, 35–40.

[25]   Palese, P.; Compans, R. W. Inhibition of influenza virus replication in tissue culture by 2-deoxy-2,3- dehydro-N-trifluoroacetylneuraminic acid (FANA): mechanism of action. *J Gen Virol*. **1976.** 33,159–163.

[26]   Palese, P.; Tobita, K.; Ueda, M.; Compans, R. W. Characterization of temperature sensitive influenza virus mutants defective in neuraminidase. *Virology*. **1974**, 61, 397–410.

[27]   Matrosovich, M. N.; Matrosovich, T. Y.; Gray, T.; Roberts, N. A.; Klenk, H. D. Neuraminidase is important for the initiation of influenza virus infection in human airway epithelium. *J Virol*. **2004**, 78, 12665–12667.

[28]   Hayden, F. G. Respiratory viral threats. *Curr. Opin. Infect. Dis*. **2006**, 19, 169–178.

[29]   Dolin, R.; Reichman, R. C.; Madore, H. P.; Maynard, R.; Linton, P. N.; Webber-Jones, J. A controlled trial of amantadine and rimantadine in the prophylaxis of influenza A infection. *N Engl J Med*. **1982,** 307, 580–584.

[30]   Nicholson, K. G.; Wood, J. M.; Zambon, M. Influenza. *Lancet*. **2003**, 362, 1733–1745.

[31]   Schnell, J. R; Chou, J. J. Structure and mechanism of the M2 proton channel of influenza A virus. *Nature*. **2008**, 451, 591-595.

[32]   Davies, W. L.; Grunert, R. R.; Haff, R. F.;, Mcgahen, J. W.; Neumayer, E. M.; Paulshock, M.; Watts, J. C.; Wood, T. R.; Hermann, E. C.; Hoffmann, C. E. Antiviral activity of 1-adamantanamine (amantadine). *Science*. **1964**, 144, 862-863.

[33]   Alves Galvão, M. G.; Rocha Crispino Santos, M. A.; Alves da Cunha, A. J. Amantadine and rimantadine for influenza A in children and the elderly. *Cochrane Database of Systematic Rev.* **2012***,* 23, 1-116.

[34]   Bright, R. A.; Medina, M. J.; Xu, X.Y.; Perez-Oronoz, G.; Wallis, T. R.; Davis, X. H. M.; Povinelli, L.; Cox, N. J.; Klimov, A. I. Incidence of adamantane resistance among influenza A (H3N2) viruses isolated worldwide from 1994 to 2005: a cause for concern. *Lancet.* **2005**, 366, 1175–1181.

[35]   Barr, I. G.; Deng, Y. M.; Iannello, P.; Hurt, A. C.; Komadina, N. Adamantane resistance in influenza A(H1) viruses increased in 2007 in South East Asia but decreased in Australia and some other countries. *Antiviral Research.* **2008**, 80, 200–205.

[36]   Suzuki, T.; Takahashi, T.; Guo, C. T.; Hidari, K. I. P. J.; Miyamoto, D.; Goto, H.; Kawaoka, Y.; Suzuki, Y. Sialidase activity of influenza A virus in an endocytic pathway enhances viral replication. *Journal of Virology.* **2005**, 79, 11705–11715.

[37]   Yen, H. L.; Hoffmann, E.; Taylor, G.; Scholtissek, C.; Monto, A. S.; Webster, R. G.; Govorkova, E. A. Importance of neuraminidase active-site residues to the neuraminidase inhibitor resistance of influenza viruses. *Journal of Virology.* **2006**, 80, 8787–8795.

[38]   Garcia, J.; Sovero, M.; Torres, A. L.; Gomez, J.; Douce, R.; Barrantes; M.; Sanchez, F.; Jimenez, M.; Comach, G.; de Rivera I.; Agudo, R.; Kochel, T. Antiviral resistance in influenza viruses circulating in Central and South America based on the detection of established genetic markers. *Influenza Other Respiratory Viruses.* **2009**, 3, 69–74.

[39]   Cao, B.; Wang, D. Y.; Yu, X. M.; We, L. Q.; Pu, Z. H.; Gao, Y.; Wang, J.; Dong, J. P.; Li, X. L.; Xu, Q.; Hu, K.; Chen, B. Y.; Yu, Y. S.; Song, S. F.; Shu, Y. L.; Wang, C. An uncontrolled openlabel, multicenter study to monitor the antiviral activity and safety of inhaled zanamivir (as Rotadisk via Diskhaler device) among Chinese adolescents and adults with influenza-like illness. *Chinese Medical Journal.* **2012**, 125, 3002–3007.

[40]   Schulman, J. L. and Palese, P. Susceptibility of different strains of influenza A virus to inhibitory effects of 2-deoxy-2,3-dehydro-N-trifluoroacetylneuraminic acid (FANA). *Virology.* **1975**, 63, 98–104.

[41]   He, G.; Massarella, J.; Ward, P. Clinical pharmacokinetics of the prodrug oseltamivir and its active metabolite Ro 64-0802. *Clinical Pharmacokinetics*. **1999**, 37, 471–484.

[42]   Greengard, O.; Poltoratskaia, N.; Leikina, E.; Zimmerberg, J.; Moscona, A. The anti-influenza virus ahent 4-GU-DANA (Zanamivir) inhibits cell fusion mediated by human parainfluenza virus and influenza virus HA. *Journal of Virology*. **2000**, 74, 11108–11114.

[43]   Bantia, S.; Arnold, C. S.; Parker, C. D.; Upshaw, R.; Chand, P. Anti-influenza virus activity of peramivir in mice with single intramuscular injection. *Antiviral Research*. **2006**, 69, 39–45.

[44]   Kubo, S.; Tomozawa, T.; Kakuta, M.; Tokumitsu, A.; Yamashita, M. Laninamivir prodrug CS-8958, a long-acting neuraminidase inhibitor, shows superior anti-influenza virus activity after a single administration. *Antimicrobial Agents and Chemotherapy*. **2010**, 54, 1256–1264.

[45]   Watson, K. G. et al. Highly Potent and Long-Acting Trimeric and Tetrameric Inhibitors of Influenza Virus Neuraminidase. *Bioorg Med Chem Lett*. **2004**, 14, 1589-1592.

[46]   Liu, K. C.; Fang, J. M.; Jan, J. T.; Cheng, T. J. R.; Wang, S. Y.; Yang, S. T.; Cheng, Y. S. E.;   Wong, C. H. Enhanced Anti-influenza Agents Conjugated with Anti-inflammatory Activity. *J. Med. Chem*. **2012**, 55, 8493–8501.

[47]   Jeong, H. J.; Ryu, Y. B.; Park, S. J.; Kim, J. H.; Kwon, H. J.; Kim, J. H.; Park, K. H.; Rho, M. C.; Lee, W. S. Neuraminidase inhibitory activities of flavonols isolated from Rhodiola rosea roots and their in vitro anti-influenza viral activities. Bioorg Med Chem. **2009**, 17, 6816-23.

[48]   Saito, R.; Sakai, T.; Sato, I.; Sano,Y.; Oshitani, H.; Sato, M.; Suzuki, H. Frequency of Amantadine-Resistant Influenza A Viruses during Two Seasons Featuring Cocirculation of H1N1 and H3N2. *J Clin Microbiol*. **2003**, 41, 2164–2165.

[49]   Shiraishi, K.; Mitamura, K.; Sakai-Tagawa, Y.; Goto, H.; Sugaya, N.; Kawaoka, Y. High frequency of resistant viruses harboring different mutations in amantadine-treated children with influenza. *J Infect Dis*. **2003**, 188, 57-61.

[50]   Du, Q. S.; Wang, S. Q.; Huang, R. B.; Chou K. C. Computational 3D structures of drug-targeting proteins in the 2009-H1N1 influenza A virus. *Chemical Physics Letters*. **2010**, 485, 191–195.

[51]   Belshe, R. B.; Burk, B.; Newman, F.; Cerruti, R. L.; Sim, I. S. Resistance of influenza A virus to amantadine and rimantadine: results of one decade of surveillance. *J Infect Dis*. **1989**, 159, 430–435.

[52]   Bertram, S.; Glowacka, I.; Steffen, I.; Kuhl, A.; Pohlmann, S. Novel insights into proteolytic cleavage of influenza virus hemagglutinin. *Rev Med Virol.* **2010**, 20, 298–310.

[53]   Skehel, J. J. and Wiley. D. C. Receptor binding and membrane fusion in virus entry: The influenza hemagglutinin. *Annual Review of Biochemistry*. **2000**, 69, 531–569.

[54]   Wilson, I. A.; Skehel, J. J.; Wiley, D. C. Structure of the haemagglutinin membrane glycoprotein of influenza virus at 3 A resolution. *Nature*. **1981**, 289, 366–73.

[55]   Webster, R. G.; Laver, W. G.; Air, G. M. Antigenic Variation Among Type A Influenza Viruses. In: Palese, P.; Kingsbury, D. W., editors. Genetics of Influenza Viruses. Vienna: Springer-Verlag. **1983**, 127-68.

[56]   Steinhauer, D. A. Role of hemagglutinin cleavage for the pathogenicity of influenza virus. *Virology*. **1999**, 258, 1–20.

CHAPTER II

Bovine lactoferrin: a novel drug target for the inhibition of influenza virus infection

Abstract

Bovine lactoferrin (bLf) is a multifunctional glycoprotein that plays an important role in innate immunity against infections, including influenza.

Therefore, bLf was considered a novel drug target for the inhibition of influenza virus infection. Previously, it was shown that inhibition of influenza virus hemagglutination and cell infection is entirely attributable to the C-lobe and that all major virus subtypes, including H1N1 and H3N2, are inhibited. By far-western blotting and sequencing studies, bLf was shown to bind to the HA_2 subunit, an HA region which is known to contain the universally conserved HA epitope. Moreover, molecular docking studies have identified some C-lobe fragments which inhibited virus hemagglutination and infection at picomolar concentration range.

Besides contributing to explain the broad anti-influenza activity of bLf, these findings lay the foundations for exploiting bLf fragments as source of potential anti-influenza therapeutics.

Keywords: Influenza, Bovine lactoferrin, C-lobe, Peptides, Antiviral.

Abbreviations

LF, lactoferrin; BLf, bovine lactoferrin; HI, hemagglutination inhibition assay; SI, selectivity index; HA, hemagglutinin.

2.1 Introduction

Lactoferrin (LF) is a non-haem iron-binding protein that is part of the transferrin protein family, whose function is to transport iron in blood serum.[1, 2]

Lactoferrin was first isolated by Sorensen and Sorensen from bovine milk in 1939. In 1960 it was concurrently determined to be the main iron binding protein in human milk by three independent laboratories.[3-5]

LF is commonly found in various secretory fluids, such as saliva, tears, nasal secretions, seminal and vaginal fluids, and in granules of polymorphonuclear leukocytes[6] of different mammalian species, including humans, cows, goats, horses, dogs, and several rodents.[7, 8]

It is also found in considerable amounts in secondary neutrophil granules ($15\mu g/10^6$ neutrophils),[9] where it plays a significant physiological role. LF is an essential player of the natural immunity. LF possesses a greater iron-binding affinity and is the only transferrin with the ability to retain this metal over a wide pH range,[10] including extremely acidic pH. It also exhibits a greater resistance to proteolysis. In addition to these differences, LF's net positive charge and its distribution in various tissues make it a multifunctional protein. It is involved in several physiological functions, including: regulation of iron absorption in the bowel; immune response; antioxidant, anticarcinogenic and anti-inflammatory properties; protection against microbial infection, which is the most widely studied function to date; and inhibiting activity towards different pathogens.[7, 11-13]

In particular, bLf has been recognized as potent inhibitor of different enveloped viruses, such as human cytomegalovirus,[14] herpes simplex viruses types 1 and 2,[15-18] human immunodeficiency virus,[19] human

hepatitis C virus,[20] hantavirus,[21] hepatitis B virus,[22] respiratory syncytial virus,[23] flavivirus,[24] alphavirus,[25] and phlebovirus.[26]

2.2 Structure and properties

Bovine lactoferrin (bLf) is a glycoprotein consisting of a single polypeptide chain of 689 amino acidic residues, with a molecular mass of 76 kDa, which binds two iron atoms with very high affinity.[27]

BLf, like lactoferrin of other mammalian species, is folded in two symmetric and globular lobes: N-lobe (residues 1-333) and C-lobe (residues 345-676) which are highly homologous with one another (33–41% homology). It is made up of α-helix and β-pleated sheet structures, which create two domains for each lobe (domains I and II). In bovine lactoferrin, the N1 stands for the sequences 1-90 and 251-333, N2 for 91-250, C1 for 345-431 and 593-676, and C2 for 432-592.[28, 29] These two lobes are linked by a three-turn connecting helix, residues 334 and 344, which provide additional flexibility to the molecule (Figure 2.1).[28] Each lobe can bind a metal atom in synergy with the carbonate ion (CO_3^{2-}). The metals that it binds are the Fe^{2+} or Fe^{3+} ions, but it has also been observed bound to Cu^{2+}, Zn^{2+} and Mn^{2+} ions.[7]
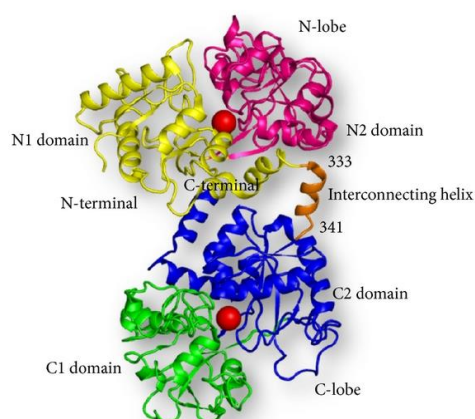
Figure 2.1 *Schematic diagram of the bovine lactoferrin molecule. The N1 and N2 domains are colored in yellow and pink, respectively, while the C1 and C2 domains are colored in green and blue, respectively. The interconnecting helix between the lobes is colored in orange. The two iron atoms are shown as red spheres. Adapted from "C-Lobe of Lactoferrin: The whole story of the half-molecule," by S. Sharma, M. Sinha, S. Kaushik, P. Kaur and T. P. Singh, 2013, Biochemistry Research International, 2013, 1-8.*

Because of its ability to reversibly bind Fe^{3+}, LF can exist free of Fe^{3+} (apo-LF) or associated with it (holo-LF),[30] and it has a different three-dimensional conformation depending on whether it is binding Fe^{3+}.[31] Apo-LF has an open conformation, whilst holo-LF is a closed molecule with greater resistance to proteolysis (Figura 2.2).[8]
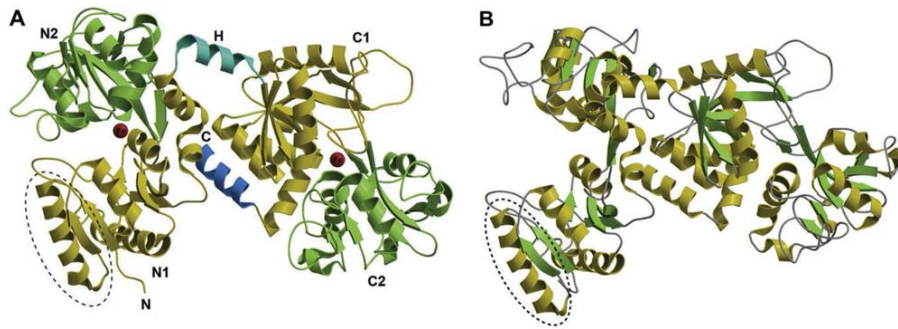
Figure 2.2 *Structure of the iron-bound (holo) form (A) and iron-free (apo) form (B) of Lf. Adapted from "A structural framework for understanding the multifunctional character of lactoferrin," by E. N. Baker and H. M. Baker, 2009, Biochimie, 91, 3–10.*

The iron-binding site is situated inside the interdomain cleft in each lobe. The iron-binding site consists of four residues: 2 tyrosines, 1 aspartate, and 1 histidine. The iron-binding residues in N-lobe are Asp 60, Tyr 92, Tyr 192, and His 253 while the corresponding iron-binding residues in C-lobe are Asp 395, Tyr 433, Tyr 526, and His 595. The iron-binding residues are coordinated to the ferric ion and a synergistic bidentate carbonate anion (Figura 2.3).[31] LF is a basic, positively charged protein with an isoelectric point of 8.0–8.5.[7]
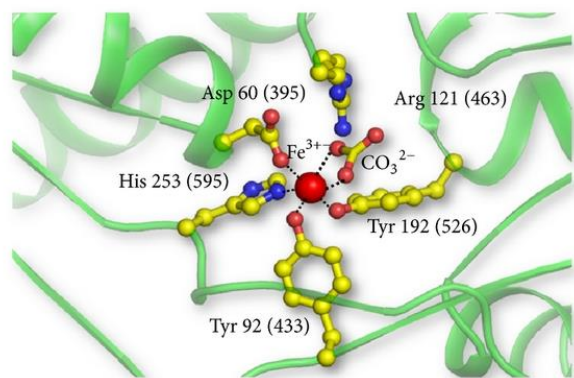
Figure 2.3 *Schematic figure of the iron-binding site of lactoferrin. The iron atom is shown as a red sphere, while the interacting amino acid residues of lactoferrin are in yellow. The residue numbers correspond to N-lobe, while the corresponding residues of C-lobe are in brackets. Adapted from "C-Lobe of Lactoferrin: The whole story of the half-molecule," by S. Sharma, M. Sinha, S. Kaushik, P. Kaur and T. P. Singh, 2013, Biochemistry Research International, 2013, 1-8.*

2.3 Biological functions of lactoferrin

Several functions have been attributed to LF. It is considered a key component in the host's first line of defence, as it has the ability to respond to a variety of physiological and environmental changes.[32] The structural characteristics of LF provide functionality in addition to the Fe^{3+} homeostasis function common to all transferrins: strong antimicrobial activity against a broad spectrum of bacteria, fungi, yeasts, viruses[33] and parasites;[34] anti-inflammatory and anticarcinogenic activities;[32] several enzymatic functions[35] and anti-influenza activity.[36]

2.4 Scientific background

Previously, Superti et al. have demonstrated that bLf binds to viral HA and inhibits hemagglutination and infection of all major virus subtypes, including H1N1 and H3N2.[37]

In particular, by far-western blotting and sequencing studies, it demonstrated that lactoferrin binds to the HA$_2$ subunit of viral HA, particularly to the fusion peptide, the only universally conserved epitope in all influenza virus hemagglutinin.[38] This behaviour explains the broad specificity of bLf and its C-lobe anti-influenza activity.[37]

Moreover, molecular docking studies have shown that the bLf C-lobe binding to HA was mediated, in most cases, by three surface-exposed loops characterized by the following amino acid sequences: SKHSSLDCVLRP (aa 418–429, **1**), AGDDQGLDKCVPNSKEK (aa 506–522, **2**) and NGESSADWAKN, (**3**) (Figure 2.4).
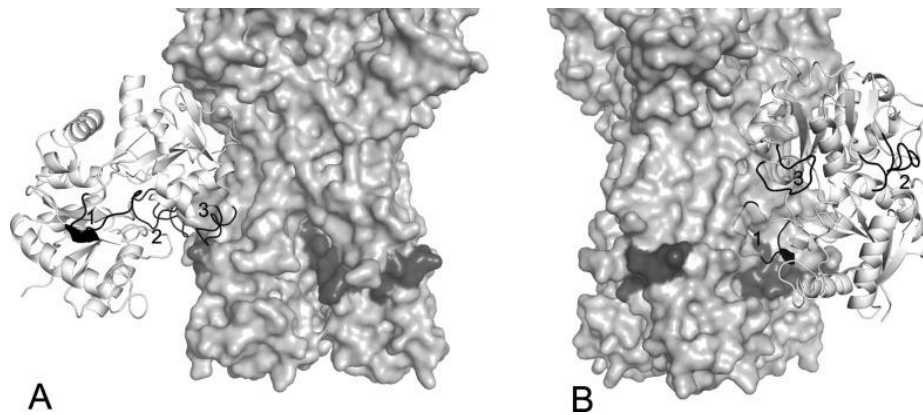
Figure 2.4 *Putative binding mode of bLf C-lobe (white ribbon) with the HA stm (light grey solid surface): (A) close to the fusion peptide (dark grey surface); (B) in the cleft between two monomers. Selected bLf sequences correspond to the numbered black loops of bLf C-lobe: (1) SKHSSLDCVLRP; (2)*

AGDDQGLDKCVPNSKEK; (3) NGESSADWAKN. Adapted from "Bovine lactoferrin-derived peptides as novel broad-spectrum inhibitors of influenza virus," by M. G. Ammendolia, M. Agamennone, A. Pietrantoni, F. Lannutti, R. A. Siciliano, B. De Giulio, C. Amici, F. Superti, 2012, Pathog. Glob. Health., 106, 12-19.

Therefore, each peptide, tested by HI, has shown to be able to inhibit HA activity of all tested virus strains at concentrations much lower than those shown by the C-lobe (Table 2.1).

Table 2.1 *Interaction of SKHSSLDCVLRP, AGDDQGLDKCVPNSKEK, and NGESSADWAKN peptides with viral HA. Adapted from "Bovine lactoferrin-derived peptides as novel broad-spectrum inhibitors of influenza virus," by M. G. Ammendolia, M. Agamennone, A. Pietrantoni, F. Lannutti, R. A. Siciliano, B. De Giulio, C. Amici, F. Superti, 2012, Pathog. Glob. Health., 106, 12-19.*

| | | HI titre | | |
Viral strain	Subtype	SKHSSL DCVLRP	AGDDQGLDK CVPNSKEK	NGESSA DWAKN
A/Roma-ISS/2/08 (Brisbane-like)	H1N1	1.4 pM	1.4 pM	0.7 fM
A/Parma/24/09 (Brisbane-like)	H1N1	1.4 pM	1.4 pM	0.3 fM
A/PR/8/34	H1N1	0.7 nM	0.35 nM	0.7 fM
A/Solomon (3/06)	H1N1	46.5 fM	46.5 fM	93.0 fM
A/Parma/5/06 (Wisconsin-like)	H3N2	0.7 pM	0.7 pM	0.3 pM
A/Wisconsin (67/05)	H3N2	23.2 fM	11.6 fM	5.8 fM
SW X-179A 1089/09	H1N1	5.8 fM	46.0 fM	0.3 fM
Avian 29/05/06	H5N1	18.0 fM	70.0 fM	93.1 fM
A/Turkey/Italy/2676/99	H7N1	18.0 fM	46.5 fM	5.8 fM

Similarly to HI data, bLf-derived peptides were better inhibitors than the entire protein, their selectivity index being about one or two order of magnitude higher, depending on virus strain (Table 2.2).

Table 2.2 *In vitro antiviral activity of SKHSSLDCVLRP, AGDDQGLDKCVPNSKEK, and NGESSADWAKN peptides towards influenza virus infection. Adapted from "Bovine lactoferrin-derived peptides as novel broad-spectrum inhibitors of influenza virus," by M. G. Ammendolia, M. Agamennone, A. Pietrantoni, F. Lannutti, R. A. Siciliano, B. De Giulio, C. Amici, F. Superti, 2012, Pathog. Glob. Health., 106, 12-19.*

	Viral strain	Subtype	CC_{50}*	EC_{50}°	SI^
SKHSSLDCVLRP	A/Roma-ISS/2/08	H1N1	>25 μM	4±0.37 pM	>6.25 × 10^6
	A/Parma/24/09	H1N1	>25 μM	3.1±0.12 pM	>8 × 10^6
	A/Parma/05/06	H3N2	>25 μM	5.8±0.7 pM	>4.3 × 10^6
AGDDQGLDKCVPNSKEK	A/Roma-ISS/2/08	H1N1	>25 μM	3.7±0.35 pM	>6.75 × 10^6
	A/Parma/24/09	H1N1	>25 μM	3.4±0.14 pM	>7.35 × 10^6
	A/Parma/05/06	H3N2	>25 μM	7.3±0.65 pM	>3.42 × 10^6
NGESSADWAKN	A/Roma-ISS/2/08	H1N1	>25 μM	225±5.8 fM	>1.11 × 10^8
	A/Parma/24/09	H1N1	>25 μM	50±1.37 fM	>5 × 10^8
	A/arma/05/06	H3N2	>25 μM	22.5±1.16 pM	>1.11 × 10^6

*CC50 the reciprocal substance dilution at which 50% of cells were protected from substance toxicity; °EC50 the reciprocal substance dilution at which 50% of cells were protected from the virus induced killing;^SI (selectivity index) the ratio between CC50 and EC50.
The mean values of three independent experiments with standard errors are shown.

This is the first demonstration that viral hemagglutination can be inhibited by a specific interaction with the HA_2 subunit. As a matter of fact, neutralizing antibodies against influenza virus have been found to act by two different mechanisms, mirroring the dual functions of hemagglutinin: (i) prevention of attachment to target cells, (ii) inhibition of entry (membrane fusion).

References

[1]   Anderson, B. F.; Baker, H. M.; Dodson, E. J.; Norris, G. E.; Rumball, S. V.; Waters, J. M.; Baker, E. N. Structure of human lactoferrin at 3.2 A resolution. *Proc. Natl. Acad. Sci. USA*. **1987**, 84, 1769–1773.

[2]   Moore, S. A.; Anderson, B. F.; Groom, C. R.; Haridas, M.; Baker, E. N. Threedimensional structure of diferric bovine lactoferrin at 2.8 A resolution. *J. Mol. Biol*. **1997**, 274, 222–236.

[3]   Groves, M. L. The isolation of a red protein from milk. *Journal of the American Chemical Society.* **1960**, 82, 3345–3350.

[4]   Johanson, B. Isolation of an iron containing red protein from human milk. *Acta Chemica Scandinavica*. **1960**, 14, 510–512.

[5]   Montreuil, J.; Tonnelat, J.; Mullet, S. Preparation and properties of lactosiderophilin (lactotransferrin) of human milk. *Biochimica et Biophysica Acta*. **1960**, 45, 413–421.

[6]   Gennaro, R.; Dewald, B.; Horisberger, U.; Gubler, H. U.; Baggiolini, M. A novelty of cytoplasmic granule in bovine neutrophils. *J Cell Biol.* **1983**, 96, 1651–1661.

[7]   van der Strate, B. W. A.; Belijaars, L.; Molema, G.; Harmsen, M. C.; Meijer, D. K. Antiviral activities of lactoferrin. *Antiviral Res*. **2001**, 52, 225–239.

[8]   Öztas-Yesim E. R.; Özgünes¸ N. Lactoferrin: a multifunctional protein. *Adv. Mol. Med.* **2005**, 1, 149–154.

[9]   Bennett, R. M. and Kokocinski, T. Lactoferrin content of peripheral blood cells. *Br. J. Haematol*. **1987**, 39, 509–521.

[10]   Aisen, P. and Leibman, A. Lactoferrin and transferrin: a comparative study. *Biochim. Biophys. Acta*. **1972**, 257, 314–323.

[11]   Levay, P. F. and Viljoen, M.   Lactoferrin: A general review. *Haematologica.* **1995**, 80, 252–267.

[12]   Vorland, L. H. Lactoferrin: A multifunctional glycoprotein. *APMIS*. **1999**, 107, 971–981.

[13]   Marchetti, M.; Superti, F. Antiviral activity of lactoferrin. In *Recent developments in antiviral research;* Trivandrum: Transworld Research Network. **2001**, 1, 193-203.

[14]   Harmsen, M. C.; Swart, P. J.; De Bèthune, M. P.; Pawels, R.; De Clercq, E.; The, T. H.; Meijer, D. K. F. Antiviral effects of plasma and milk proteins: lactoferrin shows a potent activity against both human immunodeficiency virus and human cytomegalovirus replication in vitro. *J Infec. Dis*. **1995**, 172, 380–388.

[15]   Marchetti, M.; Longhi, C.; Conte, M. P.; Pisani, S.; Valenti, P.; Seganti, L. Lactoferrin inhibits herpes simplex virus type 1 adsorption to Vero cells, *Antiviral Res*. **1996**, 29, 221-231.

[16]   Marchetti, M.; Trybala, E.; Superti, F.; Johansson, M.; Bergstrom, T. Inhibition of herpes simplex virus infection by lactoferrin is dependent on interference with the virus binding to glycosaminoglycans. *Virology*. **2004**, 18, 405-413.

[17]   Marchetti, M.; Ammendolia, M. G.; Superti, F. Glycosaminoglycans are not indispensable for the anti-herpes simplex virus type 2 activity of lactoferrin. *Biochimie***. 2009**, 91, 155-159.

[18]   Ammendolia, M. G.; Marchetti, M.; Superti, F. Bovine lactoferrin prevents the entry and intercellular spread of herpes simplex virus type 1 in Green Monkey Kidney cells. *Antivir Res*. **2007**, 76, 252–262.

[19]   Harmsen, M. C.; Swart, P. J.; De Bèthune, M. P.; Pawels, R.; De Clercq, E.; The, T. H.; Meijer, D. K. F. Antiviral effects of plasma and milk proteins: lactoferrin shows a potent activity against both human immunodeficiency virus and human cytomegalovirus replication in vitro. *J Infec. Dis*. **1995**, 172, 380–388.

[20]   Yi, M.; Kaneko, S.; Yu, D. Y.; Murakami, S. Hepatitis C virus envelope proteins bind lactoferrin. *J Virol.* **1997**, 71, 5997–6002.

[21]   Murphy, M. E.; Kariwa, H.; Mizutani, T.; Yoshimatsu, K.; Arikawa, J.; Takashima, I. In vitro antiviral activity of lactoferrin and ribavirin upon hantavirus. *Arch. Virol.* **2000**, 145, 1571–1582.

[22]   Hara, K.; Ikeda, M.; Saito, S.; Matsumoto, S.; Numata, K.; Kato, N.; Tanaka, K.; Sekihara, H. Lactoferrin inhibits hepatitis B virus infection in cultured human hepatocytes. *Hepatol Res.* **2002**, 24, 228–235.

[23]   Sano, H.; Nagai, K.; Tsutsumi, H.; Kuroki, Y. Lactoferrin and surfactant protein A exhibit distinct binding specificity to F protein and differently modulate respiratory syncytial virus infection. *Eur. J. Immunol.* **2003**, 33, 2894–2902.

[24]   Chien, Y. J.; Chen, W. J.; Hsu, W. L.; Chiou, S. S. Bovine lactoferrin inhibits Japanese encephalitis virus by binding to heparan sulfate and receptor for low density lipoprotein. *Virology*. **2008**, 379, 143–151.

[25]   Carvalho, C. A.; Sousa, I. P. Jr.; Silva, J. L.; Oliveira, A. C.; Gonçalves, R. B.; Gomes, A. M. Inhibition of Mayaro virus infection by bovine lactoferrin. *Virology*. **2014**, 452–453, 297–302.

[26]   Pietrantoni, A.; Fortuna, C.; Remoli, M. E.; Ciufolini, M. G.; Superti, F. Bovine lactoferrin inhibits Toscana virus infection by binding to heparan sulphate. *Viruses.* **2015**, 7, 480-495.

[27]   Legrand, D.; Mazurier, J.; Colavizza, D.; Montreuil, J.; Spik, G. Properties of the iron-binding site of the N-terminal lobe of human and bovine lactotransferrins. Importance of the glycan moiety and of the non-covalent interactions between the N- and C-terminal lobes in the stability of the iron-binding site. *Biochem J*. **1990**, 266, 575–581.

[28]   Moore, S. A.; Anderson, B. F.; Groom, C. R.; Haridas, M.; Bake, E. N. Three-dimensional structure of diferric bovine lactoferrin at 2.8 uA resolution. *J Mol Biol*. **1997**, 274, 222–236.

[29]   Steijns, J. M. and van Hooijdonk, A. C. Occurrence, structure, biochemical properties and technological characteristics of lactoferrin. *Br. J. Nutr*. **2000**, 84, S11-17.

[30]   Drago, S. M. E. Actividades antibacterianas de la lactoferrina. *Enf. Inf. Microbiol*. **2006**, 26, 58–63.

[31]   Shanbacher, F. L.; Goodman, R. E.; Talhouk, R. S. Bovine mammary lactoferrin: implications from messenger ribonucleic acid (mRNA) sequence and regulation contrary to other milk proteins. *J. Dairy Sci*. **1992**, 76, 3812–3831.

[32]   Connely, O. M. Antiinflammatory activities of lactoferrin. *J. Am. Coll. Nutr*. **2001**, 20, 389S–395S.

[33]   Rodriguez, D. A.; Vázquez, L.; Ramos, G. Antimicrobial mechanisms and potential clinical application of lactoferrin. *Rev. Latinoam. Microbiol*. **2005**, 47, 102–111.

[34]   Yamauchi, K.; Wakabayashi, H.; Shin, K.; Takase, M. Bovine lactoferrin: benefits and mechanism of action against infections. *Biochem Cell Biol.* **2006**, 84, 291–296.

[35]   Kanyshkova, T. G.; Babina, S. E.; Semenov, D. V.; Isaeva, N.; Valssov, A. V.; Neustroev, K. N.; et al. Multiple enzymatic activities of human milk lactoferrin. *Eur. J. Biochem.* **2003**, 270. 3353–3361.

[36]   Pietrantoni, A.; Dofrelli, E.; Tinari, A.; Ammendolia, M. G.; Puzelli, S.; Fabiani, C.; Donatelli, I.; Superti, F. Bovine lactoferrin inhibits influenza A virus induced programmed cell death in vitro. *Biometals*. **2010**, 23, 465-475.

[37]   Ammendolia, M. G.; Agamennone, M.; Pietrantoni, A.; Lannutti, F.; Siciliano, R. A.; De Giulio, B.; Amici C.; Superti, F. Bovine lactoferrin-derived peptides as novel broad-spectrum inhibitors of influenza virus. *Pathog. Glob. Health.* **2012**, 106, 12-19.

[38]   Ekiert, D. C.; Bhabha, G.; Elsliger, M. A.; Friesen, R. H.; Jongeneelen, M.; Throsby, M.; Goudsmit, J.; Wilson, I. A. Antibody recognition of a highly conserved influenza virus epitope. *Science*. **2009**, 324, 246-251.

CHAPTER III

Lactoferrin-derived Peptides Active towards Influenza: Identification of Three Potent Tetrapeptide Inhibitors

Abstract

Bovine lactoferrin, more concretely its C-lobe, is able to prevent both influenza virus hemagglutination and cell infection.

In this study, to deeper investigate the ability of lactoferrin derived peptides to inhibit influenza virus infection, we selected and synthesized new bovine lactoferrin C-lobe derived sequences that were assayed for their ability to prevent viral hemagglutination and cell infection.

We identify three tetrapeptides endowed of broad anti-influenza activity and able to inhibit viral infection in a concentration range femto- to picomolar. Our data indicate that these peptides may constitute a non-toxic approach for potential applications as anti-influenza therapeutics.

Keywords: Bovine lactoferrin; C-lobe; influenza virus; peptides; antivirals.

Abbreviations

Abbreviations used for amino acids and designation of peptides follow the rules of the IUPAC-IUB Commission of Biochemical Nomenclature in J. Biol. Chem. 1972, 247, 977-983. Amino acid symbols denote L-configuration unless indicated otherwise. The following additional abbreviations are used:

BLf, bovine lactoferrin; HA, hemagglutinin; HOBt, N-hydroxy-benzotriazole; HBTU, 2-(1H-benzotriazole-1-yl)-1,1,3,3-tetramethyluronium hexafluoro-phosphate; HOAt, 1-Hydroxy-7-azabenzotriazole; DIEA, N,N-diisopropylethyl-amine; DMF, N,N-dimethylformamide; DCM, dichloromethane; NMP, N-Methyl-2-pyrrolidone; TIS, triisopropylsilane; TFA, trifluoroacetic acid; GRK2, G Protein-Coupled Receptor Kinase 2; MDCK, Madin-Darby canine kidney;

FCS, fetal calf serum; HI, hemagglutination inhibition assay; SI, selectivity index.

3.1 Introduction

Previously, Superti et al. have deeper investigated the mechanism of the anti-influenza virus effect of bLf and the role of its tryptic fragments (the N- and C-lobes) in the antiviral activity. In particular, they have evaluated the influence of bLf on hemagglutinin-mediated functions. Hemagglutinin has been chosen since it is the major surface protein of the Influenza A virus and is essential to the entry process so representing an attractive target for antiviral therapy. An initial attachment of HA to specific receptors on the host cell surface and a membrane fusion of HA matured by protease digestion are required for virus infection. As a matter of fact, neutralizing compounds targeting HA represent a useful tool in neutralizing viral infection.

3.2 Aim of work

By protein-protein docking calculations, it was demonstrated that the binding between bLf C-lobe and HA is mediated by specific C-lobe fragments (peptides **1**, **2** and **3**).[1] These peptides strongly inhibited viral hemagglutination and infection at low picomolar concentrations and were patented.[2] However, protein-protein docking calculations suggested the possible role of other loops of bLf C-lobe that can contribute to the binding to HA. Thus, to better analyze the molecular and structural requirements that determine the bLf C-lobe-HA interaction., firstly, we decided to perform a wider mapping of C-lobe domain by designing, synthesizing, and evaluating

a new library of bLf C-lobe derivatives, corresponding to the sequences 441-454 (**4**), 478-500 (**5**), 552-563 (**6**), 619-630 (**7**), 633-638 (**8**), and 642-659 (**9**) (Figure 3.1, in yellow). As observed in Figure 3.1, the peptides **1-9** (in purple and yellow) map almost the entire C-lobe domain.
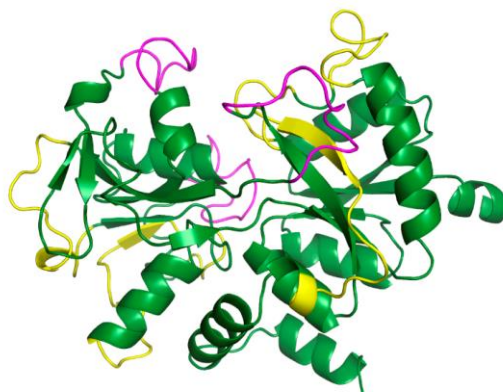
Figure 3.1 *Cartoon representation of the bLf C-lobe. The patented sequences are depicted in purple and the newly synthesized sequences in yellow.*

3.3 Design, Results and Discussion

3.3.1 Synthesis of C-lobe fragments (Peptides 4-9)

The first part of the work focused the attention on different C-lobe bLf fragments (peptides **1**, **4-9**). These peptides were synthesized and tested in order to evaluate their effectiveness to inhibit the HA activity by influenza virus belonging to subtypes H1N1 and H3N2 (Table 3.1).

3.3.1.1 Interaction with viral hemagglutinin

The first step of influenza virus entry into susceptible cells depends on the interaction between the viral HA and a specific sialic acid-containing cell receptor. This interaction can be measured by agglutination of turkey

erythrocytes. Therefore, the binding between virus and bLf was tested by checking the inhibition of viral hemagglutination activity.

In this experiment, the following influenza A virus strains were used: A/RomaISS/02/08 H1N1 oseltamivir-sensitive virus, A/Parma/24/09 H1N1 oseltamivir-resistant virus, and A/Parma/05/06 H3N2.

Table 3.1 *Sequence and HI titer of peptides 1-9.*

Frag	Pep.	Sequence	HI titer (nM)		
			A/Roma-ISS/02/08 H1N1	A/Parma/ 24/09 H1N1	A/Parma/ 05/06 H3N2
418-429	**1**	SKHSSLDCVLRP	0.0014	0.0014	0.0007
506-522	**2**	AGDDQGLDKCVPNSKEK	0.0014	0.0014	0.0007
553-563	**3**	NGESSADWAKN	$0.7 \cdot 10^{-6}$	$0.3 \cdot 10^{-6}$	0.0003
441-454	**4**	KANEGLTWNSLKDK	12	3	12
478-500	**5**	TGSCAFDEFFSQSCAPGADPKSR	-	-	97
552-563	**6**	TNGESTADWAKN	0.7	1.5	0.3
619-630	**7**	GKNGKNCPDKFC	-	-	-
633-638	**8**	KSETKN	1.5	0.3	3
642-659	**9**	NDNTECLAKLGGRPTYEE	-	2.500	-

As shown in Table 3.1, three out of six peptides were able to prevent HA activity of all tested viruses. Notwithstanding these peptides exerted a strong antiviral action (nanomolar), their activity was lower than that previously described by peptides **1**-**3** (low picomolar).[1] For example, the compound most potent of this series, dodecapeptide **6**, having a sequence similar to undecapeptide **3** proves to be 3-4 orders of magnitude less potent than reference peptides.[1]

According to these results, peptide **1** inhibits influenza virus hemagglutination at picomolar concentration, proving to be a potent antiviral peptide. During my PhD, I considered peptide **1** as a valuable starting point for the development of a novel class of antiviral drugs effective against influenza virus.

3.3.2 Design of peptides 10-17

In order to optimize the inhibitory activity of the ^{418}SKHSSLDCVLRP^{429} fragment (**1**) and to identify more potent and selective compounds, two different approaches were used: i) addition of four amino acid residues at both the N- and C-terminals (compounds **10**-**12**); ii) a truncation study, carried out via a systemic reduction of four residues at both the N- and C-terminals of the peptide **1,** to identify the shortest amino acid sequence needed for the peptide activity (compounds **13**-**17**) (Table 3.2).

3.3.2.1 Interaction with viral hemagglutinin

As shown in Table 3.2, N-terminal truncation strategy led to the most interesting results. Thus, octapeptide **13** was the most effective fragment of this series to prevent HA activity of all tested viruses in a concentration range 0.15 to 0.7 pM.

C-terminal tetrapeptide of **1**, peptide **14**, lost activity on all strains used in the assay, indicating the importance of N-terminal residue of **1** for the hemagglutination inhibition activity, while the tetrapeptide **15** maintained the same inhibition level of **1** on Influenza A/Roma-ISS/02/08 H1N1 strain. Peptide **15** showed a remarkable inhibitory selectivity against this strain (1000 fold) compared to the Parma strains. This selectivity was also observed with the compounds **16** and **17**, derived from the C-terminal deletion on the lead sequence 418-429, which were 15-40 fold more potent against A/Roma strain than against the other strains.

Table 3.2 *Sequence and HI titers of peptides 1, 10-17*.

			HI titer (nM)		
Frag.	Pep.	Sequence	A/Roma-ISS/02/08 H1N1	A/Parma /24/09 H1N1	A/Parma /05/06 H3N2
418-429	**1**	SKHSSLDCVLRP	0.0014	0.0014	0.0007
414-433	**10**	NRKSSKHSSLDCVLRPTEGY	0.3	6	0.0014
414-429	**11**	NRKSSKHSSLDCVLRP	-	12	0.4
418-433	**12**	SKHSSLDCVLRPTEGY	0.7	0.1	0.03
422-429	**13**	SLDCVLRP	0.0007	0.00015	0.0004
426-429	**14**	VLRP	0.7	0.15	1.5
422-425	**15**	SLDC	0.0014	6	1.5
418-425	**16**	SKHSSLDC	0.3	12	12
418-421	**17**	SKHS	0.1	1.5	12

The peptides **13**-**17** are acetylated and amidated at N-terminal and C-terminal, respectively.

3.3.2.2 Neutralization of influenza virus

Next, it has been examined whether, and to what extent, peptides most potent of first series (**4**, **6**, **8**) and fragments **13**-**17** derived from **1** could affect virus replication in Madin-Darby canine kidney cells (MDCK) by neutralization assay.

The influenza A virus strains A/RomaISS/02/08 H1N1 oseltamivir-sensitive virus, A/Parma/24/09 H1N1 oseltamivir-resistant virus, and A/Parma/05/06 H3N2, were used.

Table 3.3 *In vitro antiviral activity of most potent peptides against influenza virus infection.*

Pep.	Sequence	A/Roma-ISS/02/08 H1N1		A/Parma/24/09 H1N1		A/Parma0/5/06 H3N2	
		EC_{50}^{a} (pM)	SI^	EC_{50}^{a} (pM)	SI^	EC_{50}^{a} (pM)	SI^
1	SKHSSLDCVLRP	4 ± 0.37	$>6.25.10^6$	3.1 ± 0.12	$>8.10^6$	5.8 ± 0.7	$>4.4.10^6$
4	KANEGLTWNSLKDK	1 ± 0.15	$>2.5.10^7$	50.000 ± 250	$>5.10^2$	1.000 ± 360	$>2.5.10^4$
6	TNGESTADWAKN	400 ± 0.02	$>6.25.10^4$	50.000 ± 230	$>5.10^2$	10.000 ± 120	$>2.5.10^3$
8	KSETKN	0.5 ± 0.01	$>5.10^7$	500 ± 0.46	$>5.10^4$	400.000 ± 210	$>0.65.10^2$
13	SLDCVLRP	0.3 ± 0.5	$>8.33.10^7$	2.5 ± 0.37	$>1.10^7$	300 ± 0.2	$>8.33.10^4$
14	VLRP	0.45 ± 0.1	$>5.55.10^7$	1 ± 0.05	$>2.5.10^7$	250 ± 0.42	$>1.10^5$
15	SLDC	0.5 ± 0.001	$>5.10^7$	4.6 ± 0.05	$>5.4.10^6$	4.3 ± 0.03	$>5.8.10^7$
16	SKHSSLDC	80 ± 0.19	$>3.125.10^5$	0.1 ± 0.001	$>2.5.10^8$	5.0 ± 0.45	$>5.10^6$
17	SKHS	3 ± 0.61	$>8.33.10^6$	0.048 ± 0.0012	$>5.2.10^8$	5.0 ± 0.02	$>5.10^6$

[a] EC_{50}: the reciprocal substance dilution at which 50% of cells were protected from the virus induced killing; ^SI (selectivity index): the ratio between CC_{50} (the reciprocal substance dilution at which 50% of cells were protected from substance toxicity, corresponding to > 25 μM) and EC_{50}; The mean values of 3 independent experiments with standard errors are shown.

According to the results showed in Table 3.3, peptides **4**, **6**, and **8** were able to prevent infection of all tested viruses in a concentration range from about 0.5 pM to 400 nM. At these concentrations, the peptides of the first series are the most toxic (SI ≈ $10^{-2}/10^{-4}$). The octapeptide **13** (SLDCVLRP), the most active in the prevention of viral hemagglutination (HI titer 0.15-0.7 pM, Table 3.2), conserved a good antiviral activity against the two A/Roma and A/Parma H1N1 strains, with EC_{50} values of 0.3 and 2.5 pM, respectively, but lost activity against H3N2 strain respect to **1** (≈50 fold, EC_{50} = 300 pM)**.**

Tetrapeptide **14**, containing a net positive charge (Arg[428]), showed a similar activity profile to peptide **13,** in particular, **14** was more active against both H1N1 strains compared to reference peptide **1**. Tetrapeptide **15,** with net charge opposite to **14** (Asp[424])**,** was strongly effective against A/Parma/05/06 H3N2 strain at 4.3 pM. Derivatives obtained by C-terminal truncation of **1**, peptides **16** and **17**, presented a different behaviour.

Octapeptide **16** was 30 and 10 fold more potent than **1** and **13**, respectively, to prevent viral infection against A/Parma/24/09 H1N1 strain, while it was 20 and 270 fold less active than these, against A/Roma- ISS/2/08 H1N1 strain. Tetrapeptide **17**, containing two positive residues (Lys^{419}-Hys^{420}) retrieves antiviral activity on this last strain, maintaining high antiviral activity at femto- and pico-molar concentration against both A/Parma H1N1 and H3N2 strains, respectively. These results suggest that tetrapeptides **14**, **15**, and, in particular **17** could be good starting point in the search for new peptidomimetics and small molecules candidates for influenza virus treatment as well as in the search of new peptide formulation with the same aim.

3.3.3 Peptide 14 modifications (Peptides 18-23)

Focused on peptide 14, we evaluated the importance of the net positive charge (Arg^{428}) on the biological activity. Arg at position 3 was replaced with positive charged amino acid, lysine (Lys) and ornithine (Orn), and aminoacid with net charge opposite, glutamic acid (Glu) and aspartic acid (Asp).

We also synthesized peptides **22**-**23**, obtained from N- and C- terminal deletions of peptide **14** (Table 3.4).

3.3.3.1 Interaction with viral hemagglutinin

As shown in Table 3.4, no compound generated through the substitution of Arg at position 3 with positive and negative charged amino acid and N- and C- terminal deletions, was able to inhibit HA in a greater extent of peptide **14**.

The substitution of Arg with positive charged amino acid, Lys and Orn, determines an increase of the antiviral potency on influenza A/Roma-ISS/2/08 A/H1N1 virus subtype and a dramatic loss or decrease of activity against the other two influenza Parma virus subtypes, respectively.

In derivatives **20** and **21**, the absence of positive charge by substitution of Arg3 with aminoacid with net charge opposite, Glu and Asp, induces a dramatic loss of activity against influenza H1N1 virus subtypes, increasing the antiviral potency on Parma H3N2 strain.

Peptides **22** and **23**, obtained by N- and C- terminal deletions, appear not inhibit notably HA activity compared to peptides **14**.

Table 3.4 *Sequence and HI titers of peptides 14, 18-23.*

Pep.	Sequence	HI titer (nM)		
		A/Roma-ISS/02/08 H1N1	A/Parma /24/09 H1N1	A/Parma /05/06 H3N2
14	VLRP	0.7	0.15	1.5
18	VLKP	0.0031	-	8.6
19	VLOP	0.0014	-	12
20	VLEP	-	6	0.1
21	VLDP	-	7.1	0.6
22	VLR	-	3	3000
23	LRP	1.1	3.9	-

All peptides are acetylated and amidated at N-terminal and C-terminal, respectively.

3.3.4 Alanine scanning approach (Peptides 24-31)

Through a truncation library, we identified the tetrapeptides **15** and **17**, which were able to bind HA and inhibit cell infection. In order to generate peptides with improved biological activity, we decided to apply to peptides **15** and **17** an Alanine scanning approach, a classical chemical tecnique to check the relevance of side chains of each aminoacidic residue in the

interaction with the target molecule (peptides **24-31**, Table 3.5). This approach resulted in the generation of a panel of eight peptides, named peptide **24** to **31**. All new derivatives were tested for the assessment of their ability to inhibit viral hemagglutination and cell infection.

3.3.4.1 Interaction with viral hemagglutinin

As shown in Table 3.5, the substitution of Ser1 and Leu2 with an alanine determines a significant increase of inhibitory potency of the corresponding analogues **24** and **25** compared to reference peptide **15**. In derivative **26**, the absence of negative charge by substitution of Asp3 with Ala induces a decrease of activity against all influenza strains.

Peptide **30** loses the inhibitor potency on all influenza strains. It showed that Asp3 and Cys4 are important amino acids for inhibitory activity of all influenza virus subtypes.

The data showed that Ser1, Lys2, and His3 of peptide **17** are key amino acids for the antiviral activity against all influenza strains used in the assay. The substitution of a hydroxyl chain (Ser 4) with a residue more lipophilic (Ala) determines a significant increase of inhibitory potency of the corresponding analogue **31** compared to reference peptide **17**. In derivative **29**, the absence of positive charge by substitution of Lys2 with Ala induces a dramatic loss of activity against influenza A/Roma-ISS/2/08 A/H1N1 virus subtype, increasing the antiviral potency on the other two influenza Parma virus subtypes. Peptide **30** increases the inhibitor potency on Parma H1N1 strain, showing that His3 is important for inhibitory activity of influenza A/H3N2 virus subtype.

Table 3.5 *Sequence and HI titers of peptides 15, 17, 24-31.*

Pep.	Sequence	HI titer (nM)		
		A/Roma-ISS/02/08 H1N1	A/Parma /24/09 H1N1	A/Parma /05/06 H3N2
15	**SLDC**	0.0014	6	1.5
24	ALDC	0.0023	0.015	0.8
25	SADC	0.0003	0.25	0.1
26	SLAC	1.7	8.3	4
27	SLDA	-	-	3.7
17	**SKHS**	0.1	1.5	12
28	AKHS	0.6	-	12
29	SAHS	-	0.005	0.023
30	SKAS	0.1	0.0015	-
31	SKHA	0.047	0.0014	0.0003

All peptides are acetylated and amidated at N-terminal and C-terminal, respectively.

3.3.4.2 Neutralization of influenza virus

We have examined the ability of peptides **24**, **25** and **31**derived from **15** and **17** to affect virus replication in Madin-Darby canine kidney cells (MDCK) by neutralization assay.

However, it has been demonstrated that no compound, generated through the Ala scan analysis, was able to inhibit virus replication in a greater extent of peptide **15** and **17**.

Table 3.6 *In vitro antiviral activity of most potent peptides against influenza virus infection.*

Pep.	Sequence	A/Roma-ISS/02/08 H1N1		A/Parma/24/09 H1N1		A/Parma0/5/06 H3N2	
		EC_{50}^{a} (pM)	SI^	EC_{50}^{a} (pM)	SI^	EC_{50}^{a} (pM)	SI^
15	SLDC	0.5 ± 0.001	$>5.10^{7}$	4.6 ± 0.05	$>5.4.10^{6}$	4.3 ± 0.03	$>5.8.10^{7}$
24	ALDC	5.6 ± 0.41	$>4.46.10^{6}$	6.13 ± 0.67	$>4.08.10^{6}$	7.9 ± 1.01	$>3.16.10^{6}$
25	SADC	8.31 ± 1.01	$>3.01.10^{6}$	5.47 ± 0.46	$>4.57.10^{6}$	13.6 ± 2.09	$>1.84.10^{6}$
17	SKHS	3 ± 0.61	$>8.33.10^{6}$	0.048 ± 0.0012	$>5.2.10^{8}$	5.0 ± 0.02	$>5.10^{6}$
31	SKHA	8.8 ± 0.73	$>2.84.10^{6}$	3.99 ± 0.31	$>6.27.10^{6}$	23 ± 1.79	$>1.09.10^{6}$

[a] $EC_{50:}$ the reciprocal substance dilution at which 50% of cells were protected from the virus induced killing; ^SI (selectivity index): the ratio between CC_{50} (the reciprocal substance dilution at which 50% of cells were protected from substance toxicity, corresponding to > 25 μM) and EC_{50}; The mean values of 3 independent experiments with standard errors are shown.

3.3.5 Peptidomimetics

The direct application of proteins and peptides as medicinal entities has some severe limitations, including high degradation by proteolytic enzymes and poor cell membrane permeability. Many of these problems could be avoided by an alternative, modular system with a basis set of "unnatural" monomers. Once an interesting compound has been identified from a library of such nonpeptide polymers, it can serve as a lead for drug discovery, further along the road to a metabolically stable drug. Optimized analogs of a lead compound could then be developed rapidly due to the modular synthetic nature of these compounds.

3.3.6 Design of N-methyl peptides (Peptides 32-41)

N-Methylation of the peptide backbone has been shown to be a valuable tool in structure-activity relationship studies.[3.5]

The replacement of natural amino acids for N-methyl amino acids in biologically active peptides has resulted in analogs with improved pharmacological properties, such as enzymatic stability,[6, 7] receptor selectivity,[8, 10] enhanced potency[11-13] and bioavailability.[14-17] The N-methylation of backbone confers high affinity toward the targets, proteolytic stability, membrane permeability, and conformational rigidity to the peptides. Thus, in peptide chemistry N-methylation is considered as one of the most attractive and suitable modifications of a peptide structure.[18, 19]

Hence, focused on tetrapeptides **15** and **17** we decided to synthesize the corresponding N-methyl peptides (peptides **32**-**41**, Table 3.7). Every amide bond and, subsequently, the whole peptide backbone (compound **41**, Figure 3.2) were replaced sequentially by the corresponding N-methylated unit.
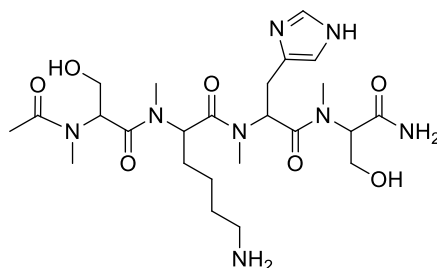
Figure 3.2 *Structure of compound 41.*

With the synthesis of a series of ten N-methylated peptides we investigated if N-methylation of a single peptide bond and all peptide bonds in the lead structures **15** and **17** has similar positive effects on activity.

3.3.6.1 Interaction with viral hemagglutinin

The influence of this N-methylation scan on biological activity was investigated and revealed a significant increase of inhibitory potency of the

corresponding analogues **35** and **40** compared to reference peptides. The other peptides showed lower activities.

Table 3.7 *Sequence and HI titers of peptides 15, 17, 32-41.*

Pep.	Sequence	HI titer (nM)		
		A/Roma-ISS/02/08 H1N1	A/Parma /24/09 H1N1	A/Parma /05/06 H3N2
15	**SLDC**	0.0014	6	1.5
32	(N-Me)SLDC	-	8.7	2.3
33	S(N-Me)LDC	1.56	7.13	0.87
34	SL(N-Me)DC	2.33	-	-
35	SLD(N-Me)C	0.0041	3.32	0.41
36	(N-Me)[SLDC]	3.7	7.91	-
17	**SKHS**	0.1	1.5	12
37	(N-Me)SKHS	0.3	5.7	13.6
38	S(N-Me)KHS	0.2	3.23	2.6
39	SK(N-Me)HS	0.13	6.07	-
40	SKH(N-Me)S	0.07	1.03	6.7
41	(N-Me)[SKHS]	0.67	-	11.17

All peptides are acetylated and amidated at N-terminal and C-terminal, respectively.

3.3.6.2 Neutralization of influenza virus

Next, we have examined the ability of peptides **35** and **40** to affect virus replication in Madin-Darby canine kidney (MDCK) by neutralization assay.

Table 3.8 *In vitro antiviral activity of most potent peptides against influenza virus infection.*

Pep.	Sequence	A/Roma-ISS/02/08 H1N1		A/Parma/24/09 H1N1		A/Parma0/5/06 H3N2	
		EC_{50}^{a} (pM)	SI^	EC_{50}^{a} (pM)	SI^	EC_{50}^{a} (pM)	SI^
15	SLDC	0.5±0.001	$>5.10^{7}$	4.6±0.05	$>5.4.10^{6}$	4.3±0.03	$>5.8.10^{7}$
35	SLD(N-Me)C	7.8±0.51	$>3.21.10^{6}$	11±1.67	$>2.27.10^{6}$	100±0.2	$>2.50.10^{5}$
17	SKHS	3±0.61	$>8.33.10^{6}$	0.048±0.0012	$>5.2.10^{8}$	5.0±0.02	$>5.10^{6}$
40	SKH(N-Me)S	5.31±0.91	$>4.71.10^{6}$	7.47±0.46	$>3.35.10^{6}$	33.6±2.49	$>7.44.10^{5}$

[a] $EC_{50:}$ the reciprocal substance dilution at which 50% of cells were protected from the virus induced killing; ^SI (selectivity index): the ratio between CC_{50} (the reciprocal substance dilution at which 50% of cells were protected from substance toxicity, corresponding to > 25 μM) and EC_{50}; The mean values of 3 independent experiments with standard errors are shown.

However, these peptides have not shown increased antiviral activity compared to peptides **15** and **17**.

3.3.7 Design of peptoids (Compounds 42-51)

Peptoids are peptidomimetic molecules that comprise of repeating poly-N-substituted glycine units (NGS).[20] They are a readily accessible class of synthetic, non-natural peptide mimic of modular design into which a plethora of structural elements can be readily incorporated. In terms of structure, peptoids differ from peptides in that their side-chain functionality is bonded to the nitrogen of the poly-amide backbone, rather than the α-carbon, leading to an achiral, flexible oligomeric backbone devoid of hydrogen bond donors (Figure 3.3). This repeating N-alkyl amide backbone motif affords peptoids with an increased stability towards proteolytic degradation compared to analogous peptides.[21] Compared to α-peptides, NSG's have distinct secondary structures (e.g., helices) characterized by steric and electronic interactions that are stable over a wider range of solvent, ionic and thermal conditions.[22] Further, the NSG backbone is not a substrate for commonly encountered proteases, which leads

to backbone proteolytic stability. In addition, NSG's can be more hydrophobic and they possess superior cellular permeability.[21-28] The schematic comparison of peptides and peptoids, provided in Figure 3.3, shows the similarities in the spacing of the side chains and the carbonyl groups, and the differences in the chirality of the two monomers.
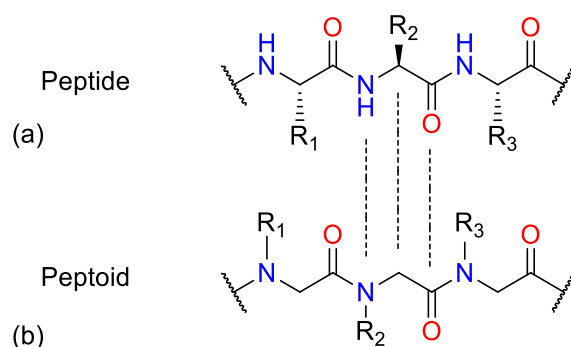
Figure 3.3 *The comparision of (a) peptide and (b) peptoid*

Hence, focused on tetrapeptides **15** and **17** we decided to synthesize the peptoid analogues (compound **51**, Figure 3.4).
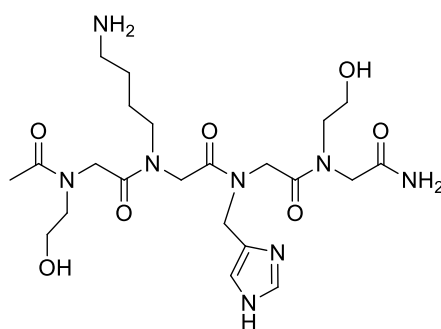
Figure 3.4 *Structure of compound 51.*

3.3.7.1 Interaction with viral hemagglutinin

Peptoids (42-51) were tested to verify if they inhibit hemagglutinin activity. Here, it has been demonstrated that no compound was able to inhibit HA activity in a greater extent of peptides **15** and **17** (compounds **42**-**51**, Table 3.9).

Table 3.9 *Sequence and HI titers of peptides 15, 17, 42-51*.

Pep.	Sequence	HI titer (nM)		
		A/Roma-ISS/02/08 H1N1	A/Parma /24/09 H1N1	A/Parma /05/06 H3N2
15	**SLDC**	0.0014	6	1.5
42	*N*hSerLeuAspCys	1.3	3.7	1.47
43	Ser*N*LeuAspCys	4.6	3.4	9.87
44	SerLeu*N*AspCys	1.3	5.7	1.95
45	SerLeuAsp*N*hCys	0.87	4.5	-
46	*N*hSer*N*Leu*N*Asp*N*hCys	0.0023	2.17	0.36
17	**SKHS**	0.1	1.5	12
47	*N*hSerLysHisSer	1.47	3.3	-
48	Ser*N*LysHisSer	2.16	-	3.7
49	SerLys*N*HisSer	4.1	0.19	-
50	SerLysHis*N*hSer	0.67	3.66	5.7
51	*N*hSer*N*Lys*N*His*N*hSer	0.067	0.13	1.23

All peptides are acetylated and amidated at N-terminal and C-terminal, respectively.

3.3.7.2 Neutralization of influenza virus

Next, we have examined the ability of peptoids **46** and **51** to affect virus replication in Madin-Darby canine kidney cells (MDCK) by neutralization assay.

As shown in Table 3.10, virus replication was inhibited by peptides **46** and **51** at concentrations several logs lower than peptides **15** and **17**.

Table 3.10 *In vitro antiviral activity of most potent peptides against influenza virus infection.*

Pep.	Sequence	A/Roma-ISS/02/08 H1N1		A/Parma/24/09 H1N1		A/Parma0/5/06 H3N2	
		EC_{50}^a (pM)	SI^	EC_{50}^a (pM)	SI^	EC_{50}^a (pM)	SI^
15	SLDC	0.5±0.001	$>5.10^7$	4.6±0.05	$>5.4.10^6$	4.3±0.03	$>5.8.10^7$
46	*N*hSer*N*Leu*N*Asp*N*hCys	6.6±0.93	$>3.79.10^6$	17±1.83	$>1.47.10^6$	10.9±2.01	$>2.29.10^6$
17	SKHS	3±0.61	$>8.33.10^6$	0.048±0.0012	$>5.2.10^8$	5.0±0.02	$>5.10^6$
51	*N*hSer*N*Lys*N*His*N*hSer	40±0.19	$>6.25.10^5$	27±0.59	$>9.26.10^5$	9.99±1.31	$>2.50.10^6$

[a] EC_{50}: the reciprocal substance dilution at which 50% of cells were protected from the virus induced killing; ^SI (selectivity index): the ratio between CC_{50} (the reciprocal substance dilution at which 50% of cells were protected from substance toxicity, corresponding to > 25 μM) and EC_{50}; The mean values of 3 independent experiments with standard errors are shown.

3.4 NMR analysis of peptide 1 and 17.

The solution-state structure (HFA/H_2O) of the oligopeptide SKHSSLDCVLRP (**1**) was obtained by 2D NMR spectroscopy. In details, according to standard procedures,[29] the chemical shift assignments of the ^{1}H resonances (Table S1) have been achieved by using DQF-COSY,[30] TOCSY[31] and NOESY[32] experiments. A set of 117 inter-proton distance restraints were collected from 2D-NOESY NMR experiments (t_{mix} = 400 ms) and used in simulated annealing protocol of the software CYANA 2.1.[33] The NMR structure bundle (Figure 3.5, left) of SKHSSLDCVLRP shows high structural agreement with RMSD of 0.29 Å referenced to the backbone atoms. By means of PROMOTIF software,[34] the quantitative analysis of φ and ψ dihedral angles of the representative structures of SKHSSLDCVLRP was carried out, highlighting a global turn conformation. In particular, **1** contains four β-turns (type IV) formed by residues: 2-5, 4-7, 6-9 and 7-10, (Table S3). It was also observed a γ-turn structure involving the residues Val9-Arg11 (Table S3).
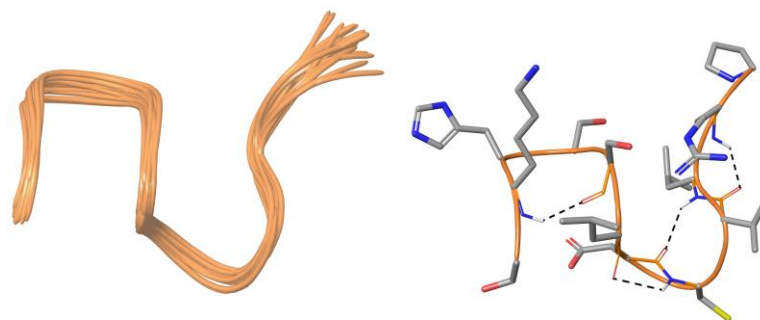
Figure 3.5 *On the left, superposition of backbone atoms of twenty NMR structures of **1** (orange ribbons) generated by using CYANA 2.1. On the right, the average NMR derived structures of **1**. The atoms are depicted in tube and colored by atom types (O, red; N, blue; S, yellow; polar hydrogen, white). The backbone C atoms of **1** are colored as for the ribbons and the side chain C atoms are in grey. The dashed lines indicate intramolecular H-bonds responsible of the global fold.*

The overall turn conformation observed for **1** is in line with spatial arrangement of the loop Ser418-Pro429 of C-terminal lobe of lactoferrin (PDB ID: 3IB0). In particular, we observed that the helix 3_{10} formed by Cys425-Leu427 of protein loop is overlapped with the γ-turn of **1** centered on Val9-Arg11 (Figure 3.6a). Moreover, we observed a very good superimposition between **1** and the loop Ser418-Pro429 in the first four amino acids (SKHS, Figure 3.6b), suggesting this conformation as a structural requirement for the resulting peptide activity as shown by **17**.
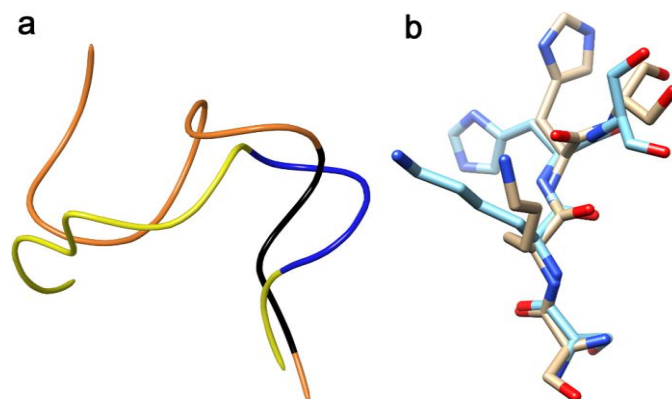
Figure 3.6 *a) Superimposition of loop Ser418-Pro429 (yellow and blue ribbon) of lactoferrin (PDB ID: 3IB0) and **1** (orange and black ribbon). The blue and black portions indicate the helix 3$_{10}$ of Ser418-Pro429 and the γ-turn of **1**, respectively. b) Superimposition of first four amino acids (SKHS) of **1** (cyan) and loop Ser418-Pro429 (tan). The atoms are depicted in tube and colored by atom types (O, red; N, blue). The C atoms of **1** and loop Ser418-Pro429 are colored as for tube.*

Similarly to **1**, we tried to assign the ^{1}H resonances of tetrapeptide **17** (SKHS) in HFA/H$_2$O, but most of resonances resulted overlapped. Thus, we assigned the ^{1}H resonances in DMSO (Table S2).[35, 36] of tetrapeptide **17** (SKHS) We also attempted to determine the solution structure of **17** by collecting interproton distance restraints from 2D-NOESY and 2D-ROESY[37] experiments at different mixing time, but the very low number of inter-residue NOE effects hampered this task. This was due to the expected high flexibility of the tetrapeptide in solution, nevertheless we can assume that the preferred conformation of **17** is similar to the spatial arrangement observed for **1** and the loop Ser418-Pro429 as highlighted by the biological activity of **17**.

3.5 Chemistry

3.5.1 General procedure for synthesis

The synthesis of peptides (**1**, **8**, **13**-**31**) was performed according to the solid phase approach using standard Fmoc methodology in a manual reaction vessel.[38] The first amino acid was linked onto the Rink resin previously deprotected by a 25% piperidine solution in N, N-dimethylformamide (DMF) (1×5min and 1×25min).

The following protected amino acids were then added stepwise. Each coupling reaction was accomplished using HBTU and HOBt as coupling reagents in the presence of DIPEA. The N^{α}-Fmoc protecting groups was removed by treating the protected peptide resin with a 25% solution of piperidine in DMF.

In addition, after each step of deprotection and after each coupling step, Kaiser test was performed to confirm the complete removal of the Fmoc protecting group, respectively, and to verify that complete coupling has occurred on all the free amines on the resin.

The N-terminal Fmoc group was removed as described above and the peptides were acetylated adding a solution of Ac_2O/DCM (1:3) shaking for 30 min. Finally, the peptides were released from the resin with trifluoroacetic acid (TFA)/ triisopropylsilane (iPr_3SiH) / H_2O (90:5:5) for 3 h. The resin was removed by filtration, and the crude peptide was recovered by precipitation with cold anhydrous ethyl ether to give a white powder and then lyophilized (Scheme 3.1).

Scheme 3.1 *Synthesis of peptide 17.*

3.5.2 Microwave peptide synthesis

Microwave- assisted SPPS is a useful and reliable tool for the synthesis of long peptides and "difficult" sequence. Fast and precise heating by microwave irradiation during solid-phase peptide synthesis (SPPS) can reduce reaction times as well as provide better purities and greater yields for the synthesis of difficult peptides.[39] Therefore, we synthesized peptides **4-7**, **9**, **10**-**12** using an Automated Microwave Peptide Synthesizer from Biotage AB (Initiator + Alstra™) (Figure 3.7).

Figure 3.7 *The Biotage Initiator + Alstra™.*

Peptides were synthesized on a Wang-ChemMatrix. The first amino acid was linked on to the resin in the presence of DMAP, using as coupling reagent HBTU, HOAt and DIEA in N-methyl-2-pyrrolidone (NMP).[40] The N^{α}-Fmoc protecting groups were removed by treating the protected peptide resin with a 25% solution of piperidine in DMF (1×3 min, 1×10 min) at room temperature. The following protected amino acids were then added on to the resin stepwise. Coupling reactions were performed using N^{α}-Fmoc amino acids, using as

coupling reagent HBTU, HOAt and DIEA in NMP. All couplings were achieved for 10 min at 75 °C (2x) and 2x45 min at RT for histidine and cysteine couplings to avoid the epimerization. After each coupling step, the Fmoc protecting group was removed as described above. The resin was washed with DMF (4×4.5 ml) after each coupling and deprotection step. Finally, peptides were released as described above.

3.5.3 Synthesis of N-methyl peptides

In SPPS the coupling of N-methyl amino acids generally occurs in low yield and in many cases requires expensive coupling reagents and double coupling. Therefore, we decided to synthesize N-methyl peptides (**32**-**41**) using microwave (MW) irradiation.[41, 42] MW irradiation was provided by an Automated Microwave Peptide Synthesizer from Biotage AB (Initiator + Alstra™) (Figure 3.7). Fmoc-Rink amide resin was used as solid phase support (Scheme 3.2). Initially, the resin was deprotected with 20% piperidine/DMF. The protected amino acids were then coupled using HBTU and HOBt as coupling reagents in the presence of DIPEA and the mixture was irradiated for 20 min with a maximum temperature of 35 °C. In addition, after each step of deprotection and after each coupling step, chloroanyl test was performed. [43] To ensure complete N^{α}-Fmoc protecting groups removal, we followed standard treatments with 20% piperidine in DMF solutions and two extra treatments of 5 min with piperidine : DBU: toluene : DMF (5: 5 : 20 : 70, v/v)

The N-terminal Fmoc group was removed and the peptides were acetylated as described above. Final peptides were cleaved from the resin with the following cleavage cocktails: TFA/DCM (95:5 v/v) for 90 min. Peptides were precipitated by addition of cold diethyl ether, the solution was decanted, and the solid was

triturated with cold diethyl ether, which was decanted again. This process was repeated twice (Scheme 3.2).
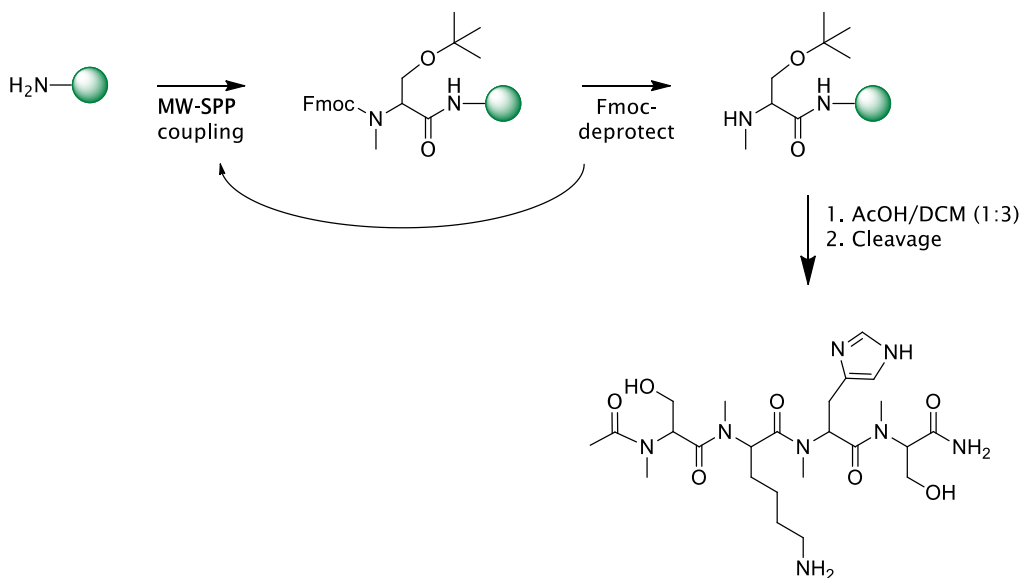
Scheme 3.2 *Synthesis of peptide 41.*

3.5.4 Synthesis of peptoids

In the solid-phase synthesis of peptoid, two different approaches can be used to introduce an N-alkylglycine (peptoid residue) on the growing peptide chain: (i) the N-substituted glycine derivative, suitably protected at the tertiary nitrogen atom, can be separately prepared and directly utilized as building block in the solid phase procedure (monomer method),[44, 45] or (ii) the peptoid residue is built during the peptide chain elongation by a combination of two submonomers, an haloacetic acid and a primary amine (submonomer method).[20]

To speed up the synthesis of peptoid, we optimized a procedure based on the submonomer method, which makes possible a direct assembling of the functionalized peptoid residue starting from commercially available reagents.

For the synthesis of compounds **42**-**51**, the peptoid residue is built during the peptide chain elongation by a combination of two submonomers, an haloacetic acid and a primary amine (submonomer method).

Initially the Rink resin was deprotected by a 25% piperidine solution in N, N-dimethylformamide (DMF) for 30 min.

Bromoacetic acid was then coupled to the NH_2-peptide resin in the presence of N, N'-diisopropylcarbodiimide (DIC), and the halogen was displaced with a large excess of primary amine. Further elongation of the peptide chain was carried out according to the standard protocol, with the addition of Bromo acetic acid and the appropriate amine. The last N-alkylglycine residue was acetylated as described above. Simultaneous deprotection and cleavage of peptoids from the resin carried out.

Typical cycle times for NSG oligomer synthesis are of the order of 150-180 minutes for the completion of one monomeric residue addition at room temperature. Thus, we synthetized peptoids using continuous-flow (CF) technique. Through the application of a CF technique these compounds were synthetized in high yields and with low amino acid and solvent consumption. This approches offer an great number of advantages over conventional batch procedures, for example, the efficient mixing of substrates, faster heat and mass transfer, and shorter reaction times (Figure 3.8).[46-54]

Figure 3.8 *Vapourtec Flow Chemistry*

The synthesis is illustrated in Scheme 3.3:
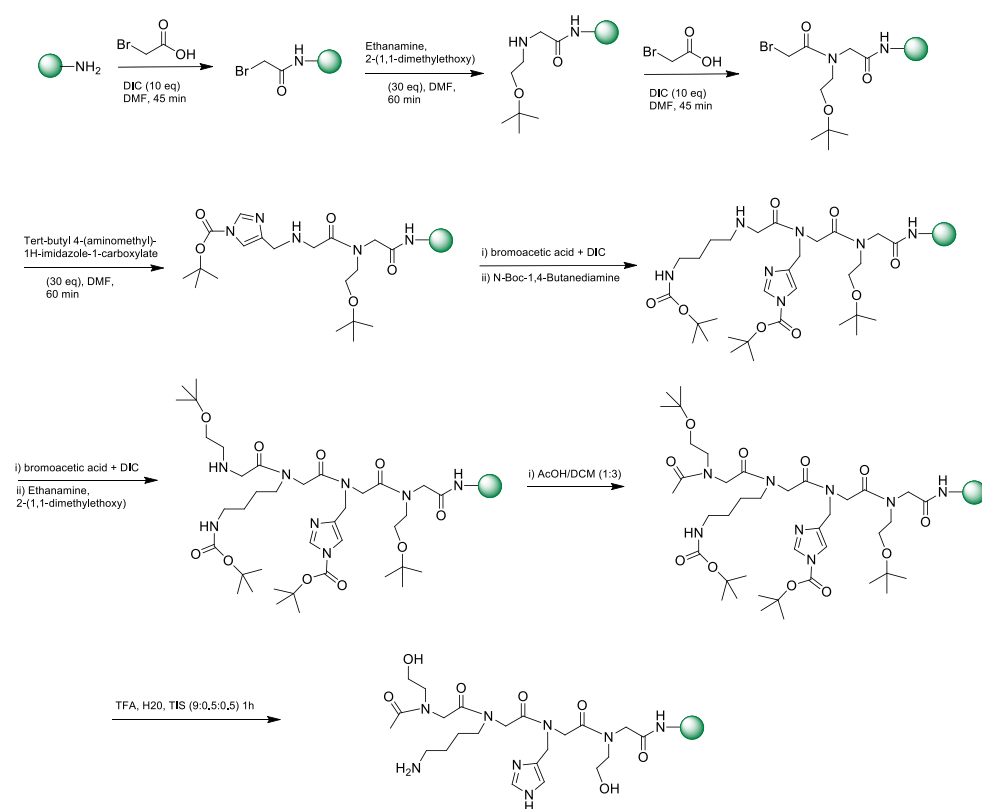
Scheme 3.3 *Synthesis of compound 51.*

The crude compounds were purified by preparative RP-HPLC. Analytical HPLC indicated a purity greater than 98%, and molecular weights were confirmed by ESI-MS.

3.6 Conclusions

The present study describes the identification of three C-lobe bLf-derived tetrapeptides as the minimum fragments expressing the broad anti-influenza activity of bLf. Peptides **14** (VLRP), **15** (SLDC), and **17** (SKHS) were designed from the fragment 418-429 (**1**, SKHSSLDCVLRP), which is involved in the C-lobe bLf-HA interaction. These tetrapeptides retain the inhibitory potency of the fragment 418-429 and inhibit the influenza virus hemagglutination and cell infection in a concentration range of femto- to picomolar. NMR spectroscopy analysis performed on compounds **1** showed a global turn conformation for this peptide and hypothesized the preferred bioactive conformation of our tetrapeptides. Our results strongly encourage the pursuit of this path for the development of a novel class of anti-influenza drugs.

3.7 Experimental section

N^{α}-Fmoc-protected amino acids, Wang resin, Rink amide-resin, 1-Hydroxy-7-azabenzotriazole (HOAt), N-hydroxy-benzotriazole (HOBt), 2-(1H-benzotriazole-1-yl)- 1, 1, 3, 3-tetramethyluronium hexafluoro-phosphate (HBTU), N, N-diisopropylethyl-amine (DIPEA), Piperidine and Trifluoroacetic acid were purchased from Iris Biotech (Germany). Wang-ChemMatrix and Rink-ChemMatrix resins were purchased from Biotage AB (Sweden). Peptide synthesis solvents, reagents, as well as CH_3CN for high performance liquid chromatography (HPLC) were reagent grade and were acquired from

commercial sources and used without further purification unless otherwise noted.

3.7.1 Synthesis of linear derivatives (peptides 1, 8, 13-31)

The synthesis of bLf analogues (**1**, **8**, **13-31**) was performed according to the solid phase approach using standard Fmoc methodology in a manual reaction vessel.[55, 56]

The first amino acid, N^{α}-Fmoc-Xaa-OH (Xaa = Pro, Asn(Trt), Cys(Trt), Ser(tBu), Arg(Pbf), Ala), was linked on to the Rink resin (100–200 mesh, 1% DVB, 0.59 mmol/g) previously deprotected by a 25% piperidine solution in N, N-dimethylformamide (DMF) for 30 min.

The following protected amino acids were then added stepwise: N^{α}-Fmoc-Arg(Pbf)-OH, N^{α}-Fmoc-Leu-OH, N^{α}-Fmoc-Val-OH, N^{α}-Fmoc-Cys(Trt)-OH, N^{α}-Fmoc-Asp(OtBu)-OH, N^{α}-Fmoc-Ser(tBu)-OH, N^{α}-Fmoc-His(N(im)trityl(Trt))-OH, N^{α}-Fmoc-Lys(Boc)-OH, N^{α}-Fmoc-Thr(tBu)-OH, N^{α}-Fmoc-Glu(OtBu)-OH, Fmoc-Orn(Boc)-OH, N^{α}-Fmoc-Ala-OH. Each coupling reaction was accomplished using a 3-fold excess of amino acid with HBTU and HOBt in the presence of DIPEA (6 eq.). The N^{α}-Fmoc protecting groups were removed by treating the protected peptide resin with a 25% solution of piperidine in DMF (1×5 min and 1×25 min). The peptide resin was washed three times with DMF, and the next coupling step was initiated in a stepwise manner. The peptide resin was washed with DCM ($3\times$), DMF ($3\times$), and DCM ($3\times$), and the deprotection protocol was repeated after each coupling step. In addition, after each step of deprotection and after each coupling step, Kaiser test was performed to confirm the complete removal of the Fmoc protecting group, respectively, and to verify that complete coupling has occurred on all the free amines on the resin. The N-terminal Fmoc group was removed as described

above, and the peptides were acetylated adding a solution of Ac_2O/DCM (1:3) shaking for 30 min. Finally, the peptides were released from the resin with TFA/TIS/H_2O (90:5:5) for 3 h. The resin was removed by filtration, and the crude peptide was recovered by precipitation with cold anhydrous ethyl ether to give a white powder and then lyophilized.

3.7.2 Microwave peptide synthesis

Peptides **4-7**, **9-12** were synthesized using an Automated Microwave Peptide Synthesizer from Biotage AB (Initiator + Alstra™). Peptides were synthesized on a Wang-ChemMatrix resin (0.150 g, loading 0.3 mmol/g). The first amino acid was linked on to the resin in the presence of DMAP (2.4 eq.), using as coupling reagent HBTU (4eq, 0.6M), HOAt (4eq, 0.5M) and DIEA (8eq, 2M) in N-methyl-2-pyrrolidone (NMP).[57] The resin was then washed with DMF (4 × 4.5ml). The N^α-Fmoc protecting groups were removed by treating the protected peptide resin with a 25% solution of piperidine in DMF (1 × 3 min, 1 × 10 min) at room temperature. The following protected amino acids were then added on to the resin stepwise.

Coupling reactions were performed using N^α-Fmoc amino acids (4.0 eq., 0.5 M), using as coupling reagent HBTU (4eq, 0.6M), HOAt (4eq, 0.5M) and DIEA (8eq, 2M) in N-methyl-2-pyrrolidone (NMP). All couplings were achieved for 10 min at 75 ºC (2x) and 2x45 min at RT for histidine and cysteine couplings to avoid the epimerization. After each coupling step, the Fmoc protecting group was removed as described above. The resin was washed with DMF (4 × 4.5 ml) after each coupling and deprotection step. Finally, peptides were released as described above.

3.7.3 Synthesis of N-methyl peptides (compound 32-41)

Fmoc-Rink amide resin (100–200 mesh, 1% DVB, 0.75 mmol/g) was placed in a peptide synthesis vessel, swollen in DMF, and deprotected with 5 ml of 20% piperidine/DMF for 4 min. Washings between the first deprotection, coupling, and subsequent deprotection steps were carried out with DMF (5 × 0.5min) and DCM (5 × 0.5 min) using 10 ml of solvent/g of resin each time. Protected amino acid (3 eq.), HBTU (3 eq.) and HOBt (3 eq.) in DMF (1–3 ml/g resin) were sequentially added to the resin and the mixture was irradiated in a Automated Microwave Peptide Synthesizer from Biotage AB (Initiator + Alstra™) for 20 min with a maximum temperature of 35 °C.

The following protected N-methyl amino acids were then added stepwise: Fmoc-N-Me-Lys(Boc)-OH, Fmoc-N-Me-His(Trt)-OH, Fmoc-N-Me-Leu-OH, Fmoc-N-Me-Asp(OtBu)-OH, Fmoc-N-Me-Cys(Trt)-OH, Fmoc-N-Me-Ser(tBu)-OH.

Two treatments with piperidine/DMF (2: 8, v/v) for 10 min, and two extra 5-min treatments with piperidine/DBU/toluene/DMF (5 : 5 : 20 : 70, v/v) were used. In addition, after each step of deprotection and after each coupling step, chloroanyl test was performed to confirm the complete removal of the Fmoc protecting group, respectively, and to verify that complete coupling has occurred on all the free amines on the resin.

The N-terminal Fmoc group was removed and the peptides were acetylated as described above. Final peptides were cleaved from the resin with the following cleavage cocktails: TFA/DCM (95:5 v/v) for 90 min (10 ml/g resin). Peptides were precipitated by addition of cold diethyl ether, the solution was decanted, and the solid was triturated with cold diethyl ether, which was decanted again. This process was repeated twice (Scheme 3.2).

3.7.4 Synthesis of peptoids (compound 42-51)

For on-resin assembling of N^κ-protected N-aminoalkylglycine residue, a 2 M solution of bromoacetic acid in DMF (10 equiv) and DIC (10 equiv) was added to the deprotected Rink resin (100–200 mesh, 1% DVB, 0.59 mmol/g). The acylation reactions and nucleophilic displacement were carried out under optimized reaction conditions: 60 bar, 70 °C, 0.15 mLmin^{-1} flow rate. After washing in DMF, a 1 M solution of the selected amine in DMF was added.

The following protected amine were then added stepwise: Tert-butyl 4-(aminomethyl)-1H-imidazole-1-carboxylate, N-Boc-1,4-butanediamine, 2-(tert-butoxy)ethan-1-amine, Glycine tert-butyl ester hydrochloride, 2-Methyl-2-propanethiol, 2-methylpropan-1-amine.

Then the beads were washed with DMF and prepared for the formation of the next residue. Cleavage of peptides from the resin and removal of the acid labile protecting groups were simultaneously achieved by treatment of the final peptoid resin with a TFA-H$_2$O-triisopropylsilane (TIS) mixture (95:2.5:2.5 by volume) for 90-120 min at room temperature. Peptides were precipitated by addition of cold diethyl ether and dried overnight under vacuum. Crude peptides were obtained in 70-80% yield.

3.7.5 Purification and characterization

All crude peptides were purified by RP-HPLC on a preparative C18-bonded silica column (Phenomenex Kinetex AXIA 100Å, 100 x 21.20mm, 5µm) using a Shimadzu SPD 20A UV/VIS detector, with detection at 210 and 254 nm. The column was perfused at a flow rate of 15 ml/min with solvent A (10%, v/v, water in 0.1% aqueous TFA), and a linear gradient from 10 to 90% of solvent B (80%, v/v, acetonitrile in 0.1% aqueous TFA) over 40 min was adopted for

peptide elution. Analytical purity and retention time (tr) of each peptide were determined using HPLC conditions in the above solvent system (solvents A and B) programmed at a flow rate of 1.500 ml/min using a linear gradient from 10 to 90% B over 10 min, fitted with C-18 column Phenomenex, Aeris XB-C18 column (150 mm x 4.60, 3.6µm). All analogues showed >97% purity when monitored at 215 nm. Homogeneous fractions, as established using analytical HPLC, were pooled and lyophilized. Peptides molecular weights were determined by ESI mass spectrometry and LC-MS in a LC-MS 2010 instrument fitted with Phenomenex, Aeris XB-C18 column (150 mm x 4.60, 3.6µm), eluted with a linear gradient from 10% to 90% B over 15 min, at a flow rate of 1.000 mL/min. ESI-MS analysis in positive ion mode, were made using a Finnigan LCQ Deca ion trap instrument, manufactured by Thermo Finnigan (San Jose, CA, USA), equipped with the Excalibur software for processing the data acquired. The sample was dissolved in a mixture of water and methanol (50/50) and injected directly into the electrospray source, using a syringe pump, which maintains constant flow at 5 ml/min. The temperature of the capillary was set at 220°C.

Peptide analytical data are reported in Table 3.11 and Table 3.12.

Table 3.11 *Analytical data of peptides 1-31.*

Pep.	Sequence	HPLC k'[a]	ESI-MS
1	SKHSSLDCVLRP	9.73	1339.69
4	KANEGLTWNSLKDK	9.56	1602.84
5	TGSCAFDEFFSQSCAPGADPKSR	12.09	2407.01
6	TNGESTADWAKN	6.19	1292.55
7	GKNGKNCPDKFC	6.78	1309.58
8	KSETKN	2.61	705.35
9	NDNTECLAKLGGRPTYEE	9.78	2008.90
10	NRKSSKHSSLDCVLRPTEGY	11.69	2276.12
11	NRKSSKHSSLDCVLRP	11.13	1825.94
12	SKHSSLDCVLRPTEGY	10.95	1790.85
13	SLDCVLRP	4.48	942.48
14	VLRP	3.67	524.33
15	SLDC	3.13	477.17
16	SKHSSLDC	4.63	916.39
17	SKHS	2.33	498.24
18	VLKP	3.17	496.32
19	VLOP	3.06	482.36
20	VLEP	3.56	497.27
21	VLDP	3.51	483.25
22	VLR	3.01	427.28
23	LRP	3.06	425.26
24	ALDC	3.27	461.18
25	SADC	3.78	435.13
26	SLAC	2.46	433.18
27	SLDA	2.95	445.20
28	AKHS	2.68	482.24
29	SAHS	3.16	441.18
30	SKAS	3.46	432.22
31	SKHA	3.01	482.24

[a] k'=[(peptide retention time-solvent retention time)/solvent retention time].

Table 3.12 *Analytical data of peptides **32**-**51***.

Pep.	Sequence	HPLC k'a	ESI-MS
32	(N-Me)SLDC	2.71	491,56
33	S(N-Me)LDC	2.81	491,56
34	SL(N-Me)DC	2.73	491,56
35	SLD(N-Me)C	2.79	491,56
36	(N-Me)[SLDC]	3.01	533,64
37	(N-Me)SKHS	3.13	512,56
38	S(N-Me)KHS	3.16	512,56
39	SK(N-Me)HS	3.16	512,56
40	SKH(N-Me)S	3.08	512,56
41	(N-Me)[SKHS]	3.41	554,64
42	*N*hSerLeuAspCys	4.07	505,59
43	Ser*N*LeuAspCys	4.01	505,59
44	SerLeu*N*AspCys	4.17	505,59
45	SerLeuAsp*N*hCys	4.27	505,59
46	*N*hSer*N*Leu*N*Asp*N*hCys	5.23	505,59
47	*N*hSerLysHisSer	5.13	526,59
48	Ser*N*LysHisSer	5.16	526,59
49	SerLys*N*HisSer	5.24	526,59
50	SerLysHis*N*hSer	5.18	526,59
51	*N*hSer*N*Lys*N*His*N*hSer	5.67	526,59

[a] k'=[(peptide retention time-solvent retention time)/solvent retention time].
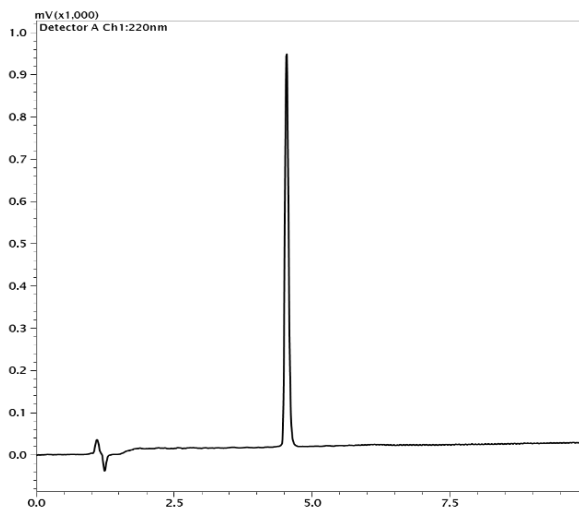
Figure 3.9 *HPLC profile of pure peptide 1.*

3.7.6 Biological assay

3.7.6.1 Virus strains

The following influenza A virus strains were used: A/RomaISS/02/08 H1N1 (Brisbane-like) oseltamivir-sensitive virus, A/Parma/24/09 H1N1 (Brisbane-like) oseltamivir-resistant virus, and A/Parma/05/06 H3N2 (Wisconsin-like). Virus titers were determined by a hemagglutinin titration and/or plaque assay according to the standard procedures.[58, 59]

3.7.6.2 Cells

Madin-Darby canine kidney (MDCK, ATCC, CRL-2936) cells were grown at 37°C in minimal essential medium (MEM, Invitrogen, Paisley, UK) containing 1.2 g/l $NaHCO_3$, and supplemented with 10% inactivated fetal calf serum (FCS, Invitrogen, Paisley, UK), 2 mM glutamine, nonessential amino acids, penicillin (100 IU/ml), and streptomycin (100 μg/ml).

3.7.6.3 Cytotoxicity assay

This procedure was performed as reported elsewhere.[60] Briefly, two-fold serial dilutions of each protein in culture medium were incubated at 37°C with confluent MDCK cells grown in 96-well tissue culture microplates (Nalge Nunc Europe Ltd, Neerijse, Belgium). After 24 hours, cell morphology, viability, and proliferation were evaluated. Protein dilutions that did not affect any of these parameters were considered as non cytotoxic concentrations and utilized for antiviral assays.

3.7.6.4 Hemagglutination inhibition assay (HI)

Virus in PBS was incubated for 1 hour at 4uC with serial dilutions of bLf or peptidic fragments in PBS. An equal volume of 0.5% turkey erythrocytes was

then added and allowed to agglutinate. Titers were expressed as the reciprocal of the protein dilutions giving 50% hemagglutination of erythrocytes by four virus-agglutinating units.

3.7.6.5 Neutralization assay

Neutralization was carried out by incubating serial twofold peptide fragment dilutions, starting from 12.5 µM, in culture medium with equal volumes of virus suspension containing 10^6 p.f.u. for 1 hour at 4 °C. In negative controls, culture medium was used instead of peptide fragments in the same volume. MDCK cells, grown in 96-well tissue culture microplates (Nalge Nunc Europe Ltd, Neerijse, Belgium), were infected with 100 µl/well (10 p.f.u./cell; in quadruplicate) of the virus-peptide mixtures. After adsorption, cells were rinsed thoroughly and incubated at 37°C for 24 hours. The viral cytopathic effect (c.p.e.) was measured by neutral red staining.[61]

3.7.7 NMR experiments and structure calculation

The NMR sample of **1** was obtained dissolving 1 mg of the oligopeptide in 50% of hexafluoroacetone and 50% of H_2O (10 mM of KH_2PO_4) and placed in a 3 mm NMR tube (200 µl). The compound **17** (3.4 mg) was dissolved in 200 µl of [D6] DMSO.

All NMR experiments were performed on a Bruker DRX 600 spectrometer equipped with a cryoprobe at $T = 300$ K. All spectra were acquired in the phase-sensitive mode, and the TPPI method was used for quadrature detection in the ω_1 dimension.[62] The residual water signal was suppressed by excitation sculpting with gradients. Data block sizes of 4096 in t_2 and 512 equidistant t_1 values were used. Before Fourier transformation, the time domain data matrices were multiplied by shifted sine bell QSINE (SSB = 2) functions in both

dimensions. For **1**, the DQF-COSY, 2D-TOCSY and 2D-NOESY experiments were executed with a number of 48 scans/t_1 and a t_{1max} value of 51.2 ms. For **17**, the DQF-COSY, 2D-TOCSY and 2D-NOESY experiments were executed with 16 scans/t_1, 24 scans/t_1 and 64 scans/t_1, respectively, with a t_{1max} value of 64.0 ms. A mixing time of 80 ms was used for the 2D-TOCSY experiments. 2D-NOESY and 2D-ROESY experiments were run with mixing times in the range of 100−550 ms. SPARKY software was used for qualitative and quantitative analyses of 2D spectra.[63] The obtained peak volumes were converted into upper distance bounds with the CALIBA routine from the CYANA software package. The pseudoatom corrections were applied for non-stereospecifically assigned protons of methylene and methyl groups. The experimentally derived constraints were used to generate an ensemble of 200 structures with the standard CYANA protocol of simulated annealing in the torsion angle space (using 50,000 steps). The best 20 structures that had low target function values and small residual violations were selected. All the 3D models were depicted using the Chimera 1.10.1[64] and Maestro 9.6.[65]

3.8 Supporting information

Table S1. *^{1}H chemical shifts (ppm) of peptide **1** in HFA/H$_2$O (600 MHz, 300 K).*

Residue	NH	αH	βH	γH	δH	εH	Others
Ser1	7.83	4.12	3.63	-	-	-	-
Lys2	7.45	3.96	1.47	1.12	1.34	2.65	-
			1.43	1.07			
His3	7.87	4.37	2.95	-	6.89 (2H)	-	-
			2.84		8.08 (4H)	-	-
Ser4	7.80	4.22	3.66	-	-	-	-
			3.54	-	-	-	-
Ser5	7.89	4.12	3.61				
Leu6	7.35	4.06	1.29	1.22	0.61	-	-
					0.51	-	-
Asp7	7.59	4.14	2.43	-	-	-	-
Cys8	7.40	4.06	2.69	-	-	-	-
			2.65				
Val9	7.25	3.76	1.81	0.61	-	-	-
Leu10	7.31	3.99	1.30	1.22	0.53	-	-
					0.51		
Arg11	7.21	4.33	1.53	1.54	2.85		6.609 (NHE)
			1.44		2.77		7.526 (NHZ)
Pro12	-	4.04	1.93	1.61	3.39	-	-
			1.71		3.25		

Table S2. *^{1}H chemical shifts (ppm) of peptide **17** in [D$_6$] DMSO (600 MHz, 300 K).*

Residue	NH	αH	βH	γH	δH	εH	Others
Acetyl	-	-	-	-	-	-	1.87
Ser1	8.12	4.33	3.62	-	-	-	-
			3.57				
Lys2	8.34	4.17	1.65	1.27	1.51	2.73	-
			1.51				
His3	8.06	4.41	2.96	-	6.82 (2H)	7.51 (4H)	-
			2.85				
Ser4	7.86	4.14	3.63	-	-	-	-

Table S3. *Mean values of φ, ψ and χ1 angles and αC distances relative to the most representative conformers of peptide **1**.*

Peptide	Sequence	i+1			i+2			αC distance	
		φ	ψ	χ1	φ	ψ	χ1	i to i+2	i to i+3
	Lys2- Ser5	-52.9	-29.7	-83.7	-138.1	-42.8	-140.3	-	4.8
	Ser4-Asp7	-76.3	166.1	-124.7	69.9	8.5	-67.0	-	6.2
1	Leu6-Val9	-108.6	75.2	-95.6	64.6	27.2	-120.6	-	5.7
	Asp7-Leu10	64.6	27.2	-120.6	71.1	42.9	-164.2	-	5.3
	Val9-Arg11	-76.1	91.0	-147.5	-	-	-	5.9	-
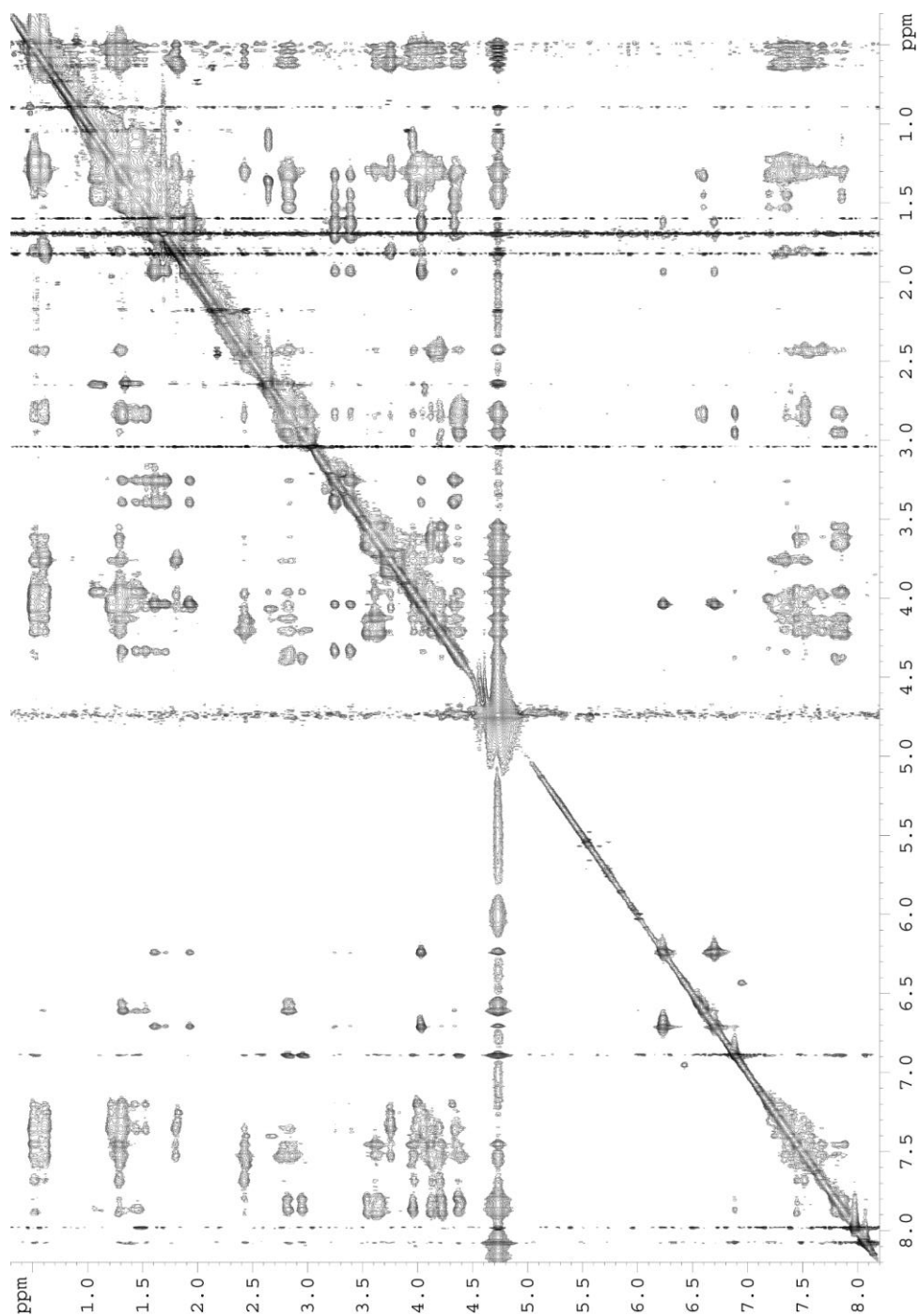
Figure S1. 2D-NOESY spectrum of peptide **1** HFA/H$_2$Osolution (600 MHz, 300 K, t_{mix} = 400 ms).

10
S K H S S L D C V L R P

$d_{NN}(i,i+1)$

$d_{\alpha N}(i,i+1)$

$d_{\beta N}(i,i+1)$

$d_{NN}(i,i+2)$

$d_{\alpha N}(i,i+2)$

$d_{\alpha N}(i,i+3)$

$d_{\alpha \beta}(i,i+3)$

$d_{\alpha N}(i,i+4)$
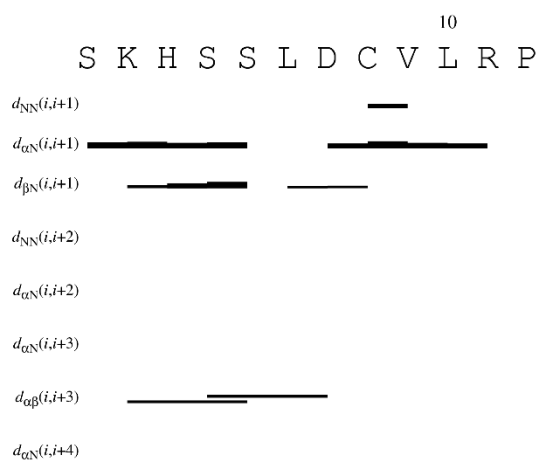
Figure S2. NOE connectivities from 2D-NOESY spectra of peptide **1** in HFA/H$_2$O (600 MHz, 300 K, t_{mix} = 400 ms).
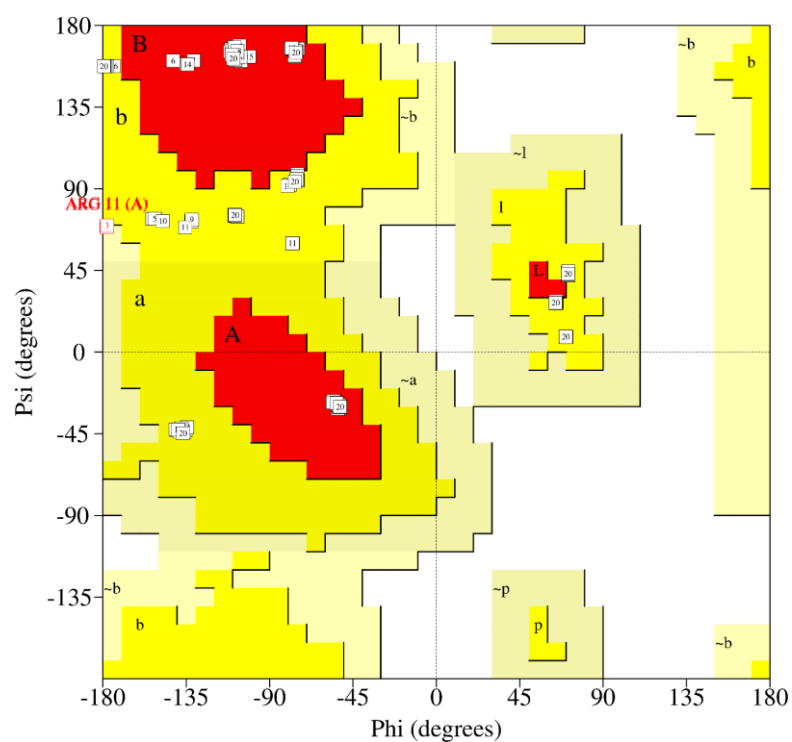
Figure S3. Ramachandran plot of NMR derived bundle of peptide **1**, calculated by PROCHECK[1] software.
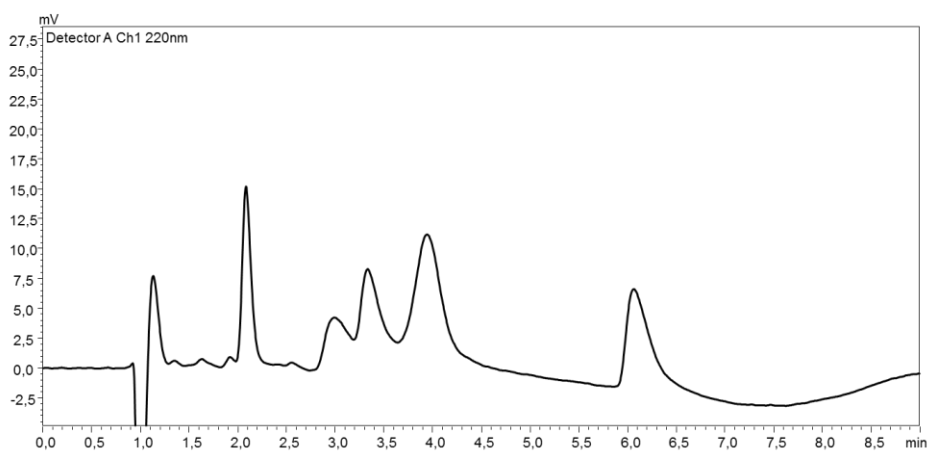
Figure S4. *HPLC profile of crude peptide 32 synthesized at room temperature.*
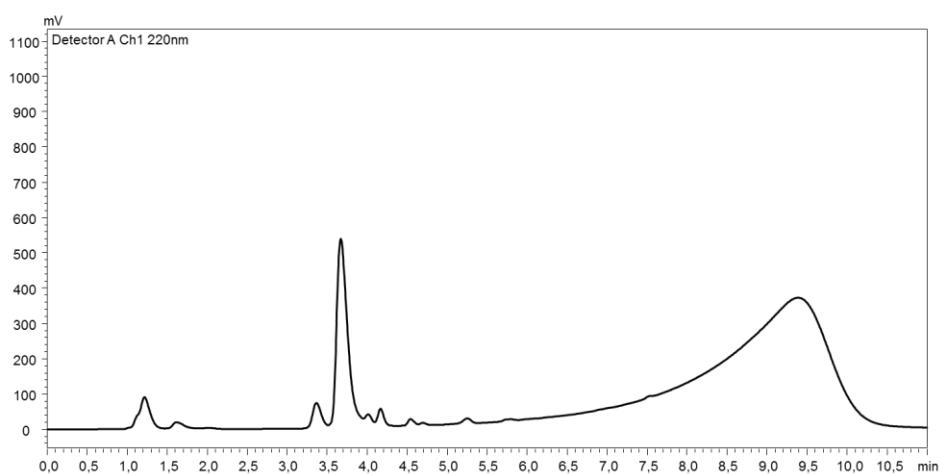
Figure S5. *HPLC profile of crude peptide 32 synthesized using microwave.*
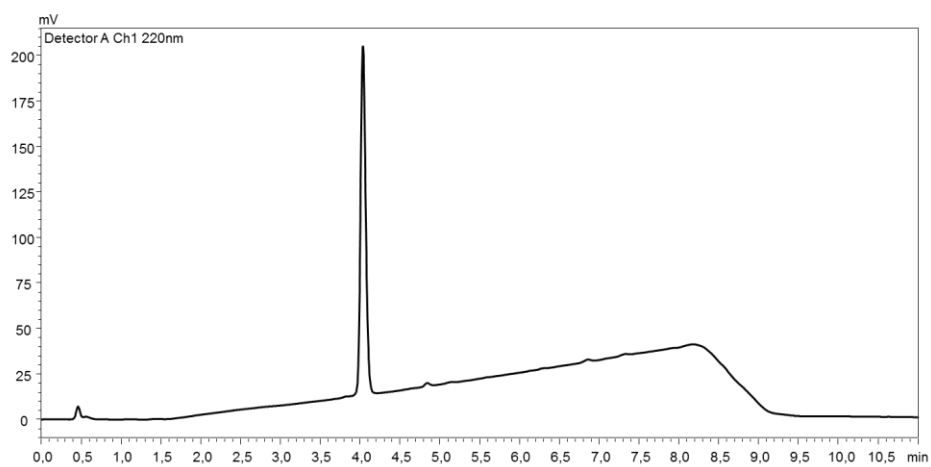
Figure S6. *HPLC profile of pure peptide 32.*

References

[1]   Ammendolia, M. G.; Agamennone, M.; Pietrantoni, A.; Lannutti, F.; Siciliano, R. A.; De Giulio, B.; Amici, C.; Superti, F. Bovine lactoferrin-derived peptides as novel broad-spectrum inhibitors of influenza virus. *Pathog. Glob. Health*. **2012**, 106, 12-19.

[2]   Superti, F. E. D.; Agamennone, M.; Ammendolia, M. G.; Pietrantoni, A.; Lannutti, F. Lactoferrin derived peptides for use as broad-spectrum inhibitors of Influenza virus infection. WO2013072946, **2014**; Istituto Superiore Di Sanità, Università Degli Studi "G. D'annunzio" (IT).

[3]   Manavalan, P.; Momany, F. A. Conformational Energy Studies on N-Methylated Analogues of Thyrotropin Releasing Hormone, Enkephalin and Luteinizing Hormone Releasing Hormone. *Biochemistry*. **1980**, 19, 1943-1973.
[4]   Tonelli, A. E. The Effects of Isolated N-Methylated Residues on the Conformational Characteristics of Polypeptides. *Biopolymers*. **1976**, 15, 1615-1622.

[5]   Ron, D.; Gilon, C.; Hanani, M.; Vromen, A.; Selinger, Z.; Chorev, M. N-Methylated Analogues of Ac[Nle28,31]CCK(26-33). *J. Med. Chem*. **1992**, 35, 2806-2811.

[6]   Haviv, F.; Fitzpatrick, T. D.; Swenson, R.E.; Nichols, C. J.; Mort, N. A.; Bush, E. N.; Diaz, G.; Bammert, G.; Nguyen, A.; Rhutasel, N. S.; Nellans, H. N.; Hoffman, D. J.; Johnson, E. S.; Greer, J. Effect of N-methyl substitution of the peptidebonds in luteinizing hormone-releasing hormone agonists. *J. Med. Chem*. **1993**, 36, 363–369.

[7]   Cody, W. L.; He, J. X.; Reily, M. D.; Haleen, S. J.; Walker, D. M.; Reyner, E. L.; Stewart, B. H.; Doherty, A. M. Design of a potent combined pseudopeptide endothelin-A/endothelin-B receptor antagonist, Ac-DBhg(16)-Leu-Asp-Ile-[NMe]Ile- Trp(21) (PD 156252): examination of itspharmacokinetic and spectralproperties. *J. Med. Chem*. **1997**, 40, 2228–2240.

[8]   Bach, A. C.; Espina, J. R.; Jackson, S. A.; Stouten, P. F. W.; Duke, J. L.; Mousa, S. A.; De Grado,W. F. Type II to type I beta-turn swap changes specificity for integrins. *J. Am. Chem. Soc*. **1996**, 118, 293–294.

[9]   Pierson, M. E.; Comstock, J. M.; Simmons, R. D.; Kaiser, F.; Julien, R.; Zongrone, J.; Rosamond, J. D. Synthesis and biological evaluation of potent,

selective, hexapeptide CCK-A agonist anorectic agents. *J. Med. Chem.* **1997**, 40, 4302–4307.

[10]   Rajeswaran, W. G.; Hocart, S. J.; Murphy, W. A.; Taylor, J. E.; Coy, D. H. Highly potent and subtype selective ligands derived by N-methyl scan of a somatostatin antagonist. *J. Med. Chem.* **2001**, 44, 1305–1311.

[11]   Laufer, R.; Wormser, U.; Friedman, Z. Y.; Gilon, C.; Chorev, M.; Selinger, Z. Neurokinin-B is a preferred agonist for a neuronal substance- P receptor and its action is antagonized by enkephalin. *Proc. Natl. Acad. Sci. USA.* **1985**, 82, 7444–7448.

[12]   Samanen, J.; Ali, F.; Romoff, T.; Calvo, R.; Sorenson, E.; Vasko, J.; Storer, B.; Berry, D.; Bennett, D.; Strohsacker, M.; Powers, D.; Stadel, J.; Nichols, A. Development of a small RGD peptide fibrinogen receptor antagonist with potent antiaggregatory activity in vitro. *J. Med. Chem.* **1991**, 34, 3114–3125.

[13]   Dechantsreiter, M. A.; Planker, E.; Mathä, B.; Lohof, E.; Hölzemann, G.; Jonczyk, A.; Goodman, S. L.; Kessler, H. N-methylated cyclic RGD peptides as highly active and selective $\alpha_v\beta_3$ integrin antagonists. *J. Med. Chem.* **1999**, 42, 3033–3040.

[14]   Barker, P. L.; Bullens, S.; Bunting, S.; Burdick, D. J.; Chan, K. S.; Deisher, T.; Eigenbrot, C.; Gadek, T. R.; Gantzos, R.; Lipari, M. T.; Muir, C. D.; Napier, M. A.; Pitti, R. M.; Padua, A.; Quan, C.; Stanley, M.; Struble, M.; Tom, J. Y. K.; Burnier, J. P. Cyclic RGD peptide analogs as antiplatelet antithrombotics. *J. Med. Chem.* **1992**, 35, 2040–2048.

[15]   Wipf, P. Synthetic studies of biologically active marine cyclopeptides. *Chem. Rev.* **1995**, 95, 2115–2134.

[16]   Romero, F.; Espliego, F.; Pérez Baz, J.; García de Quesada, T.; Gravalos, D.; De la Calle, F.; Fernández-Puentes, J. L. Thiocoraline, a new depsipeptide with antitumor activity produced by a marine micromonospora. I. Taxonomy, fermentation, isolation, and biological activities. *J. Antibiot.* **1997**, 50, 734–737.

[17]   Soto, P.; Griffin, M. A.; Shea, J. E. New insights into the mechanism of alzheimer amyloid-β fibrillogenesis inhibition by N-methylated peptides. *Biophys. J.* **2007**, 93, 3015–3025.

[18]   Conradi, R. A.; Hilgers, A. R.; Ho, N. F. H.; Burton, P. S. The influence of peptide structure on transport across caco-2 cells. II. Peptide-bond modification which results in improved permeability. *Pharm. Res*. **1992**, 9, 435–439.

[19]   Sagan, S.; Karoyan, P.; Lequin, O.; Chassaing, G.; Lavielle, S. N- and Cα-methylation in biologically active peptides: synthesis, structural and functional aspects. *Curr. Med. Chem*. **2004**, 11, 2799–2822.

[20]   Zuckermann, R. N.; Kerr, J. M.; Kent, S. B. H.; Moos, W. H. Efficient method for the preparation of peptoids [oligo(N-substituted glycines)] by submonomer solid-phase synthesis. *J. Am. Chem. Soc.* **1992**, 114, 10646-10647.

[21]   Miller, S. M.; Simon, R. J.; Ng, S.; Zuckermann, R. N.; Kerr J. M.; Moos, W. H. Comparison of the proteolytic susceptibilities of homologous L-amino acid, D-amino acid, and N-substituted glycine peptide and peptoid oligomers. *Drug Dev. Res*. **1995**, 35, 20–32.

[22]   Sanborn, T. J.; Wu, C. W.; Zuckermann, R. N.; Barron, A. E. Extreme stability of helices formed by water-soluble poly-N-substituted glycines (polypeptoids) with α-chiral side chains. *Biopolymers.* **2002**, 63, 12-20.

[23]   Figliozzi, G. M.; Goldsmith, R.; Ng, S. C.; Banville, S. C.; Zuckermann, R. N. Synthesis of Nsubstituted glycine peptoid libraries. *Methods Enzymol*. **1996**, 267, 437-447.

[24]   Patch, J. A.; Kirshenbaum, K.; Seurynck, S. L.; Zuckermann, R. N.; Barron, A. E. Versatile Oligo(N-Subsitituted) Glycines: The Many Roles of Peptoids in Drug Discovery. In Pseudopeptides in Drug Discovery; Nielsen, P.E., Ed.; Wiley-VCH Verlag, GmbH & Co. KgaA: Weinheim, Germany. **2004**, 1-31.

[25]   Richter, L. S.; Spellmeyer, D. C.; Martin, E. J.; Figliozzi, G. M.; Zuckermann, R. N. Automated Synthesis of Nonnatural Oligomer Libraries: The Peptoid Concept. In Combinatorial Peptide and Nonpeptide Libraries; Jung, G., Ed.; VCH: Weinheim, Germany. **1996**, 387-404.

[26]   Zuckermann R. N.; Kodadek T. Peptoids as potential therapeutics. *Curr. Opin. Mol. Therap*. **2009**, 11, 299-307.

[27]   Miller, S. M.; Simon, R. J.; Ng, S.; Zuckermann, R. N.; Kerr, J. M.; Moos, W. H. Proteolytic studies of homologous peptide and N-substituted glycine peptoid oligomers. *Bioorg. Med. Chem. Lett*. **1994**, 4, 2657-2662.

[28]   Lim, H. S.; Muralidhar Reddy, M.; Xiao, X.; Wilson, J.; Wilson, R.; Connell, S.; Kodadek, T. Rapid identification of improved protein ligands using peptoid microarrays. *Bioorg. Med. Chem. Lett*. **2009**, 19, 3866-3869.

[29]   Wüthrich, K. NMR of Proteins and Nucleic Acids. John Wiley & Sons: New York. **1986**.

[30]   Piantini, U.; Sorensen, O. W.; Ernst, R. R. Multiple quantum filters for elucidating NMR coupling networks. *J. Am. Chem. Soc*. **1982**, 104, 6800−6801.

[31]   Bax, A. and Davis, D. G. MLEV-17-based two-dimensional homonuclear magnetization transfer spectroscopy. *J. Magn. Reson*. **1985**, 65, 355-360.

[32]   Macura, S. and Ernst, R. R. Elucidation of cross relaxation in liquids by two-dimensional N.M.R. spectroscopy. *Mol. Phys*. **1980**, 41, 95–117.

[33]   Güntert, P.; Mumenthaler, C.; Wüthrich, K. Torsion angle dynamics for NMR structure calculation with the new program D1. *J. Mol. Biol*. **1997**, 273, 283–298.

[34]   Hutchinson, E. G. and Thornton, J. M. PROMOTIF-a program to identify and analyze structural motifs in proteins. *Protein Sci*. **1996**, 5, 212−220.

[35]   Di Micco, S.; Terracciano, S.; Bruno, I.; Rodriquez, M.; Riccio, R.; Taddei, M.; Bifulco, G. Molecular modeling studies toward the structural optimization of new cyclopeptide-based HDAC inhibitors modeled on the natural product FR235222. *Bioorganic & Medicinal Chemistry*. **2008**, 16, 8635–8642.

[36]   Maulucci, N.; Chini, M. G.; Di Micco, S.; Izzo, I.; Cafaro, E.; Russo, A.; Gallinari, P.; Paolini, C.; Nardi, M. C.; Casapullo, A.; Riccio, R.; Bifulco, G.; De Riccardis, F. Molecular Insights into Azumamide E Histone Deacetylases Inhibitory Activity. *J. Am. Chem. Soc*. **2007**, 129, 3007-3012.

[37]   Bax, A. and Davis, D. G. Practical aspects of two-dimensional transverse NOE spectroscopy. *J. Magn. Reson*. **1985**, 63, 207−213.

[38]   Atherton, E. and Sheppard, R. C. Solid-Phase Peptide Synthesis: A Practical Approach. *IRL Press: Oxford, U.K.* **1989**.

[39]   Malik, L.; Tofteng, A. P.; Pedersen, S. L.; Sorensen, K. K.; Jensen, K. J. Automated "X-Y" robot for peptide synthesis with microwave heating: application to difficult peptide sequences and protein domains. *J Pept Sci.* **2010**, 16, 506-512.

[40]   Wang, S. S.; Tam, J. P.; Wang, B. S.; Merrifield, R. B. Enhancement of Peptide Coupling Reations by 4-Dimethylaminopyridine. *Int J Pept Protein Res*. **1981**, 18, 459-467.

[41]   Zhang, H. B.; Chi, Y. S.; Huang, W. L.; Ni, S. J. Total synthesis of human urotension by microwave-assisted solid phase method. *Chin. Chem. Lett.* **2007**, 18, 902–904.

[42]   Wisén, S.; Androsavich, J.; Evans, C. G.; Chang, L.; Gestwicki, J. E. Chemical modulators of heat shock protein 70 (Hsp70) by sequential, microwave-accelerated reactions on solid phase. *Bioorg. Med. Chem. Lett.* **2008**, 18, 60–65.

[43]   Christensen, T. Qualitative test for monitoring coupling completeness in solid phase peptide synthesis using chloranil. *Acta Chem. Scand. B*. **1979**, 33, 763–766.

[44]   Gobbo, M.; Benincasa, M.; Bertoloni, G.; Biondi, B.; Dosselli, R.; Papini,E.; Reddi, E.; Rocchi, R.; Tavano, R.; Gennaro, R. Substitution of the Arginine/Leucine Residues in Apidaecin Ib with Peptoid Residues: Effect on Antimicrobial Activity, Cellular Uptake, and Proteolytic Degradation. *J Med Chem.* **2009**, 52, 5197-5206.

[45]   Simon, R. J.; Kania, R. S.; Zuckermann, R. N.; Huebner, V. D.; Jewell, D. A.; Banville, S.; Ng, S.; Wang, L.; Rosenberg, S.; Marlowe, C. K.; Spellmeyer, D. C.; Tan, R.; Frankel, A. D.; Santi, D. V.; Cohen, F. E.; Bartlett, P. A. Peptoids: amodular approach to drug discovery. *Proc Natl Acad Sci U.S.A.* **1992**, 89, 9367-9371.

[46]   Hartman, R. L.; McMullen, J. P.; Jensen, K. F. Deciding whether to go with the flow: evaluating the merits of flow reactors for synthesis. *Angew Chem Int Ed Engl*. **2011**, 50, 7502-7519.

[47]   Jhnisch, K.; Hessel, V.; Lowe, H.; Baerns, M. Chemistry in microstructured reactors. *Angew. Chem. Int. Ed. Engl*. **2004**, 43, 406 –446.

[48]   Mason, B. P.; Price, K. E.; Steinbacher, J. L.; Bogdan, A. R.; McQuade, D. T. Greener approaches to organic synthesis using microreactor technology. *Chem Rev*. **2007**, 107, 2300-2318.

[49]   Noël, T. and Buchwald, S. L. Cross-coupling in flow. *Chem. Soc. Rev*. **2011**, 40, 5010 –5029.

[50]   Watts, P. and Haswell, S. J. The application of micro reactors for organic synthesis. *Chem. Soc. Rev*. **2005**, 34, 235 –246.

[51]   Flçgel, O., Codee, J. D. C.; Seebach, D.; Seeberger, P. H. *Angew. Chem.* **2006**, 118, 7157–7160; *Angew. Chem. Int. Ed*. **2006**, 45, 7000–7003.

[52]   ötvös, S. B.; Mándity, I. M.; Fülöp, F. Asymmetric aldol reaction in a continuous-flow reactor catalyzed by a highly reusable heterogeneous peptide. *J. Catal*. **2012**, 295, 179–185.

[53]   Mandity, I. M.; Martinek, T. A.; Ferenc, D.; Ferenc, F. *Tetrahedron Lett*. **2009**, 50, 4372 – 4374.

[54]   Ahmed-Omer, B.; Brandt, J. C.; Wirth, T. Advanced organic synthesis using microreactor technology. *Org. Biomol. Chem*. **2007**, 5, 733–740.

[55]   Atherton, E. and Sheppard, R. C. Solid-Phase Peptide Synthesis: A Practical Approach. IRL Press: Oxford, U.K. **1989**.

[56]   Stewart, J. M. and Young, J. D. In Solid Phase Peptide Synthesis. Pierce Chemical: Rockford, IL. **1984**.

[57]   Wang, S. S.; Tam, J. P.; Wang, B. S.; Merrifield, R. B. Enhancement of Peptide Coupling Reations by 4-Dimethylaminopyridine. *Int J Pept Protein Res*. **1981**, 18, 459-467.

[58]   Gaush, C. R. and Smith, T. F. Replication and plaque assay of influenza virus in an established line of canine kidney cells. *Appl Microbiol*. **1968**, 16, 588–594.

[59]   Rimmelzwaan, G. F.; Baars, M.; Claas, E. C.; Osterhaus, A. D. Comparison of RNA hybridization, hemagglutination assay, titration of

infectious virus and immunofluorescence as methods for monitoring influenza virus replication in vitro. *J. Virol. Methods*. **1998**, 74, 57–66.

[60]   Pietrantoni, A.; Dofrelli, E.; Tinari, A.; Ammendolia, M. G.; Puzelli, S.; Fabiani, C.; Donatelli, I.; Superti, F. Bovine lactoferrin inhibits influenza A virus induced programmed cell death in vitro. *Biometals*. **2010**, 23, 465–475.

[61]   Marchetti, M.; Trybala, E.; Superti, F.; Johansson, M.; Bergström, T. Inhibition of herpes simplex virus infection by lactoferrin is dependent on interference with the virus binding to glycosaminoglycans. *Virology*. **2004**, 318, 405-413.

[62]   Terracciano, S.; Di Micco, S.; Bifulco, G.; Gallinari, P.; Riccio, R.; Bruno, I. Synthesis and biological activity of cyclotetrapeptide analogues of the natural HDAC inhibitor FR235222. *Bioorganic & Medicinal Chemistry*. **2010**, 18, 3252–3260.

[63]   Marion, D. and Wüthrich, K. Application of phase sensitive two-dimensional correlated spectroscopy (COSY) for measurements of 1H-1H spin-spin coupling constants in proteins. *Biochem. Biophys. Res. Commun*. **1983**, 113, 967–974.

[64]   Goddard, T. D. and Kneller, D. G. SPARKY 3, University of California, San Francisco.

[65]   Schrödinger, *LLC, New York, NY*. **2013**.

CHAPTER IV

Investigation on side-products formation during the preparation of a cyclic peptide contained a lactam bridge

Abstract

The preparation of lactam constrained cyclic peptide requires orthogonal protecting groups for side-chain amino and carboxylate functionalities involved in the cyclization process.

In this study, starting from the synthesis of a lactam peptide, H-Ser-[Lys-His-Ser-Ser-Leu-Asp]-Cys-Val-Leu-Arg-Pro-NH$_2$, we report the identification of problematic stretches during the sequence assembly process. Sequence elongation was achieved with standard Fmoc peptide synthesis and an α-allyl-protected aspartic acid residue was then coupled to the growing chain in order to allow the cyclization. Surprisingly, after the deprotection of aspartic acid Fmoc group, the formation of a mixture of desired compound, aspartimide and piperidinyl derivative was observed. Therefore, we studied this problem and described its resolution using β-2-phenylisopropyl ester as β-protecting group of aspartic acid.

Keywords

Cyclic peptide, aspartimide, allyl ester, side reactions.

Abbreviations

Abbreviations used for amino acids and designation of peptides follow the rules of the IUPAC-IUB Commission of Biochemical Nomenclature in J. Biol. Chem. 1972, 247, 977-983. Amino acid symbols denote L-configuration unless indicated otherwise. The following additional abbreviations are used: HOBt, N-hydroxy-benzotriazole; HBTU, 2-(1H-benzotriazole-1-yl)-1,1,3,3-tetramethyluronium hexafluoro-phosphate; HOAt, 1-Hydroxy-7-azabenzotriazole; DIEA, N,N-diisopropylethyl-amine; DMF, N,N-dimethylformamide; DCM, dichloromethane; NMP, N-Methyl-2-pyrrolidone; TIS, triisopropylsilane; TFA, trifluoroacetic acid; Boc, tert-butoxycarbonyl;

ESI-MS, electro spray ionization mass spectrometry; Fmoc, fluorenylmethoxycarbonyl; Mmt, 4-methoxytrityl; SPPS, solid-phase peptide synthesis.

4.1 Introduction

Cyclic peptides, in contrast to linear peptides, have been considered to have greater potential as therapeutic agents due to their increased chemical and enzymatic stability, more defined structure, and improved pharmacodynamic properties.[1, 2] Specially, side-chain lactam bridges linking amino acid residues that are spaced several residues apart in the linear sequence offer a convenient and flexible method for introducing conformational constraints into a peptide structure.

Solid phase peptide synthesis (SPPS) is the most convenient approach to prepare lactam constrained cyclic peptides. In particular, the preparation of these peptides generally require a pair of selectively cleavable protecting groups used for protection of the amine and carboxylic acid to be linked by solid-phase cyclization. Among these groups, the most used is the Allyl ester (OAll) for side chain carboxilyc acids, along with its urethane-based partner for side-chain amines, the allyloxycarbonyl group (Alloc). OAll-protecting group, stable to both acid and base, is reliably cleaved in good yield on solid supports using the Pd(0) catalyst.[3-5] Nevertheless side reactions can hamper the overall synthesis leading to decreased yields and/or quality.

In particular, aspartimide (Asi) formation, a well-documented side reaction when allyl ester is used as a protection for the aspartic acid side chain, can be observed. Its formation, which can either be acid or base catalyzed, occurs while the piperidine-catalyzed Fmoc cleavage of peptides containing aspartic acid.[6-9]

The propensity of aspartimide formation mainly depends on the aspartate carboxyl neighboring residue.[10, 11]

As a matter of fact, aspartimide is the result of an attack of an amidate species at the carbonyl carbon of the side chain carboxylate of aspartic acid. Subsequent hydrolysis of the aspartimide ring gives rise to a mixture of *α*- and *β*-aspartyl peptides. In addition, nucleophilic attack of the imide ring by piperidine results in the formation of *α*- and *β*-piperidides (Figure 4.1).
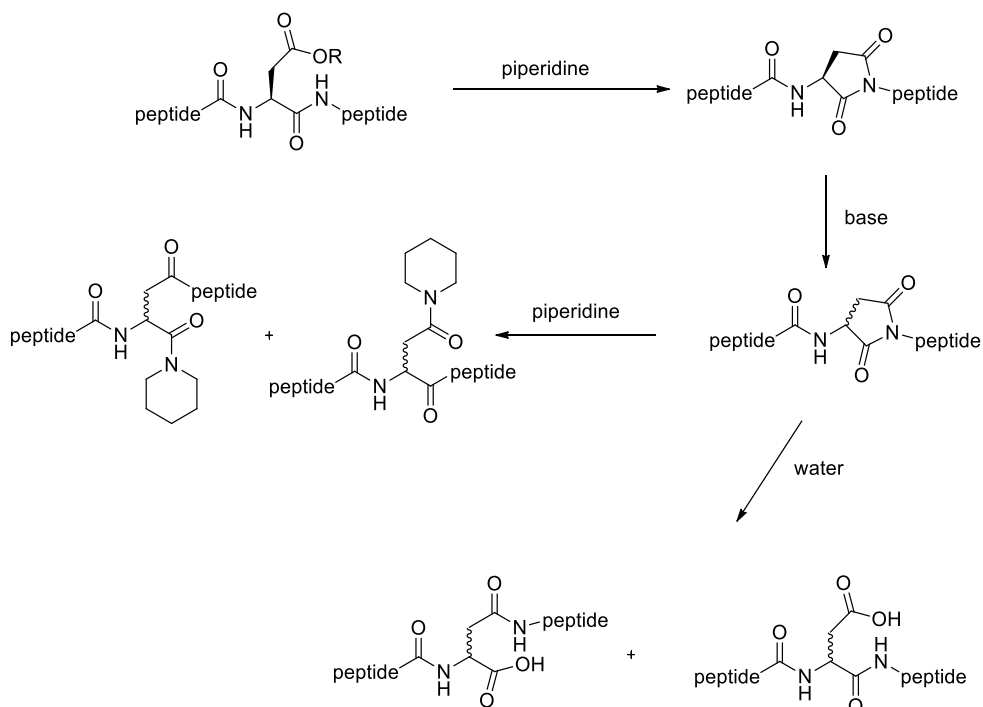
Figure 4.1 *Mechanism for aspartimide-related by-product formation.*

In recent years several strategies to avoid Asi formation have been developed.[2] Nevertheless, employing of these methods does not fully prevent Asi formation and may cause certain difficulties during synthesis, or may not be suitable for the 'on-resin' synthesis of cyclic or branched peptides.

In this work, we tried to stabilize of 3D structure of bLf C-lobe fragment 418-429 through cyclization of the peptide backbone, H-Ser-[Lys-His-Ser-Ser-Leu-Asp]-Cys-Val-Leu-Arg-Pro-NH$_2$ (Figure 4.2). Sequence elongation was achieved with standard Fmoc peptide synthesis and an α-allyl-protected aspartic acid residue was then coupled to the growing chain in order to allow the cyclization. During the synthesis of this peptide, unfortunately, the major product obtained showed a mass difference of +67 Da respect to expected cyclic peptide.
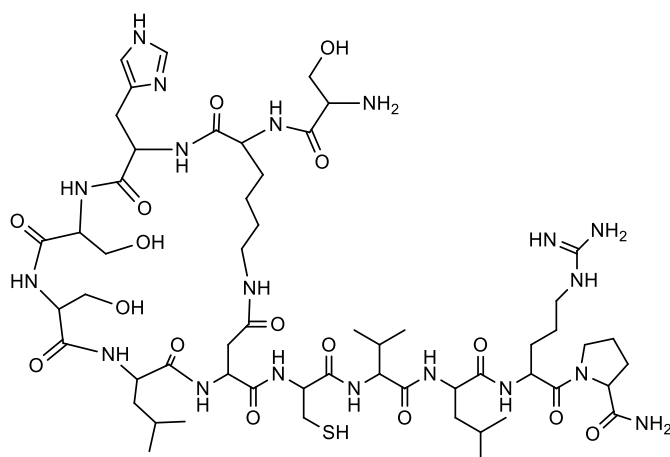
Figure 4.2 *Stucture of peptide 71.*

Therefore, the synthesis and the gradual elongation of this peptide were monitored. The formation of side products was observed after the deprotection of the Fmoc group of aspartic acid.

In particular, after the deprotection of aspartic acid Fmoc group by piperidine (25% v/v in DMF) for 30 min at room temperature, we observed a removal of Asp allyl group. LC-MS analysis revealed a mixture of three compounds (Figure 4.3): desired compound (**52**), aspartimide (Asi, **53**) and 4-(1-Piperidinyl) aspartate derivative (**54**) (Table 4.1).

Table 4.1 *Peptides obtained during the synthesis.*

Peptide	Sequence
52	H$_2$N— allyl ester —Cys-Val—Leu-Arg-Pro-NH$_2$
53	H$_2$N— succinimide N—Cys-Val—Leu-Arg-Pro-NH$_2$
54	H$_2$N— piperidide —Cys-Val—Leu-Arg-Pro-NH$_2$
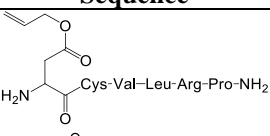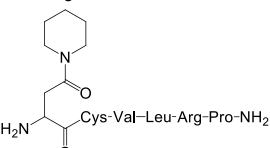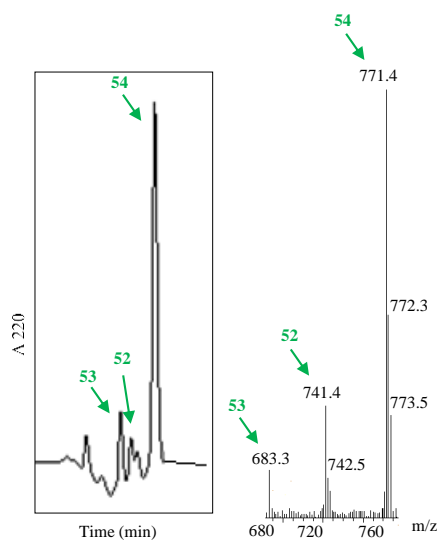
Figure 4.3 *HPLC elution profile of mixture of compounds and ESI-MS spectrum.*

NMR analysis in $DMSO_{d6}$ solution clearly demonstrated the presence of piperidinyl (pyp) derivative.
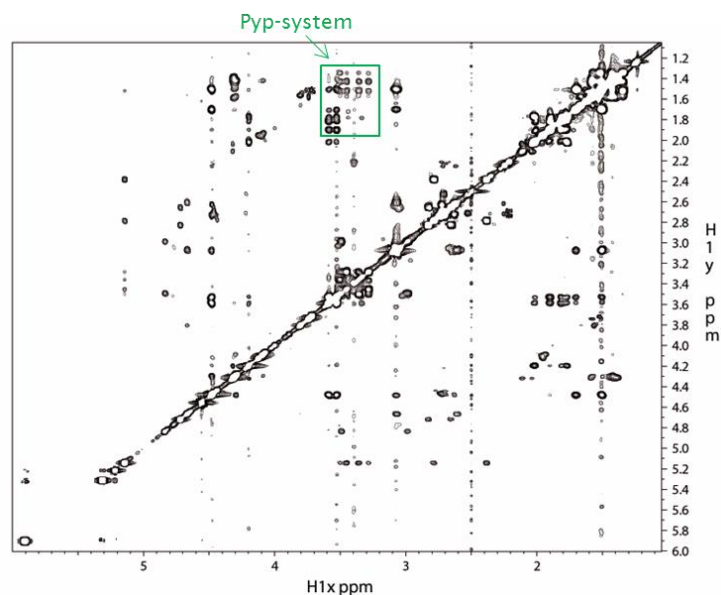
Figure 4.4 *Partial NOESY spectrum of compound 54.*

In the present study, we report the problem of Asi formation during Fmoc-based SPPS of peptide containing a lactam bridge using Allyl group to protect β-carboxy side-chain group of Asp residue.

Starting from these observations, during my PhD, I intended to identify the factors affecting Asi formation and thus to find a simple and efficient synthesis protocol to minimize the process Asi formation.

4.2 Chemistry

4.2.1 Synthesis of peptides

The synthesis of peptides (**52**-**71**) was performed according to the solid phase approach using standard Fmoc methodology in a manual reaction vessel.[12] Different resins were used: Rink-Amide, Fmoc-PAL-PEG-PG and 2-chlorotrityl chloride resin. Rink-Amide and Fmoc-PAL-PEG-PG were deprotected by a 25% piperidine solution in N, N-dimethylformamide (DMF) for 30 min and the first amino acid was linked onto the resin.

For 2-chlorotrityl chloride resin, the first N^α-Fmoc amino acid and DIPEA were dissolved in dry dichloromethane containing, if necessary, a small amount of dry DMF. This was added to the resin and stirred for 30-120 min.

The following protected amino acids were then added stepwise. Each coupling reaction was accomplished using a 3-fold excess of amino acid with HBTU and HOBt in the presence of DIPEA. The N^α-Fmoc protecting groups was removed by treating the protected peptide resin with a 25% solution of piperidine in DMF.

In addition, after each step of deprotection and after each coupling step, Kaiser test was performed to confirm the complete removal of the Fmoc protecting group, respectively, and to verify that complete coupling has occurred on all the free amines on the resin. [13]

The preparation of cyclic peptides, through a side-chain-to-side-chain cyclization, was carried out after removal of the 2-PhiPr/Mmt protection with 1% TFA/DCM.

The N-terminal Fmoc group was removed as described above. Finally, the peptides were released from the resin with trifluoroacetic acid (TFA)/ triisopropylsilane (iPr3SiH) / H2O (90:5:5) for 3 h. The resin was removed by

filtration, and the crude peptide was recovered by precipitation with cold anhydrous ethyl ether to give a white powder and then lyophilized (Scheme 4.1).

The crude peptides were purified by preparative RP-HPLC. Analytical HPLC indicated the degree of purity of the peptides and molecular weights were confirmed by ESI-MS.
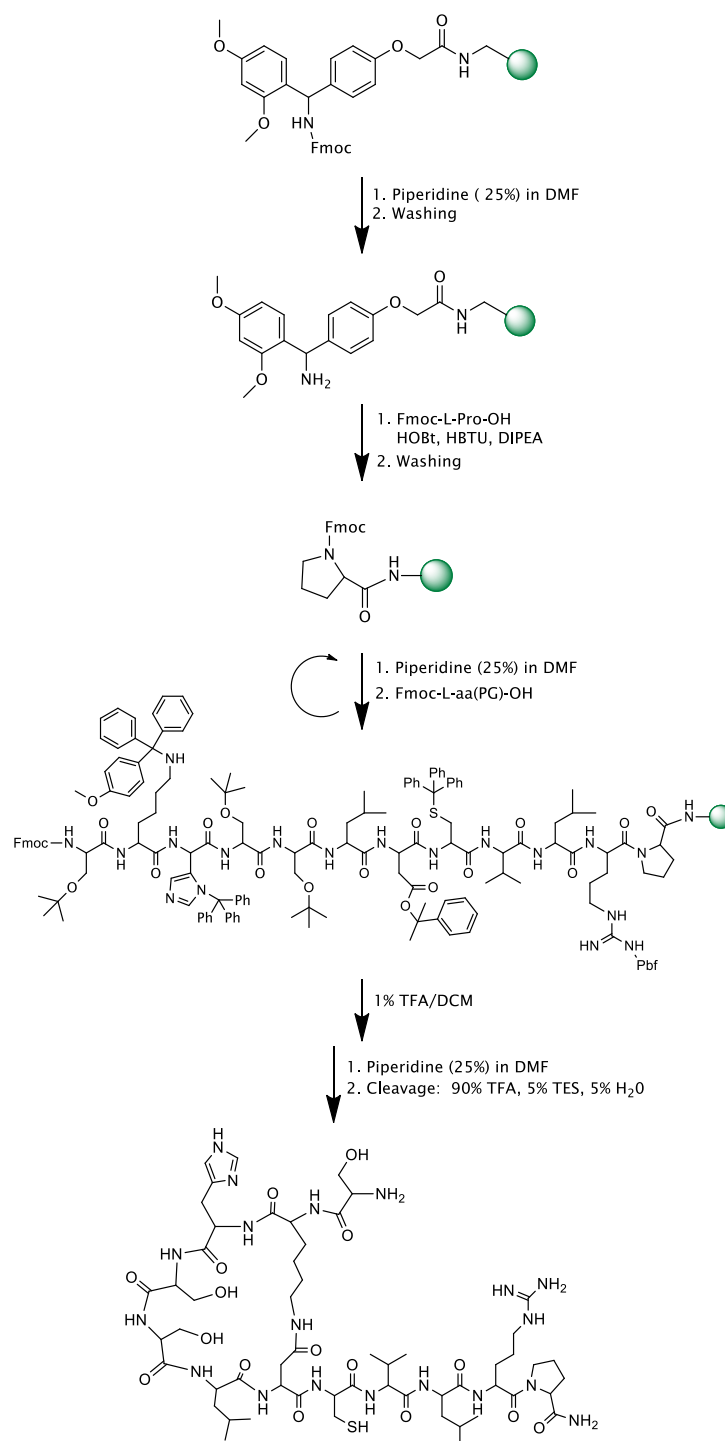
Scheme 4.1 *Synthesis and folding of peptide 71.*

4.3 Results and discussion

The preparation of the lactam peptide mentioned above requires orthogonal protecting groups for side-chain amino and carboxylate functionalities.[2, 14] Use of the allyl ester (OAll) group for this role in the protection of the aspartic acid side-chain resulted in the formation of unexpected side-products. [15, 16]

To study this phenomenon and try to get the desired sequence in a good yield we used different approaches. We study the influence of resins, protecting groups, bases and amino acid sequence on the formation of byproducts.

To simulate deprotection conditions of prolonged synthesis, all peptides were incubated with piperidine (25%v/v in DMF) for 30 min, 1h, 2h, 3h, 6h, 12h and 16h.

4.3.1 Factors influencing aspartimide formation

4.3.1.1 Solid support (peptides 52, 55 and 56)

It has been observed that the resin/linker used as a solid support in solid phase synthesis may sometimes contribute to decreasing the formation of aspartimide. Therefore, to compare the extent of side reactions formation and factors that can affect it, we studied the effect of the polymer support.

As a first resin we used a Rink Amide, a resin that releases amides rather than carboxylic acids, as required by the peptide sequence. This is a resin acid labile, thus the solution used for the cleavage of the peptide from the resin is at 90% of TFA in DCM. The synthesis did not have successful leading to the formation of the already mentioned side products.

Albericio et al. used the hydrophilic resins.[17] The most commonly used are resins, polystyrene-based always, on which are grafted chains of polyethylene glycol (PEG). These chains move away from the functional groups of the resin

core for which the reaction conditions become more "solution-like". Therefore, we used the resin Fmoc-PAL-PEG-PS (Peptide Amide Linker-polyethylene glycol-polystyrene) to avoid the problems caused steric hindrance. In the literature, however, it is reported that the use of 2-chlorotrityl chloride resin, which offers the possibility of mild acidolysis of the peptide chain, prevents this undesired cyclization.[18, 19]

Therefore, although it is used to acids peptides, we used this resin for the synthesis of our peptide to evaluate their effectiveness.

Both approaches have not been successful (Table 4.2).

Table 4.2 *Influence of the solid support on aspartimide and piperidinyl derivatives formation.*

Pep.	Protecting Group Asp	Resin		(16 h) base treatment
				α- β-piperidinyl peptide (%)
52	All	RINK-AMIDE	(structure)	100
55	All	Fmoc-PAL-PEG-PS	(structure)	100
56	All	2-Chlorotrityl-cloride	(structure)	100
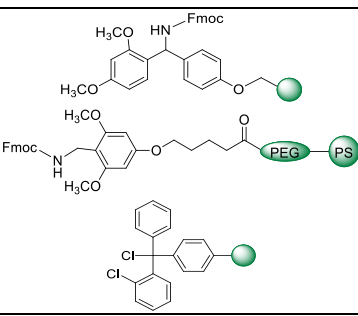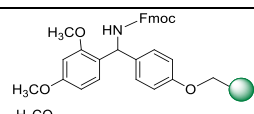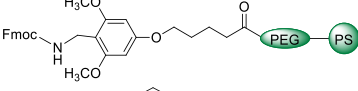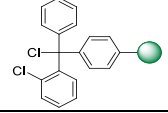
4.3.1.2 Base (peptides 52, 57-59)

Piperidine, the standard secondary amine applied in the removal of Fmoc in solid-phase, gives rise to a considerably high percentage of Aspartimide, plus the additional presence of piperidides of the α- and β-peptide.[20] The concentration of the secondary amine also affects the amount and ratio of byproducts.[21, 22] We replaced the piperidine (pKa=11.12) with the milder base piperazine (pKa = 9.73) and morfoline (pKa = 8.3), that could reduce

aspartimide formation, however, at the cost of the reaction rate. It did not show a significant effect.

N-hydroxylamine-based compounds and coupling reagents are widely used as amide bond-forming agents.[23-27] In addition, additives are beneficial in order to reduce the extent of racemization and guanidylation of the N-terminus of the growing peptide chain and to increase coupling efficiency.[28, 29] This substantial contribution to coupling strategies prompted their evaluation in the prevention of other non-coupling-derived side reactions. It was showed indeed that, in unwanted reactions, their addition can be advantageous. N-Hydroxylamine-based additives also contribute to the wide arsenal of approaches to prevent the formation of Asi and derived byproducts. This beneficial effect is observed in base-catalyzed Asi cyclization, during coupling or Fmoc removal with secondary/tertiary amines. It is proposed that the unique acidic properties of N-hydroxylamines used as additives in peptide synthesis (pKa = 2-10) are responsible for this behaviour.[30] The abstraction of the amide backbone proton is the crucial step in the cyclization that leads to Asi. Thus, addition of a relative strong acid, such as HOBt, results in competition with the Asp-X amide backbone for the base present in the medium.[30] When HOBt is used as additive, conversion into its anion by the effect of the base would decrease the percentage of negatively charged amide backbone nitrogen, which is responsible for initiating Asi formation (Figure 4.5).
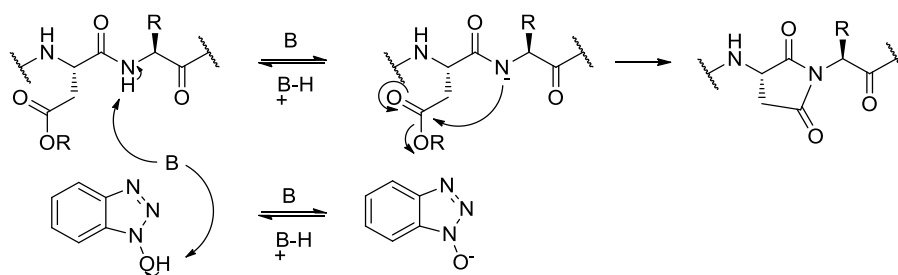
Figure 4.5 *Competition between N-hydroxylamine and amide backbone proton abstraction.*

Consequently, we studied the suppression of aspartimide formation by adding small amounts of organic acids to the deprotection agent piperidine. However, under these conditions, treatment with piperidine containing 0.1 M of HOBt caused the complete formation of aspartimide and piperidinyl derivate.

Table 4.3 *Influence of the nature of the base on byproducts formation.*

Pep.	Protecting Group Asp	Deprotection reagent		(16 h) base treatment By-products (%)
52	All	Piperidine		100
57	All	Morfoline		100
58	All	Piperazine		100
59	All	Piperidine + HOBt 0.1 M		100
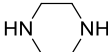
4.3.1.3 β-carboxyl protecting group (peptides 52, 60, 61)

The nature of the β-carboxyl ester, acting as protecting group, markedly influences on the impact of the aspartimide side reaction.
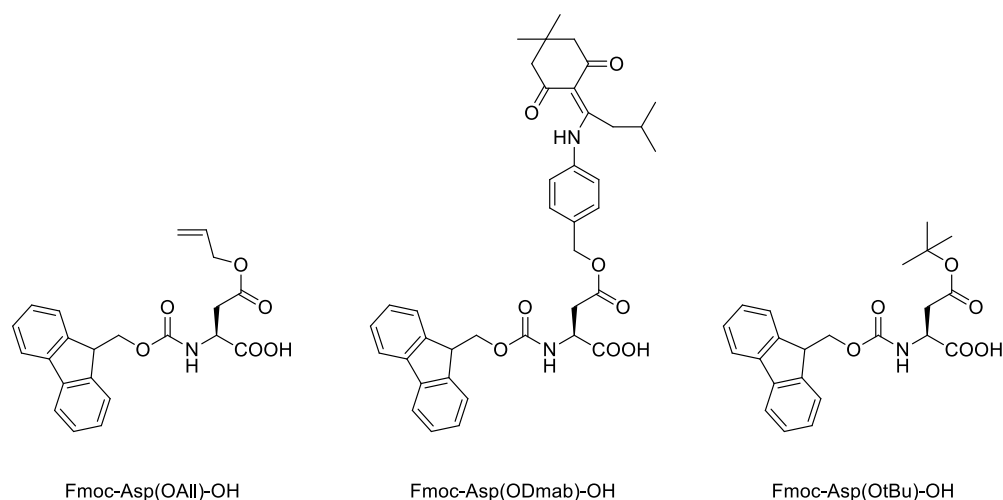
Figure 4.6 *Structures of Asp β-carboxyl protecting groups used.*

Initially, we used Asp(OAll) as protecting group of aspartic acid, but it gives rise to high percentages of aspartimide peptide and thus offers the poorest protection against this unwanted process. In order to minimize the nucleophilic attack of the preceding amide backbone nitrogen atom to Asp, ODmab [4-{N-[1-(4,4-dimethyl-2,6-dioxocyclohexylidene)-3-methylbutyl]amino}benzyl], highly sterically hindered β-protecting group, was used. However, the β-protection of Asp as ODmab does not result in improved prevention of the side reaction and is comparable to that achieved by β-allyl ester protection. Protection with the bulky tert-butyl ester has shown greater efficacy than the abovementioned strategies in preventing this side reaction in basic media.[10, 19, 32] In fact, in classical Fmoc removal conditions, it not give rise to conversion into Asi residues.

Table 4.4 *Influence of β-carboxyl protecting group on aspartimide and piperidinyl derivatives formation.*

Pep.	Protecting Group Asp	(16 h) base treatment
		α- β-piperidinyl peptide (%)
52	All	100
60	Dmab	100
61	tBu	-

4.3.1.4 Sequence

Undoubtedly, the nature of the neighbouring amino acid located at the C-terminus of the aspartic acid (Asp-X) and the amino acidic sequence determine the degree of aspartimide formation, since the cyclization of Asp to Asi is initiated by attack of the amide backbone nitrogen of the preceding residue.[22] Two different approaches were used to evaluate the influence of amino acids β-functional groups on aspartimide formation: i) L-Ala scanning analysis of peptide **52** (peptides **62**-**66**); ii) scramble peptides (peptides **67**-**69**).

Alanine scanning approach (peptides 62-66)

We decided to check the relevance of side chains of each aminoacidic residue in side products formation through L-Ala scanning analysis (peptides **62-66**, Table 4.5). These changes did not show a significant effect to suppress aspartimide formation.

Table 4.5 *Peptides synthesized by alanine scanning approach.*

Pep.	Protecting Group Asp	Sequence	(16 h) base treatment
			α- β-piperidinyl peptide (%)
62	All	DCVLRA	100
63	All	DCVLAP	100
64	All	DCVARP	100
65	All	DCALRP	100
66	All	DAVLRP	100

Scramble peptide (peptides 67-69)

Finally, the scramble analogue peptides, constructed through permutation of the original peptide sequence, were synthesized to examine the sequence dependence on Asi and piperidide formation. These side-products were not observed in scramble peptides.

Therefore, we hypothesized that the conversion of Asp into Asi units could be conformation-dependent.

Table 4.6 *Scramble peptides synthesized.*

Pep.	Protecting Group Asp	Sequence	(16 h) base treatment
			α- β-piperidinyl peptide (%)
67	All	DLPRVC	-
68	All	DVRPCL	-
69	All	DPCVLR	-

4.3.2 β-(2-phenylisopropyl) ester to minimization of aspartimide formation

Finally, in order to minimize the nucleophilic attack of the preceding amide backbone nitrogen atom to Asp, we used highly sterically hindered β-protecting group, as Asp [OPhiPr = β-(2-phenylisopropyl)]. An orthogonal protecting groups for side-chain of cysteine was used.

In peptide **70**, we used Asp(2-PhiPr) and Cys(tBu), it does not suppress the aspartimide formation.

Moreover, in order to evaluate the influence of high bulkiness of trityl, β-protecting group of cysteine, we synthetized peptide **71**. It results in increased prevention of Asi.

Asp(O-2-PhiPr)-Cys(Trt)   Asp(O-2-PhiPr)-Cys(tBu)
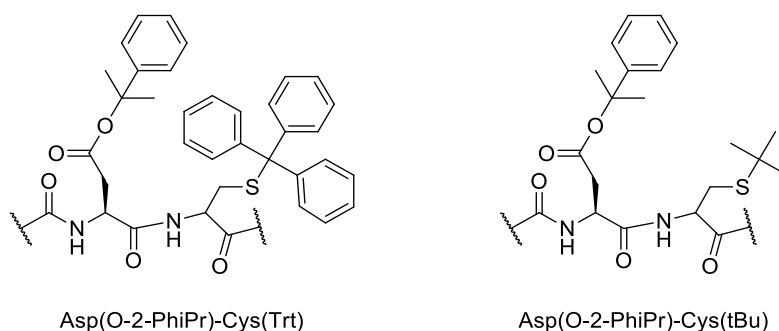
Figure 4.7 *Influence of cysteine β-protecting group on aspartimide formation.*

Table 4.7 *Peptides synthesized.*

Pep.	Protecting Group Asp	Protecting Group Cys	(16 h) base treatment
			α- β-piperidinyl peptide (%)
70	2-PhiPr	tBu	100
71		Trt	-

4.4 Conclusions

The synthesis of lactam constrained cyclic peptide requires orthogonal protecting groups for side-chain amino and carboxylate functionalities. To synthesize a cyclic peptide, H-Ser[Lys-His-Ser-Ser-Leu-Asp]-Cys-Val-Leu-Arg-Pro-NH$_2$, we used the allyl ester (OAll) group for this role in the protection of the aspartic acid side-chain.

Surprisingly, our approach to synthesize the peptide mentioned above, failed completely. In particular, after the deprotection of aspartic acid Fmoc group by piperidine (20% v/v in DMF) for 30 min at room temperature, the formation of unexpected side-products was observed.

Therefore, we studied this phenomenon and tried to obtain the desidered sequence with different approaches. We hypothesized that the aspartimide and piperidinyl derivative formation is conformation-dependent.

Finally, we synthetized the desidered peptide, using as β-protecting group of aspartic acid and lysine, β-2-phenylisopropyl ester and methoxytrityl, respectively. LC-MS analysis confirmed the presence of the desired cyclic peptide.

4.5 Experimental section

N^{α}-Fmoc-protected amino acids, Rink amide-resin, Fmoc-PAL-PEG-PS resin, 2-Chlorotrityl-cloride resin, N-hydroxy-benzotriazole (HOBt), 2-(1H-benzotriazole-1-yl)-1,1,3,3-tetramethyluronium hexafluoro-phosphate (HBTU), N,N-diisopropylethyl-amine (DIPEA), piperidine, morpholine, piperazine and Trifluoroacetic acid were purchased from Iris Biotech (Germany). Peptide synthesis solvents, reagents, as well as CH3CN for high performance liquid chromatography (HPLC) were reagent grade and were acquired from commercial sources and used without further purification unless otherwise noted.

4.5.1 Synthesis of peptides with Rink-Amide and Fmoc-PAL-PEG-PS resin

The synthesis of peptides (**52**-**55**, **57**-**71**) was performed according to the solid phase approach using standard Fmoc methodology in a manual reaction vessel.[33, 34]

The first amino acid, N^{α}-Fmoc-Xaa-OH (Xaa = Pro, Cys(Trt), Arg(Pbf), Leu, Ala), was linked on to the Rink resin (100–200 mesh, 1% DVB, 0.59 mmol/g) and Fmoc-PAL-PEG-PS resin (100–200 mesh, 1% DVB, 0.22 mmol/g) previously deprotected by a 25% piperidine solution in N, N-dimethylformamide (DMF) for 30 min.

The following protected amino acids were then added stepwise: N^α-Fmoc-Pro-OH, N^α-Fmoc-Arg(Pbf)-OH, N^α-Fmoc-Leu-OH, N^α-Fmoc-Val-OH, N^α-Fmoc-Cys(Trt)-OH, N^α-Fmoc-Cys(tBu)-OH, N^α-Fmoc-Asp(OtBu)-OH, N^α-Fmoc-Ala-OH, N^α-Fmoc-Asp(OAll)-OH, N^α-Fmoc-Asp(OtBu)-OH, N^α-Fmoc-Asp(ODmab)-OH, N^α-Fmoc-Asp(2-PhiPr)-OH.

Each coupling reaction was accomplished using a 3-fold excess of amino acid with HBTU and HOBt in the presence of DIPEA (6 eq.). The N^α-Fmoc protecting groups were removed by treating the protected peptide resin with a 25% solution of piperidine in DMF (1 × 5 min and 1 × 25 min). The peptide resin was washed three times with DMF, and the next coupling step was initiated in a stepwise manner. The peptide resin was washed with DCM (3×), DMF (3×), and DCM (3×), and the deprotection protocol was repeated after each coupling step. In addition, after each step of deprotection and after each coupling step, Kaiser test was performed to confirm the complete removal of the Fmoc protecting group, respectively, and to verify that complete coupling has occurred on all the free amines on the resin.

4.5.2 Synthesis of peptides 56 with 2-Chlorotrityl-cloride resin

The peptides **56** was synthetized using a 2-chlorotrityl chloride resin. The first N^α-Fmoc-Pro-OH, (0.6-1.2 equiv relative to the resin for 2-chlorotrityl resin) and DIPEA (4 equiv relative to amino acid) were dissolved in dry dichloromethane (DCM) (approx. 10 mL per gram of resin) containing, if necessary, a small amount of dry DMF (enough to facilitate dissolution of the acid). This was added to the resin and stirred for 30-120 min. After stirring, the resin was washed with 3×DCM/MeOH/DIPEA (17:2:1), 3×DCM, 2×DMF and 2×DCM. Other N^α-Fmoc amino acids (4 equiv) were sequentially coupled as previously described.

4.5.3 Synthesis of lactam peptide (peptide 71)

The corresponding linear peptide was synthetized as described above and the amino acids N^α-Fmoc-Asp(2-PhiPr)-OH and N^α-Fmoc-Lys(Mmt)-OH were used as lactam precursors. After linear assembly, the 2-PhiPr and the Mmt groups were removed according to the following procedure: 200 mg of peptide resin was washed with dichloromethane (DCM) and a solution of 1% TFA/DCM was added. The reaction was allowed to proceed for 30 min. The peptide resin was washed with DCM (3x), DMF (3x) and DCM (4x). The macrocyclic lactam ring formation was mediated by addition of HBTU (6 equiv), HOBt (6 equiv) and DIPEA (12 equiv) under Ar for 2 h. The process was repeated if necessary (Kaiser test used to monitor completion).

The N-terminal Fmoc group was removed as described above. Finally the peptides were released from the resin with TFA/TIS/H2O (90:5:5) for 3 h. The resin was removed by filtration, and the crude peptide was recovered by precipitation with cold anhydrous ethyl ether to give a white powder and then lyophilized.

4.5.4 Purification and characterization

All crude peptides were purified by RP-HPLC on a preparative C18-bonded silica column (Phenomenex Kinetex AXIA 100Å, 100 x 21.20mm, 5µm) using a Shimadzu SPD 20A UV/VIS detector, with detection at 210 and 254 nm. The column was perfused at a flow rate of 15 ml/min with solvent A (10%, v/v, water in 0.1% aqueous TFA), and a linear gradient from 10 to 90% of solvent B (80%, v/v, acetonitrile in 0.1% aqueous TFA) over 40 min was adopted for peptide elution. Analytical purity and retention time (tr) of each peptide were determined using HPLC conditions in the above solvent system (solvents A and

B) programmed at a flow rate of 1.500 ml/min using a linear gradient from 10 to 90% B over 11 min, fitted with C-18 column Phenomenex, Aeris XB-C18 column (150 mm x 4.60, 3.6μm). All analogues showed >97% purity when monitored at 215 nm. Homogeneous fractions, as established using analytical HPLC, were pooled and lyophilized. Peptides molecular weights were determined by ESI mass spectrometry and LC-MS in a LC-MS 2010 instrument fitted with Phenomenex, Aeris XB-C18 column (150 mm x 4.60, 3.6μm), eluted with a linear gradient from 10% to 60% B over 15 min, at a flow rate of 1.000 mL/min. ESI-MS analysis in positive ion mode, were made using a Finnigan LCQ Deca ion trap instrument, manufactured by Thermo Finnigan (San Jose, CA, USA), equipped with the Excalibur software for processing the data acquired. The sample was dissolved in a mixture of water and methanol (50/50) and injected directly into the electrospray source, using a syringe pump, which maintains constant flow at 5 ml/min. The temperature of the capillary was set at 220°C.

Peptide analytical data are reported in Table 4.8.

Table 4.8 Analytical data of peptides **52**-**71**.

Peptide	HPLC k'[a]	ESI-MS
52	9.93	740.91
53	9.67	697.85
54	6.72	767.98
55	9.93	740.91
56	9.96	741.90
57	10.26	769.96
58	10.21	768.97
59	6.72	767.98
60	9.81	700.85
61	6.72	767.98
62	9.97	741.95
63	9.23	682.87
64	9.89	725.90
65	9.91	739.93
66	9.90	735.92
67	9.95	740.93
68	9.96	740.95
69	9.92	740.89
70	6.72	767.91
71	12.31	1321.54

[a] k'=[(peptide retention time-solvent retention time)/solvent retention time].
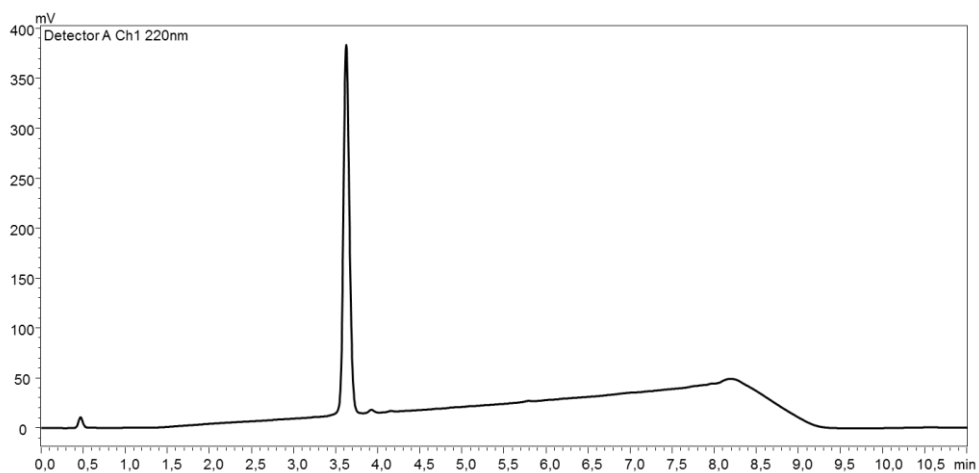

Figure 4.8 *HPLC profile of pure piperidinyl derivative.*

References

[1]   Lambert, J. N.; Mitchell, J. P.; Roberts, K. D. J. The synthesis of cyclic peptides. *J. Chem. Soc., Perkin Trans*. **2001**, 1, 471-484.

[2]   Li, P.; Roller, P. P.; Xu, J. Current Synthetic Approaches to Peptide and Peptidomimetic Cyclization. *Curr. Org. Chem*. **2002**, 6, 411-440.

[3]   Biancalana, S.; Hudson, D.; Lyttle, M. H.; Johnson, C. R.; Tsou, D.; Wright, P. B.; Barany, G.; Calnan, B. J.; Frankel, A. D.; Cohn, W. B.; Hayes, T.; Dahl, C.; Markus, M. A.; Weiss, M. A.; Hammer, R. P.; Hsu, H. T.; Jordan, R.; Kamo, K. K. and Toll, L. In Epton, R. (Ed.) Innovation and Perspectives in Solid Phase Synthesis: Peptides, Polypeptides, and Oligonucleotides. Intercept Ltd., Andover, U.K. **1992**, 135-152.

[4]   Lyttle, M. H. and Hudson, D. In Smith, J.A. and Rivier, J.E. (Eds.) Peptides: Chemistry and Biology: Proceedings of the twelfth American Peptide Symposium. ESCOM, Leiden, The Netherlands, **1992**, 583-584.

[5]   Loffet, A. and Zhang, H. X. In Epton, R. (Ed.) Innovation and Perspectives in Solid Phase Synthesis: Peptides, Polypeptides, and Oligonucleotides. Intercept Ltd., Andover, U.K., **1992**, 77-82.

[6]   Quibell, M.; Owen, D.; Packman, L. C.; Johnson, T. Supresion of piperidine-mediated side product formation for Asp(OBu^t)- containing peptides by the use of N-(2-hydroxy-4-methoxybenzyl) (Hmb) backbone amide protection. *J. Chem. Soc., Chem. Commun.***1994**, 2343–2344.

[7]   Karlström, A. H.; Undén, A. E. A new protecting group for aspartic acid that minimizes piperidine-catalysed aspartimide formation in Fmoc solid phase peptide synthesis. *Tetrahedron Lett.* **1996**, 37, 4243-4246.

[8]   Yang, Y.; Sweeney, W. V.; Schneider, K.; Thörnqvist, S.; Chait, B. T.; Tam, J. P. Aspartimide formation in base-driven 9-fluorenylmethoxycarbonyl chemistry. *Tetrahedron Lett*. **1994**, 35, 9689-9692.

[9]   Dölling, R.; Beyermann, M.; Haenel, J.; Kernchen, F.; Krause, E.; Franke, P.; Brudel, M.; Bienert, M. J. Piperidine-mediated side product formation for Asp(Obut)-containing peptides. *Chem. Soc. Chem. Commun.* **1994**, 38, 853-854.

[10]   Lauer, J. L.; Fields, C. G.; Fields, G. B. Sequence dependence of aspartimide formation during 9-fluorenylmethoxycarbonyl solid-phase peptide synthesis. *Lett. Pept. Sci.* **1995**, 1, 197-205.

[11]   Mergler, M.; Dick, F.; Sax, B.; Stähelin, C.; Vorherr, T. The Aspartimide Problem in Fmoc-Based SPPS. Part II. *J. Pept. Sci.* **2003**, 9, 518-526.

[12]   Atherton, E.; Sheppard, R. C. Solid-Phase Peptide Synthesis: A Practical Approach. IRL Press: Oxford, U.K. **1989**.

[13]   Kaiser, E.; Colescott, R. L.; Bossinger, C. D.; Cook, P. I. Color test for detection of free terminal amino groups in the solid-phase synthesis of peptides. *Anal. Biochem.* **1970**, 34, 595-598.

[14]   Lambert, J. N.; Mitchell, J.P.; Roberts, K. D. The synthesis of cyclic peptides. *J. Chem. Soc., Perkin Trans.* **2001**, 1, 471–484.

[15]   Grieco, P.; Gitu, P.M.; Hruby, V.J. Preparation of 'side-chain-to-side-chain' cyclic peptides by Allyl and Alloc strategy: potential for library synthesis. *J. Pept. Res.* **2001**, 57, 250–256.

[16]   Vigil-Cruzn, S. C. and Aldrich, J. V. Unexpected aspartimide formation during coupling reactions using Asp(OAl) in solid-phase peptide synthesis. *Lett. Pept. Sci.* **1999**, 6, 71–75.

[17]   Subirós-Funosas, R.; El-Faham, A.; Albericio, F. Aspartimide formation in peptide chemistry: occurrence, prevention strategies and the role of N-hydroxylamines. *Tetrahedron.* **2011** 67, 8595-8606.

[18]   Ruczynski, J.; Lewandowska, B.; Mucha, P.; Rekowski, P. Problem of aspartimide formation in Fmoc-based solid-phase peptide synthesis using Dmab group to protect side chain of aspartic acid. *J. Pept. Sci.* **2008**, 14, 335-341.

[19]   Dixon, M. J.; Nathubhai, A.; Andersen, O. A.; van Aalten, D. M. F.; Eggleston, I. M. Solid-phase synthesis of cyclic peptide chitinase inhibitors: SAR of the argifin scaffold. *Org. Biomol. Chem.* **2009**, 7, 259-268.

[20]   Nicolas, E.; Pedroso, E.; Giralt, E. Formation of aspartimide peptides in Asp-Gly sequences. *Tetrahedron Lett.* **1989**, 30, 497-500.

[21]   Yang, Y.; Sweeney, W. V.; Schneider, K.; Thörnqvist, S.; Chait, B. T.; Tam, J. P. *Tetrahedron Lett.* **1994**, 33, 9689-9692.

[22]   Dölling, R.; Beyermann, M.; Haenel, J.; Kernchen, F.; Krause, E.; Franke, P.; Brudel, M.; Bienert, M. 3rd International Innovation and Perspectives in Solid- Phase Synthesis Symposium, 31th Auge4th Sept., Oxford, UK, **1993**, Poster P21.

[23]   Subirós-Funosas, R.; El-Faham, A.; Albericio, F. N-hydroxylamines for Peptide Synthesis. Patai's Chemistry of Functional Groups, John Wiley & Sons. **2011**, 2, 623-730.

[24]   Carpino, L. A. 1-Hydroxy-7-azabenzotriazole. An efficient peptide coupling additive. *J. Am. Chem. Soc*. **1993**, 115, 4397-4398.

[25]   Knorr, R.; Trzeciak, A.; Bannwarth, W.; Gillessen, D. New coupling reagents in peptide chemistry. *Tetrahedron Lett.* **1989**, 30, 1927-1930.

[26]   Castro, B.; Dormoy, J. R.; Evin, G.; Selve, C. Reactifs de couplage peptidique I (1) - l'hexafluorophosphate de benzotriazolyl N-oxytrisdimethylamino phosphonium (B.O.P.). *Tetrahedron Lett.* **1975**, 16, 1219-1222.

[27]   Subiros-Funosas, R.; Moreno, J. A.; Bayo-Puxan, N.; Abu-Rabeah, K.; Ewenson, A.; Atias, D.; Marks, R. S.; Albericio, F. PyClocK, the phosphonium salt derived from 6-Cl-HOBt. *Chimica Oggi*. **2008**, 26, 10-12.

[28]   Subirós-Funosas, R.; Prohens, R.; Barbas, R.; El-Faham, A.; Albericio, F. Oxyma: An efficient additive for peptide synthesis to replace the benzotriazole-based HOBt and HOAt with a lower risk of explosion. *Chemistry - A European Journal.* **2009**, 15, 9394-9403.

[29]   El-Faham, A.; Subiros-Funosas, R.; Prohens, R.; Albericio, F. COMU: A safer and more effective replacement for benzotriazole-based uronium coupling reagents. *Chemistry - A European Journal.* **2009**, 15, 9404-9416.

[30]   Martinez, J.; Bodanszky, M. Side Reactions in Peptide Synthesis. IX. Suppression of the Formation of Aminosuccinyl Peptides With Additives. *Int. J. Pept. Protein Res*. **1978**, 12, 277-283.

[31]   Flora, D.; Mo, H.; Mayer, J. P.; Khan, M. A.; Yan, L. Z. Detection and control of aspartimide formation in the synthesis of cyclic peptides. *Bioorg. Med. Chem. Lett.* **2005**, 15, 1065-1068.

[32]   Palasek, S. A.; Cox, Z. J.; Collins, J. M. Limiting racemization and aspartimide formation in microwave-enhanced Fmoc solid phase peptide synthesis. *J. Pept. Sci.* **2007**, 13, 143-148.

[33]   Atherton, E. and Sheppard, R. C. Solid-Phase Peptide Synthesis: A Practical Approach. IRL Press: Oxford, U.K. **1989**.

[34]   Stewart, J. M. and Young, J. D. In Solid Phase Peptide Synthesis. Pierce Chemical: Rockford, IL, **1984**.

Conclusions

The present study describes the identification of three C-lobe bLf-derived tetrapeptides as the minimum fragments expressing the broad anti-influenza activity of bLf. Peptides **14** (VLRP), **15** (SLDC), and **17** (SKHS) were designed from the fragment 418-429 (**1**, SKHSSLDCVLRP), which is involved in the C-lobe bLf-HA interaction. These tetrapeptides retain the inhibitory potency of the fragment 418-429 and inhibit the influenza virus hemagglutination and cell infection in a concentration range of femto- to picomolar. NMR spectroscopy analysis performed on compounds **1** showed a global turn conformation for this peptide and hypothesized the preferred bioactive conformation of our tetrapeptides. Our results strongly encourage the pursuit of this path for the development of a novel class of anti-influenza drugs.

Moreover, based on conformational analysis, we tried to stabilize 3D structure of fragment 418-429, SKHSSLDCVLRP, through cyclization of the peptide backbone.

The synthesis of lactam constrained cyclic peptide requires orthogonal protecting groups for side-chain amino and carboxylate functionalities. To synthesize this peptide, we used the allyl ester (OAll) group for this role in the protection of the aspartic acid side-chain.

Surprisingly, our approach to synthesize the peptide mentioned above, failed completely. In particular, after the deprotection of aspartic acid Fmoc group by piperidine (20% v/v in DMF) for 30 min at room temperature, the formation of unexpected side-products was observed.

Therefore, we studied this phenomenon and tried to obtain the desidered sequence with different approaches. We hypothesized that the aspartimide and piperidinyl derivative formation is conformation-dependent.

Finally, we synthetized the desidered peptide, using as β-protecting group of aspartic acid and lysine, β-2-phenylisopropyl ester and methoxytrityl, respectively. LC-MS analysis confirmed the presence of the desired cyclic peptide.